

INFORMATION TO USERS

This manuscript has been reproduced from the microfilm master. UMI films the text directly from the original or copy submitted. Thus, some thesis and dissertation copies are in typewriter face, while others may be from any type of computer printer.

The quality of this reproduction is dependent upon the quality of the copy submitted. Broken or indistinct print, colored or poor quality illustrations and photographs, print bleedthrough, substandard margins, and improper alignment can adversely affect reproduction.

In the unlikely event that the author did not send UMI a complete manuscript and there are missing pages, these will be noted. Also, if unauthorized copyright material had to be removed, a note will indicate the deletion.

Oversize materials (e.g., maps, drawings, charts) are reproduced by sectioning the original, beginning at the upper left-hand corner and continuing from left to right in equal sections with small overlaps.

Photographs included in the original manuscript have been reproduced xerographically in this copy. Higher quality 6" x 9" black and white photographic prints are available for any photographs or illustrations appearing in this copy for an additional charge. Contact UMI directly to order.

**ProQuest Information and Learning
300 North Zeeb Road, Ann Arbor, MI 48106-1346 USA
800-521-0600**

UMI[®]



Université d'Ottawa • University of Ottawa

**Delving Into the Rare-Earth Metal Chemistry of Pyrrole Based Ligands:
Synthesis and Analysis of Divalent Samarium and Ytterbium Pyrrolide
Complexes**

A Thesis Submitted to the
School of Graduate Studies and Research

In Partial Fulfillment of the Requirements
for the Degree of

Master of Science

In the Ottawa-Carleton Chemistry Institute

Department of Chemistry

University of Ottawa

Ottawa, Ontario

© Christian Bérubé, 2001

Candidate

Christian Denis Bérubé

Supervisor

Professor Sandro Gambarotta



**National Library
of Canada**

**Acquisitions and
Bibliographic Services**

**395 Wellington Street
Ottawa ON K1A 0N4
Canada**

**Bibliothèque nationale
du Canada**

**Acquisitions et
services bibliographiques**

**395, rue Wellington
Ottawa ON K1A 0N4
Canada**

Your file Votre référence

Our file Notre référence

0-612-66010-9

The author has granted a non-exclusive licence allowing the National Library of Canada to reproduce, loan, distribute or sell copies of this thesis in microform, paper or electronic formats.

The author retains ownership of the copyright in this thesis. Neither the thesis nor substantial extracts from it may be printed or otherwise reproduced without the author's permission.

L'auteur a accordé une licence non exclusive permettant à la Bibliothèque nationale du Canada de reproduire, prêter, distribuer ou vendre des copies de cette thèse sous la forme de microfiche/film, de reproduction sur papier ou sur format électronique.

L'auteur conserve la propriété du droit d'auteur qui protège cette thèse. Ni la thèse ni des extraits substantiels de celle-ci ne doivent être imprimés ou autrement reproduits sans son autorisation.

Abstract

The reaction of $\text{YbI}_2(\text{THF})_2$ with diphenylmethyldipyrrolide leads to a complex reaction from which is obtained an octameric divalent Yb macrocycle (Diphenyldipyrromethane-di-yl-Yb)₈ **2.1** as a major product, but from which is also isolated a tetrameric cyclic Yb(II)-oxo complex [(diphenyldipyrrolyl-methane-di-yl)Yb]₄[(K₂)(THF)₆](μ-O)₂(THF) **2.2** and a monomeric Yb(III) complex, Yb(diphenyldipyrrolylmethane-di-yl)₃(K₃THF₃) **2.3**, as minor products. Complex **2.1** is analogous to the Sm(II) dipyrrolide octameric clusters obtained under an argon atmosphere, which are thought to represent the intermediate species in the formation of dinitrogen complexes.

The reactions of $\text{SmI}_2(\text{THF})_2$ and $\text{YbI}_2(\text{THF})_2$ with the alkali salts of 2,5-dimethylpyrrole, or the reaction of $\text{SmCl}_3(\text{THF})_3$ and $\text{YbCl}_3(\text{THF})_3$ with the same ligands followed by reduction with the appropriate alkali metals, led to the formation of divalent mono- and polynuclear complexes. This mono-pyrrolide is used by virtue of its resemblance to the cyclopentadienyl molecule, and because of its increased stability compared to pyrrole. Analysis of the complexes obtained brings forth the observation that the bonding mode adopted by the ligand and the lanthanide metal is dependent on the nature of the alkali cation present in the structure.

The reaction of $[\text{Sm}\{\text{N}(\text{SiMe}_3)_2\}_2(\text{THF})_2]$ with highly delocalized pyrrole supporting schiff base ligands yields three distinct complexes, two of which bear an oxidized trivalent samarium. The first of these complexes, **4.1**, is formed by ligand dimerization through the formation of a C-C bond, arrangement created through radical

intermediates induced by the presence of Sm(II). The third complex, **4.3**, is also formed by the dimerization of two species, but the units are linked through π interaction. X-ray characterization of this last complex clearly indicates the presence of divalent samarium centers while the compound displays a light colouring, quality usually attributed to trivalent samarium containing complexes.

The reaction of $[\text{Sm}\{\text{N}(\text{SiMe}_3)_2\}_2(\text{THF})_2]$ with two dipyrrolide ligands, diethyldipyrromethane and methylphenyldipyrromethane, gives rise to two new dinitrogen complexes **5.1** and **5.3**, where the dinitrogen molecule is reduced by an electron from four different samarium centers. The same reaction with diethyldipyrromethane under an argon atmosphere produces a divalent samarium macrocyclic structure **5.2**, which is a good representation of the highly reactive precursor responsible for dinitrogen activation. Finally, a serendipitous result from the reaction of divalent samarium and methylphenyldipyrromethane gives the first example of a lanthanide complexed with a tripyrrane ligand.

To the three children in my life,

Alyssa, Samuel and France

Acknowledgements

There are many people who I have to thank for helping me over my seven year stay at the University of Ottawa, but first in my thoughts is my supervisor Professor Gambarotta. After a few semesters of his flamboyant exuberance towards chemistry early in my career, which included a short but engaging discussion on the uses of crown ethers as untraceable poisons for the disposal of “unwanted lifetime co-habitants”, I had no choice but to join Professor Gambarotta and his group to pursue my graduate studies. Sandro has proven to be a great teacher through his vivacity, his great knowledge, and his very interesting (if not slightly over-the-top) reference letters. I hope I can live up to his view of me as “a rising star in the Canadian scientific scenario”.

I would also like to thank both Professor Darrin Richeson, who introduced me to inorganic synthesis, and Professor Gerd Rabe, who proved to me that crystal structures of lanthanide elements actually exist. I would be remiss if I didn't acknowledge Dr. Glenn Yap who proved invaluable in the analysis of all my crystals, big, small and powdery. Thanks also go to all my lab mates that have always been there to give me advice, to carry the fire extinguishers and to steal my glassware. You are truly the people I will remember from my graduate experience.

I would like give my thanks and my love to my father, Réal, who gave me the love for the sciences, and to my mother, Odette, who taught me that anything that deserves to be done deserves to be well done.

Finally, all my love and affection goes to France who was always by me, or at least as close as she could get with an ocean between us.

List of Publications

1. G. W. Rabe, C. D. Bérubé, and G. P. A. Yap ; Terphenyl Ligand Systems in Lanthanide Chemistry: Use of the 2,6-Di(1-naphthyl)phenyl Ligand for the Synthesis of Kinetically Stabilized Complexes of Trivalent Ytterbium, Thulium, and Yttrium, *Inorganic Chemistry*; **2001**; 40(12); 2682-2685
2. G. W. Rabe, C. D. Bérubé, and G. P. A. Yap. Synthesis and X-ray Crystal Structure Determination of First Examples of Donor-Functionalized Terphenyl Lanthanide Complexes, *Inorganic Chemistry*; **2001**; 40(18); 4780-4784.
3. D. Freckmann, T. Dubé, C. D. Bérubé, S. Gambarotta, G. P. A. Yap. Cyclic Di- and Trivalent Yb Clusters Supported by Dipyrrolide Ligands, submitted.
4. M. Ganesan, C. D. Bérubé, S. Gambarotta, G. P. A. Yap. Synthesis of Samarium and Ytterbium Complexes with 2,5-Dimethylpyrrole: Alkali Cations as a determining factor in determining the Ligand Bonding Mode to Divalent Lanthanide Centres, submitted
5. C. D. Bérubé, S. Gambarotta, G. P.A. Yap. Synthesis of Pyrrole Supporting Schiff-Base Samarium Dinuclear Complexes, submitted
6. C. D. Bérubé, S. Gambarotta, G. P.A. Yap. Dinitrogen Activation by Diethyl- and Methylphenyl- Dipyrrolide Divalent Samarium Complexes, submitted

List of Abbreviations

Å	angström
Anal.	Analysis
atm	atmosphere
br	broad
°C	degrees Celsius
Calcd.	calculated
cat.	catalyst
cm⁻¹	wave number
Cp	cyclopentadienyl
δ	chemical shift
D_{calcd}	calculated density
DME	dimethylethyleneglycol
Et	ethyl
F000	electronic density
FTIR	Fourier transform infrared spectroscopy
F.W.	Formula weight
g	grams
G.o.F.	goodness of fit
h	hour
K	Kelvin
kg	kilogram
L	ligand

m	medium
M	molar
mmoles	millimoles
Me	methyl
MHz	megahertz
min	minute
mL	millilitre
mmol	millimole
NMR	nuclear magnetic resonance
ORTEP	Oak Ridge thermal ellipsoid program
Ph	phenyl
R	alkyl group (found in reaction schemes)
R	reliability factor (crystallographic tables)
s	strong
T	temperature
THF	tetrahydrofuran
THF-d₈	deuterated THF
TMEDA	N, N, N', N'-tetramethylethylenediamine
TMS	trimethylsilane
μ_{calcd}	absorption coefficient
μ_{eff}	effective magnetic moment in Bohr magnetons
V	volume
w	weak

Table of Contents

Abstract	ii
Dedication	iv
Acknowledgements	v
List of Publications	vi
List of Abbreviations	vii
Chapter I Introduction	1
I.1 Lanthanides-General Considerations	2
I.2 Cyclopentadienyl Lanthanide Complexes	5
I.3 Calix-Tetrapyrrole Lanthanide Complexes	8
I.4 Dipyrrolide Lanthanide Complexes	10
I.5 Summary of Thesis	12
References	16
Chapter II Cyclic Di- and Trivalent Yb Clusters Supported by Dipyrrolide Ligands	21
II.1 Summary	22
II.2 Introduction	22
II.3 Experimental Section	25
II.4 Results and Discussion	31
II.5 Structural Considerations	39
II.6 Conclusions	48
References	49

Chapter III	Synthesis of Samarium and Ytterbium Complexes with 2,5-Dimethylpyrrole: The Effect of the Alkali Cation on the Bonding Mode of Divalent Lanthanide Centres	52
III.1	Summary	53
III.2	Introduction	53
III.3	Experimental Section	56
III.4	Results and Discussion	62
III.5	Structural Considerations	71
III.6	Conclusions	80
	References	81
Chapter IV	Synthesis of Pyrrole Supporting Schiff-Base Samarium Dinuclear Complexes	86
IV.1	Summary	87
IV.2	Introduction	87
IV.3	Experimental Section	89
IV.4	Results and Discussion	94
IV.5	Structural Considerations	98
IV.6	Conclusions	105
	References	106
Chapter V	Dinitrogen Activation by Diethyl- and Methylphenyl-Dipyrrolide Divalent Samarium Complexes	110
V.1	Summary	111
V.2	Introduction	111
V.3	Experimental Section	113
V.4	Results and Discussion	118

V.5	Structural Considerations	122
V.6	Conclusions	131
	References	132
Chapter VI	Conclusion	135
Appendix		140

Introduction

I.1: Lanthanides-General Considerations

To follow the development of the chemistry of samarium is akin to reading the fairytale of Cinderella. Only until three decades ago, when organometallic chemistry was still enjoying a major development, was it believed that lanthanides would not offer much chemical interest. First and foremost, a very limited chemistry was expected for the lanthanides comparatively to transition metals.¹ All the lanthanide metals were seen as having similar chemical properties, and their ionic behavior made them seem as the trivalent equivalents of the alkali and alkali-earth metals.^{1,2} Given the marked stability of the lanthanides in the trivalent state, their derivatives seemed unexciting in comparison with transition metals where drastic change of chemical behavior is commonly observed within the same group of metals and where a single metal could often adopt multiple oxidation states. While limited chemical possibilities were the largest obstacle to organo-lanthanide chemistry, the added constraints brought on by the air- and moisture-sensitivity of most compounds and the NMR incompatibilities linked to the inherent paramagnetism of most lanthanides discouraged the development of lanthanide complex research.³ All these obstacles were in time overcome, and organo-lanthanide chemistry has developed into a very important field of chemical research. All the traits that originally made it undesirable when compared to transition metal were found to offer new and exciting compounds, bonding modes, and an incredible wealth of chemical reactivity.⁴

Officially, the lanthanides include the 14 elements from cerium to lutetium, although a debate has been questioning whether this list should be expanded to 15 elements and to include lanthanum, since its chemical characteristics and behavior are similar to those of the other lanthanides.⁵ Additionally, most discussion pertaining to lanthanides as a whole usually mention the elements scandium and yttrium as they also often behave in a comparable manner to the rare-earth metals. The most distinguishing trait of lanthanides as a whole is that they all display uniform properties. These similarities are linked to the fact that the lanthanides all have the possibility of utilizing the 4-f orbitals as their valence orbitals. These f-block orbitals are weakly shielded from the atomic core by the underlying $5s^25p^6$ orbitals, contracting their radii towards the closed shell.⁶ This poor shielding is at the essence of why all the lanthanides are stabilized in the trivalent state, as any change in outer-core charge of the atom greatly affects the valence orbitals. A lower charge (+2) leads to loosely held electrons that are easily abstracted, thus introducing a strong reducing power. Conversely, an increase in charge (+4) leads to strongly held electrons that are less apt to react and to a consequent strong oxidizing capacity. Since the valence orbitals do not extend very far out from the closed electron shell, they do not interact to a great extent with the ligands and electrostatic interactions become important in the determination of the structure and the stability of the complexes formed. Because these electrostatic interactions do not vary drastically from one lanthanide metal to another, the chemistry observed with a specific ligand is often reproducible with a variety of trivalent lanthanides.^{7,8}

While being the cornerstone of their uniformity, these weakly shielded f-orbitals are also linked to the few differences seen between the lanthanide elements. As the

inner-core charge augments, the change is strongly felt by the valence electrons, causing a greater than normal contraction of the atomic radii. Thus, the radius goes from 1.16 Å for La^{3+} to 0.98 Å for Lu^{3+} , observation for which the term “lanthanide contraction” was coined.⁹ This change in ionic size does lead to variations in the chemical reactivity, especially when ligands are large enough to limit coordination numbers⁷. When the oxidation of the lanthanide metals deviates from the trivalent state, the chemistry observed is far removed from what is normally obtained, but even this is linked to the f-block valence electrons. While changes to the outer-core charges destabilize the atom as previously mentioned, some lanthanides adopt the +2 and the +4 oxidation state while retaining an acceptable level of stability. This happens when an ion can attain an empty (f^0), half-filled (f^7) or filled (f^{14}) valence shell. This explains the stability of the atypical Ce^{+4} , Eu^{+2} , and Yb^{+2} ions, as they have a f^0 , a f^7 and a f^{14} valence shell, respectively. Other than these few examples, some additional lanthanides have the possibility of adopting di- or tetravalent states, but these compounds are usually difficult to prepare and highly unstable and thus often confined to the role of chemical curiosities.

Of all the available divalent lanthanides, samarium(II) produces the most spectacular reactivity. While recent results have established the availability of new and more reactive divalent lanthanides (Tm(II) , -2.35 V; Dy(II) , -2.6 V; Nd(II) , -2.75 V), these new compounds do not lend themselves readily to experimental work as they decompose through contact with many solvents and through exposure to light sources.¹⁰ Samarium enjoys a slightly increased stability compared to these (-1.56 V), while still offering enough reactivity to perform many chemical transformations. While samarium still offers opportunities in terms of novel products, the amount of research already listed

in the literature offers a strong base of knowledge that is useful, such as preparation of starting materials and predictions of chemical behavior. The only negative aspect of using Sm for experimental chemistry is the obstacles it faces with NMR analysis. Both di- and trivalent samarium are paramagnetic, with the trivalent species displaying a magnetic susceptibility of about 1.36 to 1.90 μ_B and divalent samarium of about 3.5 to 3.8 μ_B . Despite the paramagnetism of Sm(III) complexes, the NMR resonances are usually very narrow, such that the proton and the carbon resonances are observable in most cases.¹¹ For Sm(II) however, the linewidths of the NMR resonances are very broad and displaced, yielding spectra that prove difficult to analyze and are often uninformative.

The use of divalent ytterbium in conjunction with samarium can be an effective experimental tool. While both lanthanides have very similar chemical and structural properties, the ytterbium displays a much lower reactivity. Since divalent samarium has been shown to decompose certain solvents and to attack certain ligands¹², ytterbium is useful in determining the identity and the structure of certain intermediates. Ytterbium is also useful because its divalent ion is diamagnetic and it can be used to indirectly identify equivalent samarium complexes through NMR analysis.

I.2: Cyclopentadienyl Lanthanide Complexes

When the field of organo-lanthanide finally started to develop, most of the compounds were based upon the Cp systems.¹³ This *quasi*-monopoly of the chemistry was not due to a lack of available ligand systems, but it was fueled by the quality and promise of the complexes obtained. This chemistry showed that while lanthanide starting

materials were not amenable towards useful compounds such as CO, isocyanides and unsaturated hydrocarbons, Cp-complexes for these same metals opened up avenues to new and rich transformations.^{11,14} Continued efforts with this ligand system led to catalytic systems that could readily form C-H, C-C and C-halogen bonds.^{1,2b,4a,4c,4d,15} These catalytic pathways ushered the Cp-lanthanide complexes into uses for polymerization,^{16,17} hydrogenation,^{17,18} hydroboration,¹⁹ hydrosilylation²⁰ and hydroamination/cyclization²¹ of olefins.

Almost every bis-(cyclopentadienyl) lanthanide complex has already been synthesized,^{8,22} and while most of these compounds include additional ligands to supply the required bonding saturation, the divalent Cp*₂Sm complex certainly eclipses the record for producing interesting chemistry²³. This complex (Fig 1.1), which is reminiscent of ferrocene (Fig 1.2), is formed by two π -bonded pentamethylcyclopentadienyl units covering a single divalent samarium atom. While the cyclopentadienyl rings in ferrocene are at 180° to one another, in samarocene they are found much closer, forming an angle of 140.1°.

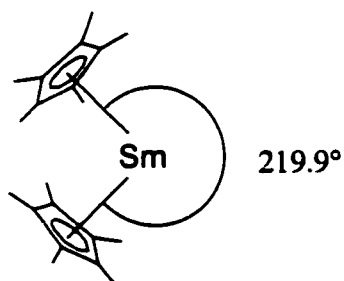


Fig 1.1

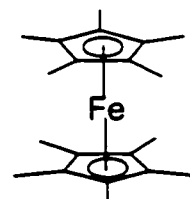


Fig 1.2

A similar structure was obtained where two additional molecules of THF were also bound to the samarium atom, but the presence of these extra atoms barely changed

the bonding angle between the ligands (136.7°). The reason for this curious bonding mode still remains unresolved. Many hypotheses have been put forth to explain the phenomenon, such as attraction between the Cp moieties as the large lanthanide center separates them, but there has been no conclusive answer that seems acceptable by all.

When the previously discussed reaction was carried out under a nitrogen atmosphere instead of under argon, an even more intriguing result was achieved. Slow crystallization of the compound from toluene gave rise to the discovery of the first dinitrogen complex of an f-element (Fig. 1.3).²⁴

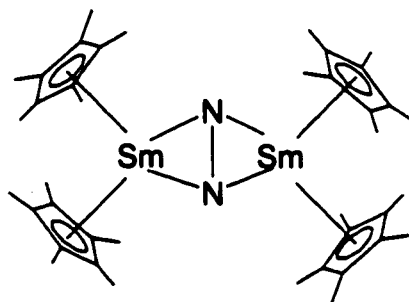


Fig 1.3

While other dinitrogen complexes had been previously observed in the literature, this complex was the first with a lanthanide and also the first to display a side-on bonding mode with the dinitrogen molecule. Analysis of the X-ray crystal structure led to the observation that the nitrogen-nitrogen bond, while coordinated by the lanthanides, was not reduced to any appreciable degree. This was indicated by the fact that the N-N bond distance was unchanged from that observed for free dinitrogen and also by the fact that the dinitrogen activation was reversible through resolubilization of the compound in toluene.

I.3: Calix-Tetrapyrrole Lanthanide Complexes

Given the caliber of the previously mentioned transformations, it is no surprise that considerable efforts have been made to develop alternative ligand systems for the chemistry of low-valent lanthanides. This line of research not only looks at duplicating the transformations made with the Cp systems but also at improving such systems. For example, a more electron deficient metal, such as one bound by an amide or an alkoxide, would lead to a more stable alkyl complex which suppresses chain termination by β -hydrogen transfer in olefin processes.²⁵ As a replacement for cyclopentadienyl ligands, pyrrole based ligands offer many promising characteristics (Fig. 1.4). The pyrrole anion has available the same π -bonding mode as Cp, which is extremely important when coordinating the large radii of the lanthanide elements. The pyrrole ring also has an additional versatility in forming σ -bonds through the nitrogen atom present in the ring. Since lanthanide metals have limited oxidation state ranges, this extra bonding mode can be very useful to form aggregates of multiple metals. This aggregation is important since it permits multiple metal centers to affect a single substrate in multi-electron transformations.²⁶

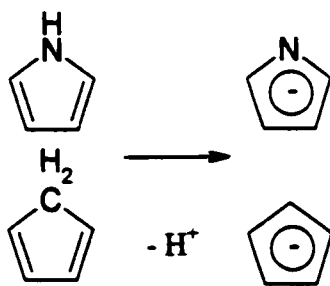


Fig 1.4

One of the first pyrrole-based ligands used on lanthanides was the calix-tetrapyrrole ligand. Use of these ligands with lanthanides led to very interesting complexes and to a rich chemistry.²⁷ One of the common patterns in this chemistry is the formation of “ate” complexes²⁸ (compounds with salt coordination), which are obtained through retention of alkali metals and solvent molecules. Many of these complexes also retain alkoxide fragments, which are formed through solvent cleavage reactions.²⁹ These salt complexes are far from useless as they can be used as starting materials that have novel chemical behaviors. Reactions starting from these “ate” complexes have led to the formation of Ln-hydrides, Ln-alkyls, and Ln-vinyl compounds and they also have the possibility of aggregating around a substrate to perform multi-metal transformations.³⁰ The reaction of the $\{\text{Sm}[\text{Et}_8\text{-calix-tetrapyrrole}][\text{Li}(\text{THF})_4]\}$ with ethylene³¹ and acetylene³² yielded both a reversible and an irreversible complex respectively, where the guest molecule was coordinated by two Sm-tetrapyrrole sub-units. Formation of the same “ate” complex under a nitrogen atmosphere lead to another aggregate, where a dinitrogen molecule was held between two samarium atoms (Fig. 1.5).³³ In this complex, the presence of

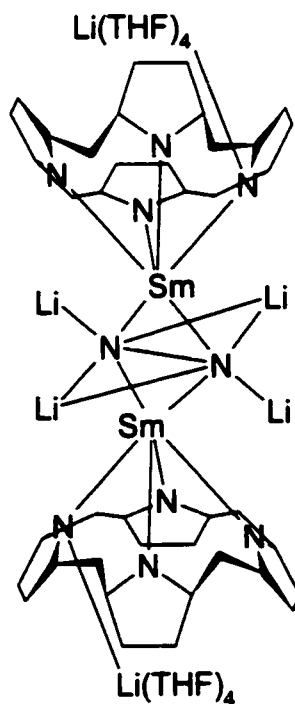


Fig 1.5

additional lithium ions permitted the four-electron reduction of the dinitrogen molecule, yielding a nitrogen-nitrogen single bond. This compound was reminiscent of previous reactions, where neodymium and praseodymium complexes of [Et₈-calix-tetrapyrrole][Na(THF)₂] formed in the presence of N₂ gave rise to two dinitrogen complexes.³⁴ In these cases, however, the dinitrogen moiety was only reduced by two electrons to form a nitrogen-nitrogen double bond. These dinitrogen compounds demonstrate that pyrrole based ligands are viable substitutes to the Cp systems, as they display certain chemical transformations that were unavailable in previously seen systems.

I.4: Dipyrrole Lanthanide Complexes

From the interesting results obtained in the reactions of calix-tetrapyrroles, it was natural that more pyrrole-based ligands were pursued for use with lanthanides. The next logical step was to assay dipyrroles, sub-units of porphyrinogens, to see if they would sustain unique structures and transformations. As hoped, the dipyrrole moieties produced very interesting chemistry with low-valent lanthanides. Losing the rigidity imposed upon the calix-tetrapyrroles, the dipyrrole compounds tend to encourage the formation of clusters³⁵. The aggregation is performed through networks of σ and π -bonds, with each pyrrole ring usually performing both. Most complexes found in the literature were obtained through the reaction of divalent samarium and diphenyl,³⁵ cyclohexyl³⁶ or methylphenyldipyrrolide³⁶ ligands (Fig. 1.6). The compounds formed are usually clusters of four to eight Sm-ligand sub-units that host one or two atoms in their interstitial space,

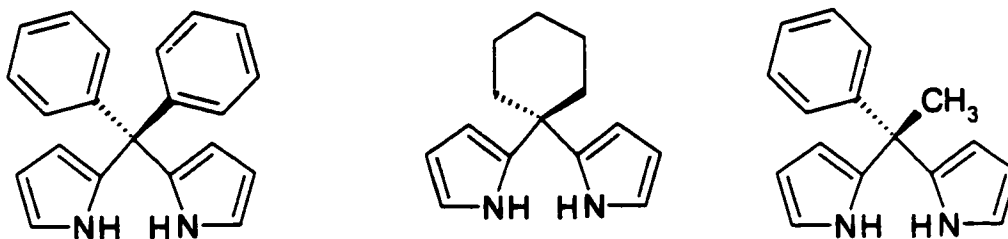


Fig 1.6

atoms that are usually halides obtained from the samarium starting materials. Solvent cleavage is less frequent than in the tetrapyrrole chemistry, and the guest molecule obtained in these cases is usually an oxygen atom instead of the alkoxo molecule observed with the porphyrinogens.³⁶ Consistent with the tetrapyrrole chemistry, the nature of the alkali cation and of the bridging substituents play an important role on the reactivity of the systems. This was observed in the reaction of $[\text{SmI}_2(\text{THF})_2]$ and the dipotassium salt of diphenyldipyrrole, which yielded a dinitrogen complex.³⁵ When one of the phenyl substituents was replaced with a methyl group the product isolated was a 5 membered cluster hosting an iodine atom³⁶. Another example is the reaction of $[\text{SmCl}_3(\text{THF})_3]$ with the di-sodium salt of cyclohexyldipyrrole followed by the reduction with metallic sodium, which yielded a second dinitrogen complex.³⁷ As with the previous dinitrogen complex, this result was not reproducible when a different alkali salt and reduction metal was used. Both of these dinitrogen complexes reduced the nitrogen-nitrogen bond by four electrons as with the Sm(II) calix-tetrapyrrole reaction (Fig. 1.7). Contrary to this earlier result, the less restricting dipyrrole ligand permits four Sm atoms to surround the dinitrogen molecule and bind it in both a side-on and end-on fashion. This is important since the presence of more reducing atoms near the dinitrogen

been shown to enhance chemical reactivity and to display electronic flexibility while polypyrrolides, more specifically, have been used to coordinate low-valent lanthanides and to promote polynuclear aggregation. Pyrrole based ligands offer great advantages in this chemistry, as they resemble the very successful Cp systems in their ability to form π -bonds with the metals while also being able to form σ -bonds through the presence of a nitrogen atom on the ring.

Both samarium and ytterbium were used in this investigation since they complement each other well in terms of reactivity and analysis. Samarium is a very strong reductant, and while it might not be the most reducing of the lanthanide series, it is much easier to synthesize, manipulate and store than other, more reactive species. Divalent samarium is by far the most developed system of low-valent lanthanides and it has been shown reactive enough to interact with the highly inert N_2 molecule. Using the Cp* ligand system, a reversible dinitrogen complex was obtained, and with both di- and tetrapyrrolide systems an irreversible four electron reduction of N_2 was achieved. Divalent ytterbium is very useful in conjunction with Sm(II), as it offers insight into the intermediate species produced transiently by the latter. Yb(II) is also diamagnetic, and as such it is very useful as an analytical tool compared to samarium (II) as the latter produces fairly uninformative NMR spectra because of its paramagnetism.

In order to complement the previously published reactions between samarium and diphenyldipyrrolide, we proceeded to investigate the reaction of divalent ytterbium with the same ligand system. This reaction proved to be fairly complex, yielding three different compounds. The major compound was discovered to be an octameric macrocycle reminiscent of the dinitrogen precursor obtained for samarium under an

argon atmosphere. This product validates the previous results as to the nature of the dinitrogen intermediate species. The reaction also yielded minor products discovered to be a divalent ytterbium tetrameric oxo-species and a trivalent monomeric species. This second compound was reproduced through a trivalent ytterbium starting material but the tetrameric complex proved harder to synthesize through alternate methods. Using an analogous dipyrrolide ligand, a similar compound was obtained where the same basic structure was duplicated except that it is a mixed-valent species.

We next delve into the chemistry of monopyrrolides as ligands for low-valent lanthanides. We look at different salts of dimethylpyrrole, which is more stable than the simple pyrrole moiety, and we pursue the reactions with divalent samarium and ytterbium. With this ligand system, we rely on the σ and the π interaction of each ring to form polynuclear species and we see what happens when no bridging substituents are present to influence structural configuration. We observe that the monopyrrole complexes are not greatly influenced by the choice of halide used in the lanthanide starting materials but that the choice of alkali metal used to form the ligand salt has a direct influence on the bonding experienced by the samarium or ytterbium metal centers.

The next investigation uses a modified salen-type ligand to further study the chemistry of dipyrrolides. Instead of supporting two alkoxide moieties, we use a ligand that has two pyrrole rings available for coordination. Changing the bridging substituents between the imino nitrogens and alkylating the imino carbon leads to different results when the ligands react with $[\text{Sm}(\text{N}(\text{TMS}_2)_2)(\text{THF})_2]$. Using phenyl-based substituents that have an imino C-H bond, we obtain two different trivalent samarium species, one of which is achieved through a radical induced ligand dimerization. Changing the bridging

substituent from phenylene to ethylene and using an imino-alkyl yielded a divalent samarium complex where no ligand dimerization was observed. Using this Schiff-base as a bridging substituent between pyrrole fragments seems to stabilize the divalent samarium centers, compared to other dipyrrolides, since no solvent deoxygenation or dinitrogen activation is observed.

Previous investigations into the production of dinitrogen complexes with dipyrrolide ligands, while proving successful, had also yielded many macrocyclic compounds where the coordinated atom was a halide from the lanthanide starting material. Using a halide-free divalent samarium starting material, $[\text{Sm}(\text{N}(\text{TMS}_2)_2)(\text{THF})_2]$, we were able to synthesize two new dipyrrolide dinitrogen complexes, one of which had proven unobtainable through the originally used methods. The precursor to one of these dinitrogen complexes was also obtained through reactions under an argon atmosphere. During this investigation into new dinitrogen complexes, an unintentional reaction yielded the first example of a tripyrrolide complex. This compound, while obtained through happenstance, does give insight into the bonding mode adopted by these exciting new ligands.

References:

- 1 Evans, W.J., *Polyhedron*, **1987**, 6(5), 803
- 2 a) Marks, T.J., Fragala, I.L., Reidel, D., *Fundamental and Technological Aspects of Organo-f-Element Chemistrh*: Dordrecht, **1985**
b) Schumann, H., *Angew. Chem. Int. Ed. Engl.*, **1984**, 23, 474
c) Evans, W.J., *J. Organomet. Chem.*, **1983**, 250, 817
- 3 a) Van Vleck, J.H. *Theory of Electric and Magnetic Susceptibilities*, Oxford. Univ.Press, New York
b) Siddall III, T.H., Casey, A.T., Mitra, S., in Bodreaux, E.A. and Mulay, L.N. (Eds.). *Theory and Applications of Molecular Paramagnetism*. Wiley, New York (1976) Ch. 4, 5
- 4 a) Schumann, H., Meese-Marktscheffel, J.A., Esser, L. *Chem. Rev.*, **1995**, 95, 865;
b) Edelmann, F.T., in *Comprehensive Organometallic Chemistry II*; Abel, E.W., Stone, R.G.S., Wilkinson, G.; Pergamon Press: Oxford, U.K., 1995; Vol. 4. Chapter 2 and references therein.;
c) Schaverien, C.J., *Adv. Organomet. Chem.*, **1994**, 36, 283 and references therein.;
d) Evans, W.J., *Adv. Organomet. Chem.*, **1985**, 24, 31 and references therein.;

- e) Kagan, H.B.; Namy, J.L., in *Handbook on the Physics and Chemistry of Rare Earths*; Gschneider, K.A., Eyring, L.; Elsevier: Amsterdam, 1984; Chapter 50;
- f) Marks, T.J., Ernst, R.D., in *Comprehensive Organometallic Chemistry*, Wilkinson, G., Stone, F.G.S., Abel, E.W.; Pergamon Press: Oxford, U.K., 1982; Chapter 21 and references therein.
- 5 Jensen, W.B., *J. Chem. Edu.*, **1982**, 59, 634
- 6 Freeman, A.J., Watson, R.E., *Phys.Rev.*, **1962**, 127, 2058
- 7 Freeman, A.J., Watson, R.E., *Phys. Rev.*, **1976**, 9,217
- 8 a) Fischer, E.O., Fischer, H., *J. Organomet. Chem.*, **1965**, 3, 181
b) Manastyrskij, S., Dubeck, M., *Inorg. Chem.*, **1964**, 3, 1647
- 9 a) Huheey, J.E., *Inorganic Chemistry; Principles of Structure and Reactivity. 2nd edition*, Harper and Row: New York, **1978**, 681
b) Shannon, R.D., *Acta. Cryst.*, **1976**, A32, 751
- 10 a) Bochkarev, M.N., Fedushkin, I.L., Fagin, A.A., Petrovskaya, T.V., Ziller, J.W., Broomhall-Dillard, R.N.R., *Angew. Chem. Int. Ed. Engl.*, **1997**,36, No. 1/2
b) Bochkarev, M.N., Fagin, A.A., *Chem. Eur. J.*, **1999**, 5, no.10
- 11 W.J. Evans, W.J., Bloom, I., Hunter, W.E., Atwood, J.L., *J. Am. Chem. Soc.*, **1981**, 103, 6507
- 12 for example
a) Guan, J., Dube, T., Gambarotta, S., Yap, G.P.A., *Organometallics*, **2000**, 19, 4820-4827;
b) Dube, T., Gambarotta, S., Yap, G.P.A., *Organometallics*, **2000**, 19, 817-823;

- c) Dube, T., Conoci, S., Gambarotta, S., Yap, G.P.A., *Organometallics*, **2000**, 19, 1182-1185;
- 13 a) Wilkinson, G., Birmingham, J.M., *J. Am. Chem. Soc.*, **1954**, 76, 6210
b) Maginn, R.E., Manastyrskyj, S., Dubeck, M., *J. Am. Chem. Soc.*, **1963**, 85, 672
- 14 a) Evans, W.J., Grate, J.W., Hughes, L.A., Zhang, H., Atwood, J.L., *J. Am. Chem. Soc.*, **1985**, 107, 3728
b) W.J. Evans, W.J., Bloom, I., Hunter, W.E., Atwood, J.L., *J. Am. Chem. Soc.*, **1981**, 103, 1401
c) Evans, W.J., Hughes, L.A., Drummond, D.K., Zhang, H., Atwood, J.L., *J. Am. Chem. Soc.*, **1986**, 108, 1722
- 15 Kohn, R.D., Kociok-Kohn, G., Schumann, H., in *Encyclopedia of Inorganic Chemistry*: Wiley, New York, **1994**
- 16 a) Thompson, M.E., Baxter, S.M., Bulls, A.R., Burger, B.J., Nolcan, M.C., Santarsiero, B.D., Schafer, W.P., Bercaw, J.E., *J. Am. Chem. Soc.*, **1987**, 109, 203
b) Den Haan, K.H., Wielstra, Y., Teuben, J.H., *Organometallics*, **1987**, 6, 2053
c) Heeres, H.J., Renkema, J., Boij, M., Meetsma, A., Teuben, J.H., *Organometallics*, **1988**, 7, 2495
d) Evans, W.J., Chamberlain, L.R., Ulibarri, T.A., Ziller, J.W., *J. Am. Chem. Soc.*, **1988**, 110, 6423
e) Watson, P.L., *J. Chem. Soc. Chem. Commun.*, **1983**, 276
f) Watson, P.L., *J. Am. Chem. Soc.*, **1983**, 105, 6491
g) Burger, B.J., Thompson, M.E., Cotter, W.D., Bercaw, J.E., *J. Am. Chem. Soc.*, **1990**, 112, 1566

- 17 Jeske, G., Lauke, H., Mauermann, H., Schumann, H., Marks, T.J., *J. Am. Chem. Soc.*, **1985**, 107, 8111
- 18 Molander, G.A., Hoberg, J.O., *J. Org. Chem.*, **1992**, 57, 3266
- 19 Harrison, K.N., Marks, T.J., *J. Am. Chem. Soc.*, **1992**, 114, 9220
- 20 Sakakura, T., Lautenschlager, H.-J., Tanaka, M., *J. Chem. Soc. Chem. Commun.*, **1991**, 40-42
- 21 Gagne, M.R., Stern, C.L., Marks, T.J., *J. Am. Chem. Soc.*, **1992**, 114, 275
- 22 Birmingham, J.M., Wilkinson, G., *J. Am. Chem. Soc.*, **1956**, 78, 42
- 23 a) Evans, W.J., Hughes, L.A., Hanusa, T.P., *Organometallics*, **1986**, 5, 1285
b) Tilley, T.D., Anderson, R.A., Spencer, B., Ruben, H., Zalkin, A., Templeton, C., *Inorg. Chem.*, **1980**, 19, 2999
- 24 Evans, W.J., Ulibarri, T.A., Ziller, J.W., *J. Am. Chem. Soc.*, **1988**, 110, 6877
- 25 for example
a) Allen, A.D., Senoff, C.V., *J. Chem. Soc. Chem. Commun.*, **1965**, 621
b) Gynane, M.J.S., Jeffery, J., Lappert, M.F., *J. Chem. Soc. Chem. Commun.* **1978**, 37
- 26 a) Bruno, J.W., Stecher, H.A., Morss, L.R., Sonnenberg, D.C., Marks, T.J., *J. Am. Chem. Soc.*, **1986**, 108, 7275
b) Labinger, J.A., Bercaw, J.E., *Organometallics*, **1988**, 7, 926
- 27 a) Floriani, C., *Chem. Commun.*, **1996**, 1257
b) Floriani, C., *Pure Appl. Chem.*, **1996**, 68, 1
- 28 a) Evans, W.J., Anwander, R., Doendens, R.J., Ziller, J.W., *Angew. Chem.*, **1994**, 106, 1725 ; *Angew. Chem. Intl. Ed.* **1994**, 33, 1641.

- 29 for example Jubb, J., Gambarotta, S., Duchateau, R., Teuben, J.H., *J. Chem. Soc. Chem. Commun.*, **1994**, 2641
- 30 Dube, T., S. Gambarotta, Yap, G.P.A., *Organometallics*, **2000**, 19, 121
- 31 Dube, T., S. Gambarotta, Yap, G.P.A., *Angw. Chem. Intl. Ed. Engl.*, **1999**, 38, 1432
- 32 Dube, T., S. Gambarotta, Yap, G.P.A., *Chem. Eur. J.*, **2001**, 7(2), 374
- 33 Jubb, J., Gambarotta, S., *J. Am. Chem. Soc.* **1994**, 117, 4477
- 34 Campazzi, E., Solari, E. Floriani, C., Scopelliti, R., *J. Chem. Soc. Chem. Commun.*, **1998**, 2603
- 35 for example: Dube, T., Conoci, S., Gambarotta, S., Yap, G.P.A., Vaspollo, G., *Angew. Chem. Int. Ed.*, **1999**, 38, 3657
- 36 for example: Dube, T., Conoci, S., Gambarotta, S., Yap, G.P.A., *Organometallics*, **2000**, 19, 1182
- 37 Dube, T., Ganesan, M., Conoci, S., Gambarotta, S., Yap, G.P.A., *Organometallics*, **2000**, 19, 3716
- 38 Evans, W.J., Drummond, D.K., Zhang, H., Atwood, J.L., *Inorg. Chem.*, **1988**, 27, 575
- 39 Dube, T., Gambarotta, S., Yap, G.P.A., *Organometallics*, **2000**, 19, 115-117;
- 40 Ganesan, M., Gambarotta, S., Yap G.P.A., *Angew. Chem. Int. Ed.*, **2001**, 40, 766-769

Chapter II:

Cyclic Di- and Trivalent Yb Clusters Supported by Dipyrrolide Ligands

Summary

22

Introduction

22

Experimental Section

25

Results and Discussion

31

Structural Considerations

39

Conclusions

48

References

49

Balsamum	MB
Balsamum Virginicum	V
Bene	bn
Borax	W
Calamare	C
Calx	UET
Calx viva	UET
Calx aurum	UET
Caryophyllus	UET
Camphora	UET
Cera	UET
Christallum	UET
Cinis	UET
Cinroscolyellus	UET
Cinroscor	UET
Coagulum	UET
Cochon	UET
Coccus	UET
Croci	UET
Crucibulum	UET
Cucurbitum	UET
Dies	UET
Digerere	UET
Distillare	UET
Distillatum	UET
Effluere	UET
Emulsio	UET
Ferens	UET
Flegma	UET
Flores	UET
Gumma	UET
Hora	UET
Jgms	UET
Jgnis rora	UET
Lignis	UET
Lutae	UET
Lutum	UET
Magnas	UET
Marchia	UET
Materia	UET
Motivum	UET

Cyclic Di- and Trivalent Yb Clusters Supported by Dipyrrolide Ligands

II.1: Summary

The reaction of $\text{YbI}_2(\text{THF})_2$ with diphenylmethyldipyrrolide leads to a complex reaction from which is obtained an octameric divalent Yb macrocycle (Diphenyldipyrromethanedi-yl-Yb)₈ 2.1 as a major product, but from which a tetrameric cyclic Yb(II)-oxo complex $[(\text{diphenyldipyrrolyl-methane-di-yl})\text{Yb}]_4[(\text{K}_2)(\text{THF})_6](\mu\text{-O})_2(\text{THF})$ 2.2•2(THF) and a monomeric Yb(III) complex, $\text{Yb}(\text{diphenyldipyrrolylmethane-di-yl})_3(\text{K}_3\text{THF}_3)$ 2.3 were also isolated as minor products.

II.2: Introduction

The unique versatility of the cyclopentadienyl-based ligand system has been a significant factor in contributing to the spectacular development of lanthanide chemistry in the early eighties.¹ The most striking example of the uniqueness of cyclopentadienyl anions as ligand systems is provided by their ability to stabilize low-valent states for a few of the lanthanide metals. Among the few lanthanides for which the oxidation state +2 has been documented (Sm, Yb, Eu, and Tm), samarium certainly displays the most remarkable reactivity.² In spite of acting as a one-electron reductant, divalent samarium displays a unique ability to perform multi-electron reductions through the cooperative attack of several metals on the same substrate. Deoxygenation/oligomerization of carbon monoxide,³ dimerization of a large variety of substrates,⁴ dinitrogen reversible fixation,⁵ and oxidative addition reactions are only a few of a large variety of attractive and diversified chemical reactions reported for samarocene derivatives.⁶

Given the calibre of the previously mentioned transformations, it is no surprise that considerable efforts have been made to develop the chemistry of low-valent lanthanides with alternative ligand systems. Divalent lanthanide alkoxides,⁷ phosphide⁸ and amide⁹ have been prepared and characterized, yielding interesting mono- and polynuclear structures. None of these systems can, however, duplicate the enormous reactivity demonstrated by the Cp-based ligand systems. The Cp derivatives remain unsurpassed in terms of the richness and importance of their chemical transformations.

A few years ago, efforts in the preparation of divalent complexes of samarium were made in our laboratory by using a calix-tetrapyrrole tetranion. Attempts to prepare a simple Sm(II)(calix-tetrapyrrole)Sm(II)Li₂ species resulted in the formation of a dinuclear complex where a dinitrogen unit was encapsulated in the center of a Sm₂Li₄ octahedron.¹⁰ The four-electron reduction undergone by the dinitrogen moiety during the formation of this dinuclear species could not be easily explained. Nevertheless, the isolation of this complex reiterates that polypyrrolide anions may in fact support an even higher level of reactivity at divalent samarium. Incidentally, a structural analysis of this and many other recently discovered complexes of lanthanide of this particular ligand system have the common feature that two of the four pyrrolyl rings bond to the lanthanide in a π fashion thus conferring on the metal with a samarocene-type of structure. With these considerations in mind, the chemistry of divalent samarium supported by dipyrrolide dianions was the most obvious target for our continuing synthetic efforts.

Recently, we have been investigating the chemistry of low-valent samarium supported by dipyrrolide dianions¹¹ which bear some electronic and steric resemblance to the *ansa*-metallocene-type ligands. However, the presence of a hard nitrogen donor atom in the five-membered rings renders these anions more versatile for assembling polynuclear structures via formation of additional M-N σ -bonds. Given that a low-valent lanthanide atom

may perform only one-electron redox reactions, the presence of two or more metal centers in the same molecular framework may be desirable for performing molecular activation processes through cooperative attack on the same substrate when availability of several electrons is required. Reactivity studies carried out with this particular ligand system have so far revealed a promising feature in the chemistry of divalent samarium, having shown the ability of this ligand to assemble tetranuclear clusters able to carry out four-electron reduction of dinitrogen. Thus, in an attempt to better understand the chemistry of this particular ligand system and its ability to both assemble polynuclear structures and to tune the redox properties of low-valent lanthanide complexes, the less reducing and NMR accessible Yb^{2+} ion was chosen for this study. We describe herein the formation of a novel ytterbium octameric cluster formed as part of a complex reaction.

II.3: Experimental Section

All operations were performed under an inert atmosphere of a nitrogen-filled dry box or by using Schlenk-type glassware in combination with a nitrogen-vacuum line.¹² Solvents were dried by passing through a column of Al_2O_3 under an inert atmosphere prior to use, degassed *in vacuo* and transferred and stored under inert atmosphere. $\text{YbI}_2(\text{THF})_2$ ¹³ and $\text{YbCl}_3(\text{THF})_3$ ¹⁴ were prepared according to literature procedures. The NaH and KH suspensions in mineral oil (Aldrich) were washed with hexane, dried and stored under nitrogen in sealed ampules. THF- d_8 was dried over Na/K alloy, vacuum transferred into ampules, and stored under nitrogen prior to use. NMR spectra were recorded on a Varian Gemini 200 and on a Bruker AMX-500 spectrometer using vacuum sealed NMR tubes prepared inside a dry box. Infrared spectra were recorded on a Mattson 3000 FTIR instrument from Nujol mulls prepared inside a dry box. Samples for magnetic susceptibility measurements were carried out at room temperature using a Gouy balance (Johnson Matthey) and corrected for underlying diamagnetism. Elemental analyses were carried out using a Perkin-Elmer Series II CHN/O 2400 analyser.

Diphenyldipyrrolylmethane

A solution of benzophenone, (27.0 g, 0.15 mol) and methanesulfonic acid (0.5 mL) in 99% EtOH was stirred and heated at 60-70°C until complete dissolution. Neat pyrrole (10 mL, 0.14 mol) was added over a period of 30 minutes and the mixture was stirred at 60-70°C for 4 hours, upon which the colour of the solution changed from dark red to dark brown. The mixture was diluted with 99% EtOH (100 mL) and allowed to crystallise at 50°C. A red solid was obtained, which was filtered and washed with portions of warm 99% EtOH (100 mL, 50°C) until complete discoloration. The compound was dried *in vacuo* yielding analytically pure diphenylmethyldipyrrole (5.8 g, 19.5 mmol, 13 %).

M.p: 258°C

M.S.- E.I. m/e⁺ : 298.

IR (KBr, Nujol mull, cm⁻¹) v: 3412(s), 3367(s), 2954(s), 2922(vs), 2854(s), 1660(w), 1596(m), 1544(m), 1454(vs), 1409(m), 1377(vs), 1255(w), 1229(w), 1184(m), 1080(s), 1029(s), 887(m), 797(s), 733(vs), 701(vs), 624(m), 514(s).

¹H NMR (CDCl₃, 200 MHz, 25°C) δ: 7.92 (broad s, NH, 2H), 7.25 (m, CH-benzene, 6H), 7.10 (m, CH-benzene, 4H), 6.74 (m, CH-pyrrole, 2H), 6.17 (pseudo-quadruplet, CH-pyrrole, 2H), 5.93 (m, CH-pyrrole, 2H).

¹³C NMR (CDCl₃, 50.29 MHz, 25°C) δ: 128.8 (CH-benzene), 128.5 (CH-benzene), 127.4 (CH-benzene), 117.1 (CH-pyrrole), 110.2 (CH-pyrrole), 108.6 (CH-pyrrole).

El. Anal. Calcd (found) for C₂₁H₁₈N₂: C 84.53 (84.44), H 6.08 (5.99), N 9.39 (9.31).

1,1'-dipyrrolylcyclohexane

A 250ml flask was fitted with a magnetic stirrer and a dropping funnel and placed in an ice bath. Neat pyrrole (25 mL, 0.36 mol) was added to the flask. The cold mixture was treated with cyclohexanone (20 mL, 0.192 mol) and methanesulfonic acid (0.4 mL) in 99% EtOH (20 mL) dropwise over a period of five minutes. The resulting green mixture was allowed to react overnight and cooled to -35°C for two days. Colourless crystals of analytically pure meso-cyclohexyldipyrrolylmethane were obtained (9.23 g, 43.1 mmol, 45%).

M.S.- E.I. m/e⁺ : 214.

IR (KBr, Nujol mull cm⁻¹) v: 3479 (m), 3398 (m), 3303 (m), 2924 (s), 2854 (s), 1562 (m), 1450 (s), 1411 (m), 1377 (m), 1288 (m), 1178 (m), 1047 (m), 766 (m), 704 (m).

^1H NMR (CDCl_3 , 200 MHz, 25°C) δ : 7.66 (broad s, NH, 2H), 6.60 (m, CH-pyrrole, 2H), 6.14 (quadruplet, CH-pyrrole, 4H), 2.07 (m, CH_2 -cyclohexyl, 4H), 1.55 (m, CH_2 -cyclohexyl, 6H).

^{13}C NMR (CDCl_3 , 50.29 MHz, 25°C) δ : 130.4 (CH-pyrrole), 117.3 (CH-pyrrole), 108.5 (CH-pyrrole), 104.9 (CH-pyrrole), 40.5 (CH_2 -cyclohexyl), 37.9 (CH_2 -cyclohexyl), 28.6 (CH_2 -cyclohexyl), 23.4 (CH_2 -cyclohexyl).

El. Anal. Calcd (found) for $\text{C}_{14}\text{H}_{18}\text{N}_2$: C 78.46 (78.41), H 8.47 (8.44), N 13.07 (13.00)

Reaction of $\text{YbI}_2(\text{THF})_2$ with diphenyldipyrrolylmethane. Isolation of a) $(\text{Diphenyldipyrromethanedi-yl-Yb})_8$ (2.1), b) $[(\text{diphenyldipyrrolyl-methane-di-yl})\text{Yb}]_4[(\text{K}_2)(\text{THF})_6](\mu\text{-O})\cdot 2(\text{THF})$ (2.2)·2(THF) and c) $\text{Yb}(\text{diphenyldipyrrolyl-methane-di-yl})_3(\text{K}_3\text{THF}_3)$ (2.3)

Solid diphenyldipyrrolylmethane (1.0 g, 3.4 mmol) was added to a stirred suspension of KH (0.25 g, 6.7 mmol) in THF (100 mL). A vigorous reaction took place and solid $\text{YbI}_2(\text{THF})_2$ (1.92 g, 3.36 mmol) was added to the resulting clear solution. The colour changed immediately to dark red. The 3 products were isolated in the following manner:

a) After stirring overnight, the reaction mixture was centrifuged, to eliminate a small amount of greenish material, concentrated to small volume (20 mL) and layered with hexane (20 mL). Standing at room temperature for four days produced dark red diamagnetic crystals of **2.1** (0.31 g, 0.08 mmol, 19 % yield).

IR (KBr, Nujol mull cm^{-1}): 3064 (m), 2848 (s), 1598 (m), 1492 (s), 1465 (vs), 1416 (m), 1378 (s), 1260 (w), 1228 (w), 1183 (w), 1152 (s), 1080 (m), 1039 (s), 978 (m), 923 (w), 895 (m), 852 (m), 799 (w), 762 (vs), 743 (vs), 701 (vs), 657 (m), 636 (s).

^1H NMR (THF, 500 MHz, 25°C) δ : 7.24(m, CH-benzene, 6H), 7.13(m, CH-benzene, 4H), 6.09(s, CH-pyrrole, 2H), 5.23(s, CH-pyrrole, 2H), 4.99(s, CH-pyrrole, 2H).

^{13}C NMR (THF, 125.8 MHz, 25°C) δ : 130.4(CH-benzene), 128.0(CH-benzene), 126.9(CH-benzene), 118.4(CH-pyrrole), 110.3(CH-pyrrole), 107.3(CH-pyrrole)

El. Anal. Calcd (Found) for $\text{Yb}_8\text{N}_{16}\text{C}_{168}\text{H}_{128}$: C 53.73 (53.31), H 3.44 (4.10), N 5.97 (5.26).

b) After 7 days of continual stirring, the solution was centrifuged, concentrated (40 mL) and layered with hexanes (30 mL). After a few days colourless and green crystals formed over a red powder. After manual separation of the crystals, several extractions with THF solubilized the red powder leaving the emerald green crystals of **2.2** behind. (0.06g, 0.03mmol, 5 % yield). The red solutions were concentrated to small volume (20 mL) and layered with hexane (20 mL), upon which red crystals of **2.1** separated.

IR (Nujol mull cm^{-1}): 2923(vs), 1470(vs), 1360(vs), 1261(s), 1228(w), 1151(s), 1091(m), 1079(m), 1037(s), 894(w), 850(m), 800(s), 761(s), 742(s), 721(m), 700(s)

El. Anal. Calcd (found) for $\text{C}_{92}\text{H}_{80}\text{N}_8\text{O}_3\text{Yb}_4$: C 54.22 (54.19), H 3.96 (3.90), N 5.50 (5.47).

The compound was diamagnetic but solubility was too low to obtain meaningful NMR data

c) Stirring proceeded over 7 days and the solution was centrifuged, concentrated (40 mL) and layered with hexane (30 mL). Within a few days, a small number of large colourless crystals of **2.3** formed next to green crystals and a red powder. In the dry box, the colourless crystals were separated from the green and red compounds.

IR (Nujol mull cm^{-1}): 2923(vs), 1590(w), 1464(vs), 1414(m), 1378(vs), 1312(w), 1281(m), 1260(w), 1242(w), 1179(w), 1141(m), 1096(w), 1075(w), 1042(s), 968(s), 894(m), 872(w), 849(w), 739(vs), 728(s), 713(s), 702(s), 658(m), 638(m), 609(w).

$\mu_{\text{eff}} = 4.34 \mu_{\text{B}}$

Preparation of (1,1'-dipyrrolylcyclohexane-di-yl-Yb)₄(μ -O)(THF)₂ (2.4)**Method A :**

The addition of KH (0.2 g, 5.2 mmol) to a THF solution (100 mL) of 1,1'-dipyrrolylcyclohexane (0.7g, 2.6 mmol) resulted in a vigorous reaction. After 1 hour, YbCl₃(THF)₃ (1.4 g, 2.7 mmol) was added to the slightly cloudy solution leading to a colour change to beige. Stirring was continued overnight at room temperature followed by addition of K-metal (0.14 g, 3.6 mmol). Within 4 days, the color of the reaction mixture changed to dark red. The solution was centrifuged, concentrated to small volume (30 mL) and layered with ether (30 mL). Upon standing one day at room temperature dark red blocks of 2.4 formed (0.06 g, 0.04 mmol, 6 % yield).

Method B:

A similar procedure as above was followed but using NaH (0.24 g, 10 mmol) and 1,1'-dipyrrolylcyclohexane (1.1g, 5.0 mmol) in 100 mL THF. Treatment with YbCl₃(THF)₃ (2.4 g, 4.8 mmol), followed by addition of Na-metal (0.2 g, 7.4 mmol) under the usual reaction conditions resulted in the same colour changes. The solution was centrifuged and concentrated to 15 mL. Layering with ether (15 mL) and standing at room temperature for 3 days produced dark red crystals of 2.4 (0.2 g, 0.09 mmol, 2% yield).

IR (KBr, Nujol mull cm⁻¹): 3367(w), 2917(vs), 2363(m), 1560(w), 1542(w), 1461 (vs), 1377(vs), 1302(m), 1277(m), 1264(m), 1236(w), 1195(w), 1159(w), 1145(m), 1126(m), 1100(m), 1088(m), 1033(s), 960(m), 903(m), 873(m), 830(w), 789(s), 743(s), 727(s), 670(w), 630(m).

El. Anal. Calcd (Found) for Yb₄C₆₄H₈₀N₈O₃Yb₄: C 45.18(44.50), H 4.74(4.84), N 6.59(6.37).

$\mu_{\text{eff}} = 6.63 \mu_{\text{B}}$

Synthesis of Yb(diphenyldipyrrolylmethane-di-yl)₃ (2.3)

A stirred suspension of KH (0.5 g, 11.7 mmol) in THF (100 mL) was added with diphenyldipyrrolylmethane (1.8 g, 5.9 mmol) resulting in a vigorous reaction. After 30 min., the addition of YbCl₃(THF)₃ (1.0 g, 2 mmol) turned the colour grey-beige. The reaction mixture was stirred overnight, centrifuged, concentrated to small volume (30 mL) and layered with hexane (30 mL). Colourless blocks of 2.3 separated upon standing 3 days at room temperature (0.41 g, 0.3 mmol, 15% yield).

Preparation of [(diphenyldipyrrolylmethane-di-yl)₈Yb₈(μ-O)(μ-I)][Li(THF)₄]₂THF (2.5)

A solution of diphenylmethyldipyrrolide (1.81 g, 6.1 mmol) in THF (100 mL) was treated at 0°C with MeLi (1.4 M solution in diethyl ether, 8.5 mL). Stirring proceeded as the solution was warmed to room temperature over a 15 minute period. Subsequent addition of YbI₂(THF)₂ (3.46 g, 6.1 mmol) produced a fast reaction with colour change to deep red. After stirring for 20 min. red solid began to separate out. Standing at room temperature for 24 hours resulted in the accumulation of bright red 2.5 (1.57 g, 40% yield)

I.R. (Nujol mull, cm⁻¹)ν: 3080(w), 3053(w), 2729(w), 2667(w), 1597(w), 1491(m), 1464(s).
1417(m), 1377(s), 1261(w), 1232(w), 1155(s), 1078(w), 1036(vs), 980(w), 926(w), 881(w).
850(w), 800(w), 760(vs), 742(vs), 700(vs), 660(m), 638(m).

μ_{eff}: 6.73 BM.

II.4: Results and Discussion

In previous reactions,¹⁵ the formation of divalent Yb complexes of dipyrrolyl dianions afforded remarkably different compounds depending on the choice of the alkali counter-cation and the reaction pathway. While the reaction of the lithium derivatives with $\text{YbCl}_3(\text{THF})_3$ followed by reduction afforded an octameric $(\{[\text{Ph}_2\text{C}(\text{C}_4\text{H}_3\text{N})_2]\text{Yb}\}_8(\mu\text{-Cl})_4\{\text{Li}(\text{THF})_4\})_2$ species containing four bridging chlorine anions in the center and two THF-solvated lithium cations in the lattice, the reaction of the sodium salt with $\text{YbI}_2(\text{THF})_2$ afforded a monomeric anionic metallate $\{[\text{Ph}_2\text{C}(\text{C}_4\text{H}_3\text{N})_2]\text{Na}(\text{THF})_2\}_2\text{Yb}$. This remarkable diversity prompted us to investigate similar reaction by employing the potassium salt and the lithium salts of the same ligand system.

The room temperature reaction of $\text{YbI}_2(\text{THF})_2$ with the dipotassium salt of diphenyldipyrrolylmethane in THF formed a dark red, air-sensitive solution from which dark red blocks of the diamagnetic (diphenyldipyrromethane-di-yl-Yb)₈ (**2.1**) were obtained as the major component of a crystalline mixture. The NMR spectrum was not particularly informative, simply displaying the characteristic resonances of the pyrrolyl and phenyl moieties. The solid state crystal structure revealed an octameric macrocyclic structure (Figure 2.1). The structure of **2.1** consists of a symmetric macrocycle, composed of eight $[\text{Ph}_2\text{C}(\text{C}_4\text{H}_3\text{N})_2\text{Yb}]$ units arranged in a flat ring with a large interstitial space. The complex is reminiscent of the Sm(II) octamer reported with the same ligand under an argon atmosphere.¹⁶ Each diphenyldipyrrolyl ligand adopts the same bridging bonding mode already observed in similar samarium-dipyrrolyl clusters, with each pyrrolyl ring being π -bonded to one Yb [$\text{Yb}(1)\text{-N}(2) = 2.639(14)\text{\AA}$], [$\text{Yb}(1)\text{-C}(5) = 2.737(17)\text{\AA}$], [$\text{Yb}(1)\text{-C}(6) = 2.785(17)\text{\AA}$], [$\text{Yb}(1)\text{-C}(7) = 2.735(16)\text{\AA}$], [$\text{Yb}(1)\text{-C}(8) = 2.637(17)\text{\AA}$]. The nitrogen atom of each pyrrolyl ring is also σ -bonded to the second Yb atom [$\text{Yb}(2)\text{-N}(2) = 2.451(15)\text{\AA}$] which in turn is π -bonded to the second pyrrolyl ring of the same ligand. Each ytterbium is also π -

bonded to a second pyrrolyl ring of another ligand and thus acts as a bridging link to assemble the macrocyclic structure. As a result, the coordination geometry around each ytterbium is bent ytterbocene-like and is determined by two π -bonded rings from two different ligands and two σ -bonded N atoms [$\text{N}(1)\text{-Yb}(1)\text{-N}(3) = 117.5(5)^\circ$] from the other two rings of the same pair of ligands. The macrocycle is rather symmetric, in the sense that the eight Yb atoms define a nearly ideal circumference (Figure 2.2).

The formation of **2.1** is a straightforward metathetic process where two iodide anions have been replaced by the dipyrrolyl dianionic ligand. The large macrocyclic structure is likely to be the result of geometry optimization as required by the particular bridging bonding mode almost always adopted by this class of ligands. The reaction is in principle a simple one, but the presence of two additional products in the reaction mixture indicates a more complex behavior. The first compound is a green diamagnetic solid that was obtained as a minor product in the reaction. Elemental analysis, magnetic moment and X-ray crystallography (Figure 2.3) permitted the characterization of compound **2.2**. The structure is formed by four $\{[\text{Ph}(\text{C}_4\text{H}_3\text{N})_2]\text{Yb}\}$ units forming a tetrametallic cavity. This cavity is occupied by an oxygen atom [$\text{O}(1)\text{-Yb}(1)=2.340(4)\text{\AA}$], [$\text{O}(1)\text{-Yb}(2)=2.390(4)\text{\AA}$] that forms a 5 atom plane with the four metal atoms [$\text{Yb}(1)\text{-O}(1)\text{-Yb}(2\text{A})=179.7(9)^\circ$], [$\text{Yb}(1\text{A})\text{-O}(1)\text{-Yb}(2)=179.7(9)^\circ$]. As observed for most ligands of this type, the ligand-metal bonding is achieved through both σ [$\text{Yb}(1)\text{-N}(2)=(2.560)\text{\AA}$] and π -bonding modes to provide ytterbocene-like metal centers. The presence of two potassium atoms in the complex sustains a two-fold symmetry in the structure. Both alkali metals are bonded to two THF molecules [$\text{K}(1)\text{-O}(2)=2.716(5)\text{\AA}$]; [$\text{K}(1)\text{-O}(3)=2.685(5)\text{\AA}$], [$\text{K}(1)\text{-O}(4)=2.720(5)\text{\AA}$] and to the same diphenylmethyldipyrrolyl ligand, being π -bonded by both a pyrrole [$\text{K}(1)\text{-N}(4\text{A})\text{cent}=2.940(5)\text{\AA}$] and a phenyl ring [$\text{K}(1)\text{-C}(38)\text{cent}=3.075(5)\text{\AA}$]. The cationic charges

borne by the potassium atoms serve to counter balance the dianionic charge conferred by the central oxygen atom to yield four Yb(II) metal centers.

Since the reaction of $\text{YbCl}_3(\text{THF})_3$ with diphenyldipyrrole followed by reduction with metallic potassium affords $(\{[\text{Ph}_2\text{C}(\text{C}_4\text{H}_3\text{N})_2]\text{Yb}\}_8(\mu\text{-Cl})_4\{\text{Li}(\text{THF})_4\})_2^{15}$, we had no obvious way of rationally synthesizing this complex. Therefore, we attempted the preparation of the same type of complex with the cyclohexyldipyrrole analog. The reaction of this ligand with $\text{YbCl}_3(\text{THF})_3$ and subsequent reduction with either metallic potassium or sodium yielded a dark crystalline material that was successfully analyzed by IR, elemental analysis and X-ray crystallography (Figure 2.5). Complex **2.4** is very similar to complex **2.2**, with four $\{[\text{Cy}(\text{C}_4\text{H}_3\text{N})_2]\text{Yb}\}$ units arranged to form a tetrametallic planar core. One oxygen atom is located in the center of the tetrametallic structure $\{[\text{O}(1)\text{-Yb}(1)=2.428(7)\text{\AA}], [\text{O}(1)\text{-Yb}(2)=2.146(6)\text{\AA}], [\text{O}(1)\text{-Yb}(3)=2.679(7)\text{\AA}], [\text{O}(1)\text{-Yb}(4)=2.139(6)\text{\AA}], [\text{Yb}(4)\text{-O}(1)\text{-Yb}(1)=92.2(2)^\circ], [\text{Yb}(2)\text{-O}(1)\text{-Yb}(1)=89.5(2)^\circ], [\text{Yb}(4)\text{-O}(1)\text{-Yb}(3)=90.1(2)^\circ], [\text{Yb}(2)\text{-O}(1)\text{-Yb}(3)=88.2(2)^\circ]\}$ and is coplanar with the four metal centers $\{[\text{Yb}(1)\text{-O}(1)\text{-Yb}(3)=177.7(2)^\circ], [\text{Yb}(2)\text{-O}(1)\text{-Yb}(4)=178.3(4)^\circ]\}$. Again in this case, four ligands bridge the four metal centers adopting both the σ - $\{[\text{Yb}(1)\text{-N}(2)=2.529(7)\text{\AA}], [\text{Yb}(1)\text{-N}(7)=2.593(8)\text{\AA}]\}$ and π -bonding modes $\{[\text{Yb}(1)\text{-C}(47)=2.771(9)\text{\AA}], [\text{Yb}(1)\text{-N}(1)=2.570(8)\text{\AA}], [\text{Yb}(1)\text{-N}(8)=2.607(7)\text{\AA}]\}$. The metallocenic-type structure of each ytterbium is realized with two π -bonded pyrrolyl rings from two different ligands. Unlike complex **2.2**, complex **2.4** retains no potassium atoms in its structure, yielding a mixed-valent Yb(II)/Yb(III) structure which is paramagnetic.

The formation of complexes **2.2** and **2.4** arises from a THF deoxygenation reaction. The oxygen abstraction from THF is a two-electron process and is accompanied by the formation of two equivalents of ethylene. Although we could not obtain a reliable

quantitative estimate of the amount of ethylene formed during the reactions, its presence was clearly detected by GC and GC-MS analysis of the reaction mother liquor, thus confirming that a THF deoxygenation reaction occurred in parallel to the formation of complex **2.1**. The formation of **2.4** can be rationalized in terms of donation of two electrons from two of the four Yb atoms composing a tetranuclear moiety with consequent oxygen abstraction from THF and formation of the final compounds. Even this process is fairly straightforward although implies the cooperative interaction of two metal centers to achieve the two-electron reduction necessary for the oxygen abstraction. However, this cannot be the case in the case of **2.2** given that the four Yb atoms have maintained the original divalent oxidation state. The formation of **2.2** is more likely the result of the ability of the octanuclear cluster to scavenge a “K₂O” unit and to rearrange during the process into a tetrameric structure. The ability of the potassium counterions to π -bond both the pyrrolide rings and the phenyl groups may play some important role in this respect. The situation is clarified somewhat by a third compound that was also isolated from the original reaction mixture. This new species is a trianionic metallate Yb complex Yb(diphenyldipyrrolylmethane-di-yl)₃ (**2.3**) and its formation implies a major molecular reorganization. Not only does its formation require one electron oxidation of the metal center but one ligand also needs to be acquired in the process as well. Compound **2.3** was rationally prepared in good yield from trivalent YbCl₃ starting material by appropriately adjusting the reaction stoichiometry.

Complex **2.3** (Figure 2.4) is monomeric with one trivalent ytterbium atom surrounded by three dypyrrolyl ligands. Three potassium atoms each solvated by one molecule of THF complete the structure. The ytterbium atom is located in a pseudo-octahedral coordination environment {[N(5)-Yb-N(2)=167.19(11)Å], [N(4)-Yb-N(1)=171.51(11)Å], [N(3)-Yb-N(6)=169.99(11)Å]}. Four nitrogen atoms from four pyrrolyl rings, two from one ligands and two from the other two ligands, are σ -bonded {[Yb-N(1)=2.334(3)Å], [Yb-N(3)=2.326(3)Å],

[Yb-N(4)=2.318(3)Å], [Yb-N(6)=2.336(3)Å]} and define the distorted equatorial plane. Two other pyrrolyl ring nitrogen atoms are located on the axial positions. The deviation of the axes from linearity is presumably due to steric reasons. The structure also incorporates three potassium atoms, each displaying different coordination geometries. One potassium is located in the region between two of the pyrrolyl rings which define the equatorial plane around Yb. The potassium appears to be symmetrically π -ligated to two rings [K(1)-N(1)_{centroid}=2.800(2)Å], [K(1)-N(6)_{centroid}=2.790(3)Å], again forming a bent-potassocene type of structure. One molecule of THF is also bonded to potassium in the region between the two rings pointing to the exterior of the molecule [K(1)-O(1)=2.649(4)Å]. Two carbon atoms from two phenyl rings also form a curiously short K-C contact [K(1)-C(62)=3.450(4)Å] not far from the bonding range possibly indicating the presence of an agostic interaction. The second potassium atom is π -bonded to one "equatorial" pyrrolyl ring [K(2)-N(3)_{centroid}=3.273(3)Å], is coordinated to the N atom of the "axial" pyrrolyl [K(2)-N(2)=3.083(3)Å] and displays a remarkable interaction with two phenyl rings from two ligands [K(2)-C(2)_{centroid}=3.038(3)Å], [K(2)-C(36)_{centroid}=3.193(3)Å]. The coordination environment of the third potassium atom appears to be very similar, except that only one phenyl ring is coordinated to the metal and it is π -bonded to the axial pyrrole ring.

The formation of **2.3** gives the key to rationalize the previous reaction. Assuming a rapid reaction of the initially formed (ligand)Yb intermediate with the still unreacted dipotassium salt, a divalent Yb(ligand)₃K₄ species may form. The THF solvent is the possible recipient of the potassium cation and the electron (two of each are necessary) to form ethylene gas and "K₂O". Reaction of this species with **2.1** may give rise to **2.2**.

The complexity of the overall reaction is remarkable and strongly indicates that the in situ generated low-nuclearity species (ligand)Yb has different reactivity patterns available before getting stabilized into the octameric cluster structure. Since the potassium alkali cation

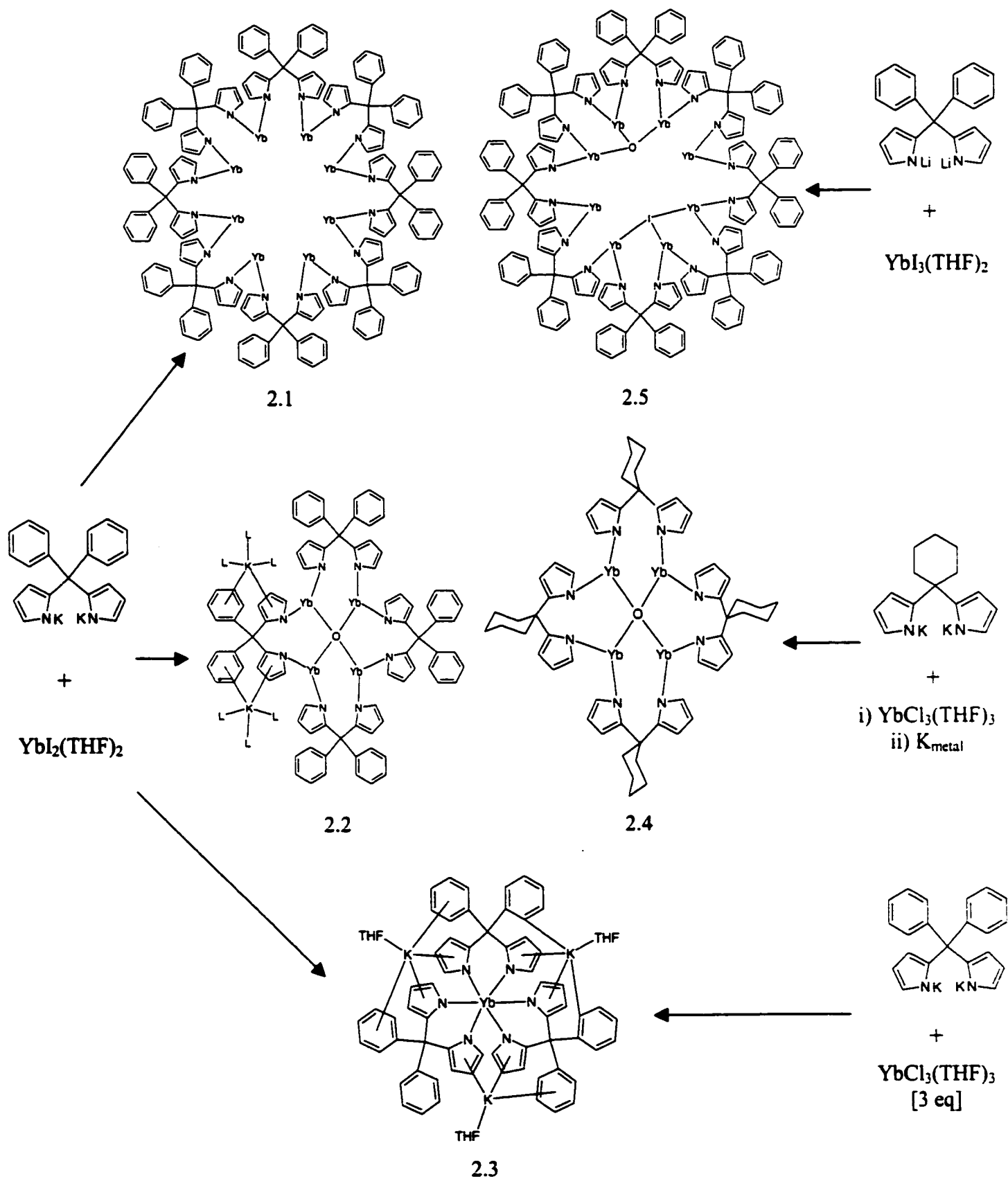
played such an important role in this reaction we have also decided to investigate the reaction of $\text{YbI}_2(\text{THF})_2$ with the lithium salt of diphenyldipyrrolyl methane. The reaction proceeded in a similar manner leading to a new complex also containing mixed valence Yb(II)/Yb(III) and which is formulated as $[(\text{diphenyldipyrrolylmethane-di-yl})_8\text{Yb}_8(\mu\text{-O})(\mu\text{-I})][\text{Li}(\text{THF})_4]_2$ (**2.5**). The crystal structure revealed that **2.5** is an octameric complex that contains two atoms in its intermetallic space, with each of these two binding three Yb metal atoms in an overall anionic structure. Two lithium atoms, each solvated by four molecules of THF and unconnected with the octameric dianion, complete the structure

Complex **2.5** (Figure 2.6) is octameric with an arrangement very similar to that observed in complex **2.1**. Unlike complex **2.1** however, this macrocycle hosts two atoms, each bridging three ytterbium atoms. Two lithium atoms, each solvated by four molecules of THF, are located in the lattice and complete the molecular structure. The presence of the two bridging atoms in the interior of the macrocycle causes a deviation of the nearly cyclic arrangement of the eight ytterbium atoms forcing an ellipsoidal conformation (Figure 2.7). The identity of the central atoms was obtained from the agreement of both analytical data and the successful refinement of the thermal parameters. The two atoms have been identified as one oxygen and one iodine disordered over the two positions with a relative occupancy of 80% oxygen against 20% iodine. This is obviously reflected in the bond distances and angles originated by the two atoms, which are averaged and not particularly informative. In other words, the structure may be formally regarded as the average of five identical octameric units, four of which host two oxygen atoms while the fifth is hosting two iodine anions. The valence of the Yb atoms is also averaged accordingly.

Even in this case the oxygen atoms present in the molecular core arise from a THF deoxygenation process since the presence of ethylene could be clearly observed in the GC-MS of the reaction mixture. The amount of ethylene observed seems to be far lower than

expected, and combined with the poor yield of **2.5**, indicates that another compound is likely to be present in the reaction mixture.

Scheme 2.1



II.5: Structural Considerations

Suitable crystals were selected, mounted on thin, glass fibres using paraffin oil and cooled to the data collection temperature. Despite repeated attempts, **2.5·10(thf)** consistently crystallizes as small, highly mosaic, multiple plates and the data presented represent the results from the best efforts. Data were collected on a Bruker AX SMART 1k CCD diffractometer using 0.3° ω -scans at 0, 90, and 180° in ϕ . Unit-cell parameters were determined from 60 data frames collected at different sections of the Ewald sphere. Semi-empirical absorption corrections based on equivalent reflections were applied (Blessing, R., *Acta Cryst.*, **1995**, A51, 33-38).

No symmetry higher than triclinic was observed for **2.5·10(thf)**. Systematic absences in the diffraction data and unit-cell parameters were consistent with $C2/c$ and Cc for **2.2·2(thf)**, $P2_1$ and $P2_1/m$ for **2.4**, $P4/n$ and $P4/nmm$ for **2.1**, and, uniquely, $P2_1/n$ for **2.3**. In cases of ambiguous space group assignment, solutions were tried in available options, and packing diagrams of candidate acentric solutions were scrutinized for any overlooked centrosymmetry. Refinement in the reported space groups yielded computationally stable and chemically reasonable results of refinement. The structures were solved by direct methods, completed with difference Fourier syntheses and refined with full-matrix least-squares procedures based on F^2 . The absolute configuration parameter in **2.4** refined to nil indicating that the true hand of the data had been determined.

The compound molecule of **2.5·10(thf)** resides on an inversion center. The compound molecule of **2.2·2(thf)** is located at a two-fold rotation axis. Two symmetry-unique but chemically identical molecules are located at four-fold rotation axes in **2.1**. One, and five molecules of tetrahydrofuran (thf) solvent were located cocrystallized in the asymmetric units of **2.2·2(thf)**, and **2.5·10(thf)**, respectively.

An atomic position in **2.5·10(thf)** was refined as a disordered iodine/oxygen atom with a site occupancy distribution of 20/80. In order to conserve a favourable data/parameter ratio, only the ytterbium, nitrogen, and disordered iodine/oxygen atoms were refined anisotropically in **2.5·10(thf)**. The phenyl groups and thf molecules in **2.5·10(thf)** were treated as idealized, rigid, flat, polygons with the atoms having smallest isotropic parameter per thf ring, or atoms coordinated to metal ions, assigned oxygen atom identities. All non-hydrogen atoms, except the carbon atoms in **2.5·10(thf)**, were refined with anisotropic displacement parameters. All hydrogen atoms were treated as idealized contributions. All scattering factors and anomalous dispersion coefficients are contained in the SHEXTL 5.10 program library (Sheldrick, G. M., Bruker AXS, Madison, WI, 1997).

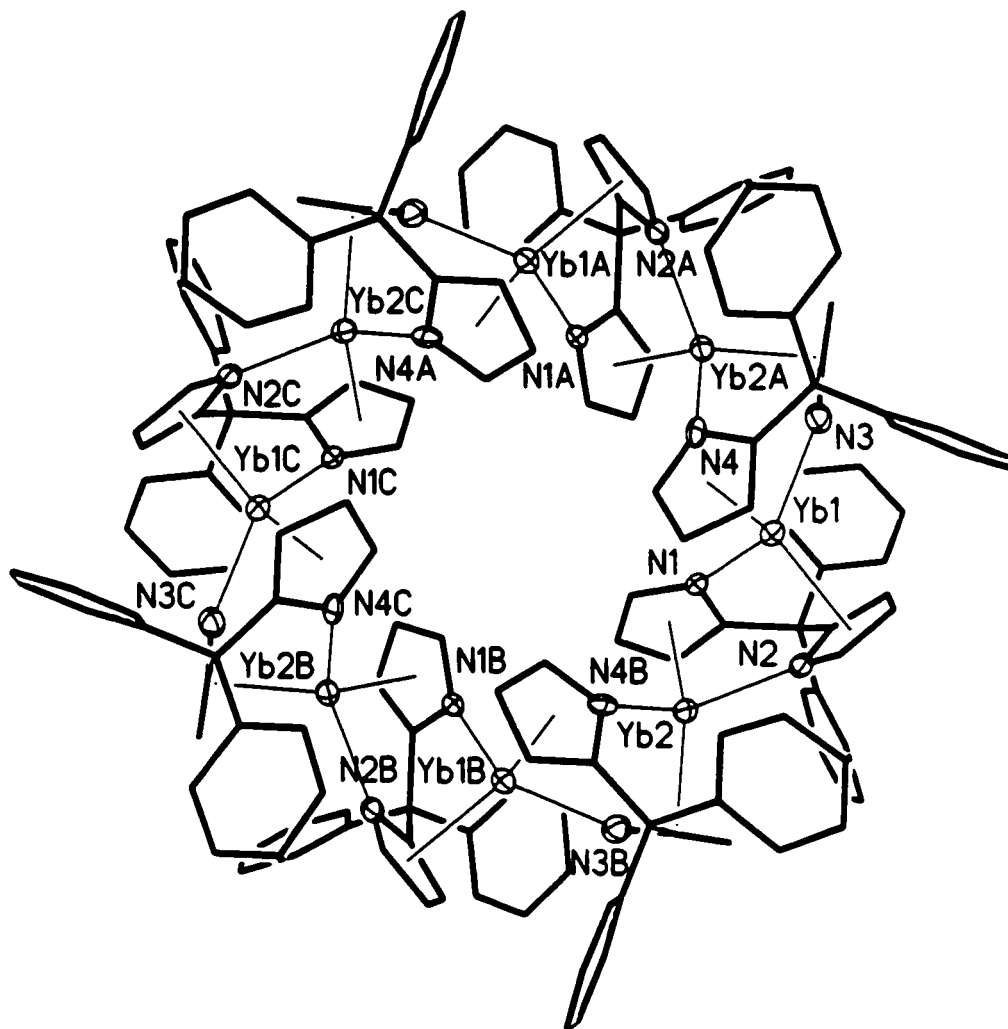


Figure 2.1: Thermal ellipsoid plot of (Diphenyldipyrromethanedi-yl-Yb)₈ (2.1). Thermal ellipsoids are drawn at the 30% probability level. All carbon atoms were resolved anisotropically but are not shown as ellipsoids.

Selected Bond Distances (Å) and Angles (deg): Yb(1)-N(3)=2.446 (16), Yb(1)-N(1)=2.469(14), Yb(1)-N(4)_{centroid}=2.434(15), Yb(1)-N(2)_{centroid}=2.431(15), Yb(1)-N(4)=2.648(13), Yb(2)-N(4B)=2.463(14), Yb(2)-N(2)=2.451(15), Yb(2)-N(3B)_{centroid}=2.451(15), Yb(2)-N(1)_{centroid}=2.459(15), N(3)-Yb(1)-N(1)=117.7(6), N(3)-Yb(1)-N(2)_{centroid}=115.8(6), N(3)-Yb(1)-N(4)_{centroid}=89.2(5), N(2)-Yb(2)-N(4B)=117.6(6), N(2)-Yb(2)-N(1)_{centroid}=87.7(5), N(2)-Yb(2)-N(3B)_{centroid}=115(6),

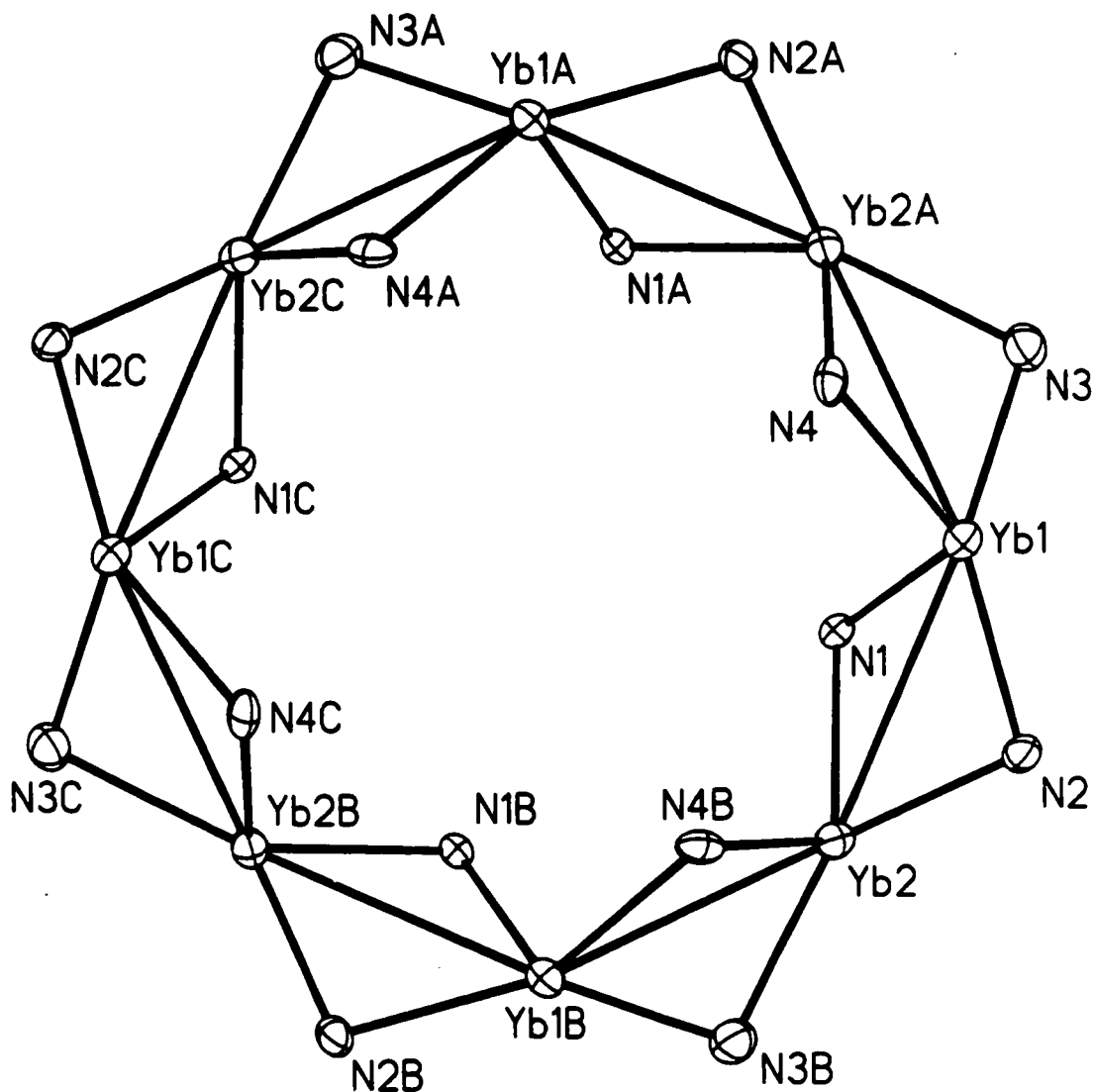


Figure 2.2: Thermal ellipsoid plot of (Diphenyldipyrromethanedi-yl-Yb)₈ (2.1) showing the circular arrangement of Yb atoms. Thermal ellipsoids are drawn at the 30% probability level. Carbon atoms were omitted for clarity.

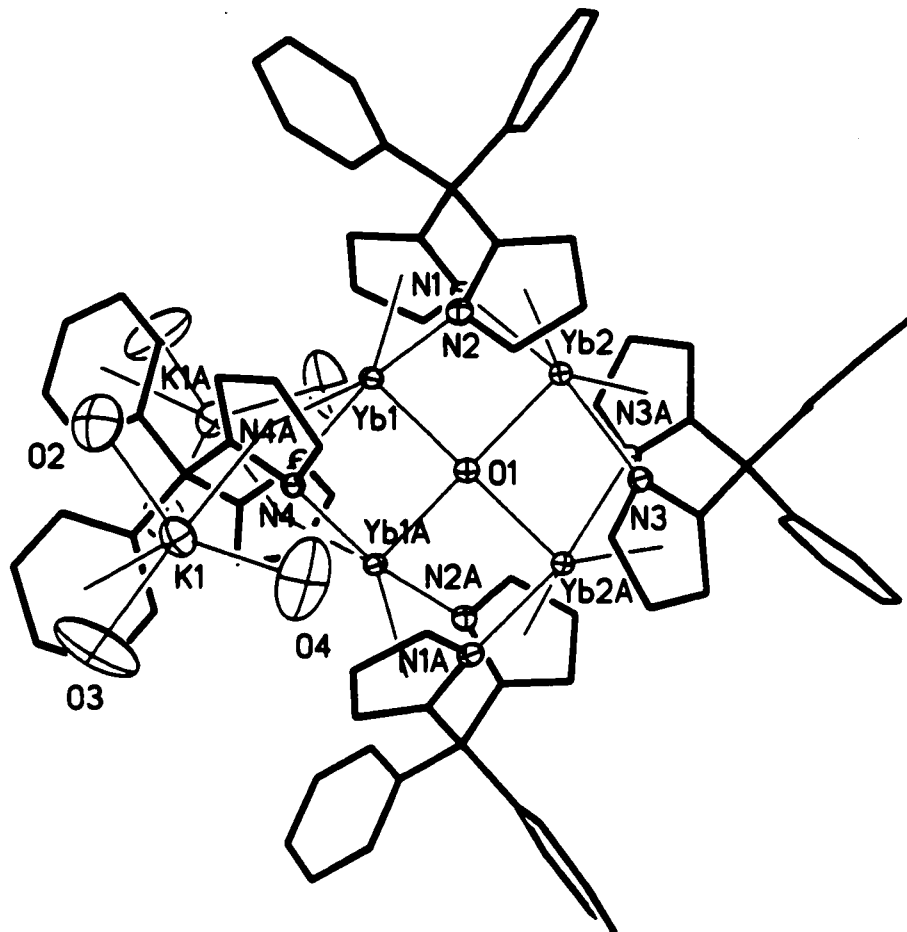


Figure 2.3: Thermal ellipsoid plot of [(diphenyldipyrrolyl-methane-diyl)Yb]₄[(K₂)(THF)₆](μ-O)•2(THF) (2.2). Thermal ellipsoids are drawn at the 30% probability level. All carbon atoms were resolved anisotropically but are not shown as ellipsoids. The carbon atoms from the THF molecules were omitted for clarity.

Selected Bond Distances (Å) and Angles (deg): Yb(1)-O(1)=2.340(4), Yb(2)-O(1)=2.390(4), Yb(1)-N(1)_{centroid}=2.518(5), Yb(1)-N(2)=2.560(4), Yb(1)-N(4)_{centroid}=2.629(5), Yb(1)-N(4A)=2.593(5), Yb(2)-N(1)=2.605(5), Yb(2)-N(2)_{centroid}=2.544(5), Yb(2)-N(3)=2.598(5), Yb(2)-N(3A)_{centroid}=2.524(5), K(1)-N(4)_{centroid}=2.940(5), K(1)-C(38)_{centroid}=3.075(5), K(1)-O(2)=2.716(5), K(1)-O(3)=2.685(5), K(1)-O(4)=2.720(5), Yb(1)-O(1)-Yb(2A)=179.7(9), Yb(1A)-O(1)-Yb(2)=179.7(9), O(3)-K(1)-N(4A)_{centroid}=177.7(9), O(3)-K(1)-O(2)=82.2(9), O(3)-K(1)-O(4)=79.9(9), O(3)-K(1)-C(28)_{centroid}=91.8(9),

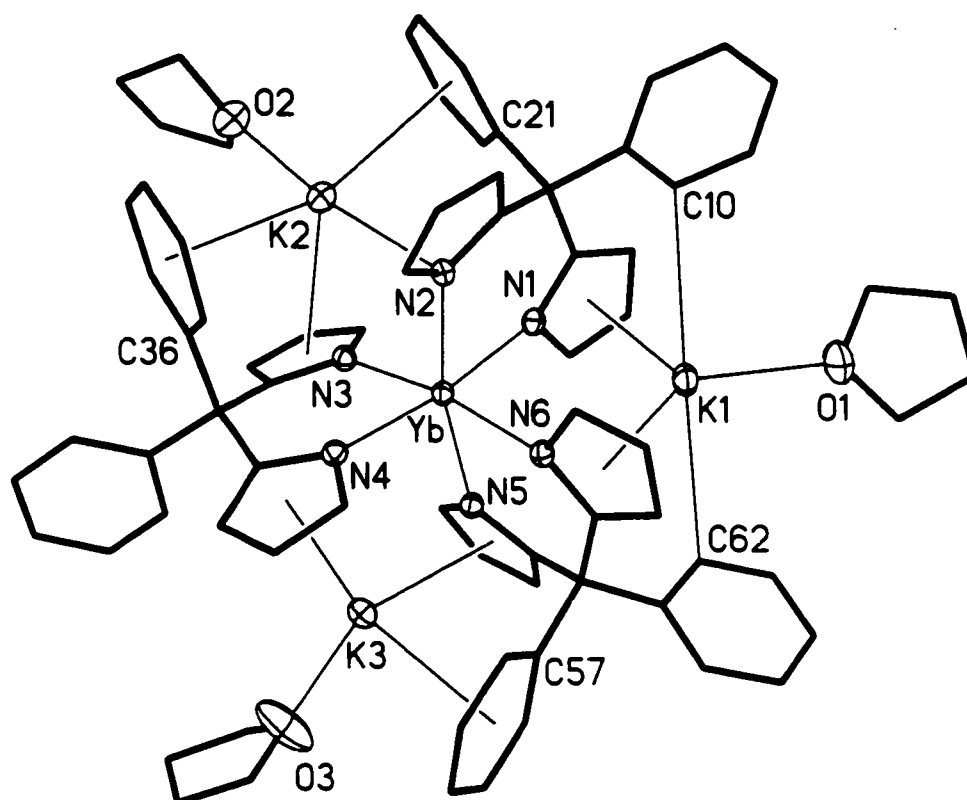


Figure 2.4: Thermal ellipsoid plot of $\text{Yb}(\text{diphenyldipyrrolyl-methane-di-yl})_3(\text{K}_3\text{THF}_3)$ (**2.3**).

Thermal ellipsoids are drawn at the 30% probability level. All carbon atoms were resolved anisotropically but are not shown as ellipsoids.

Selected Bond Distances (Å) and Angles (deg): $\text{Yb-N}(1)=2.334(3)$, $\text{Yb-N}(2)=2.327(3)$, $\text{Yb-N}(3)=2.326(3)$, $\text{Yb-N}(4)=2.318(3)$, $\text{Yb-N}(5)=2.332(3)$, $\text{Yb-N}(6)=2.336(3)$, $\text{K}(1)\text{-O}(1)=2.649(3)$, $\text{K}(1)\text{-C}(10)=3.515(3)$, $\text{K}(1)\text{-C}(62)=3.450(3)$, $\text{K}(1)\text{-N}(1)_{\text{centroid}}=2.800(3)$, $\text{K}(1)\text{-N}(6)_{\text{centroid}}=2.790(3)$, $\text{K}(2)\text{-O}(2)=2.728(3)$, $\text{K}(2)\text{-N}(2)=3.038(3)$, $\text{K}(2)\text{-C}(21)_{\text{centroid}}=3.186(3)$, $\text{K}(2)\text{-C}(36)_{\text{centroid}}=3.193(3)$, $\text{K}(2)\text{-N}(3)_{\text{centroid}}=3.273(3)$, $\text{K}(3)\text{-O}(3)=2.603(3)$, $\text{K}(3)\text{-N}(4)_{\text{centroid}}=2.861(3)$, $\text{K}(3)\text{-N}(5)_{\text{centroid}}=3.197(3)$, $\text{K}(3)\text{-C}(57)_{\text{centroid}}=3.161(3)$, $\text{N}(1)\text{-Yb-N}(2)=78.4(9)$, $\text{N}(1)\text{-Yb-N}(3)=94.4(10)$, $\text{N}(1)\text{-Yb-N}(4)=171.5(12)$, $\text{N}(1)\text{-Yb-N}(5)=92.9(10)$, $\text{N}(1)\text{-Yb-N}(6)=91.1(10)$,

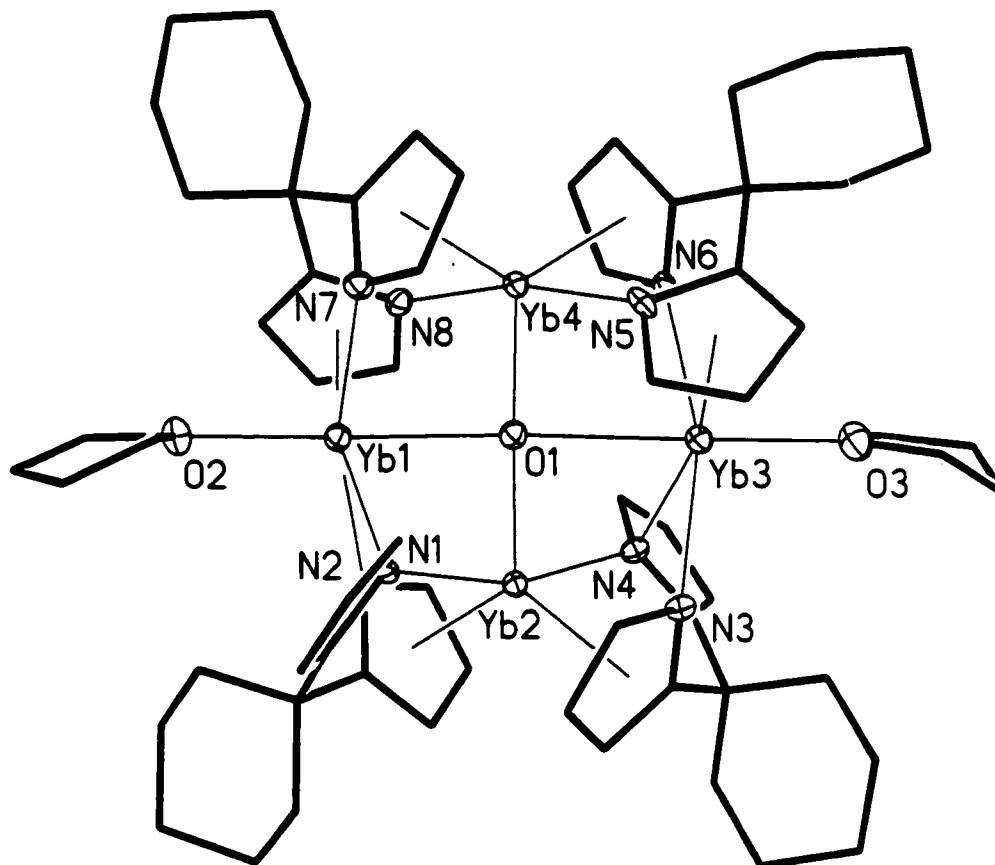


Figure 2.5: Thermal ellipsoid plot of $(1,1'$ -dipyrrolylcyclohexane-di-yl-Yb) $_4(\mu\text{-O})(\text{THF})_2$ (2.4). Thermal ellipsoids are drawn at the 30% probability level. All carbon atoms were resolved anisotropically but are not shown as ellipsoids.

Selected Bond Distances (Å) and Angles (deg): Yb(1)-O(2)=2.428(7), Yb(1)-N(1)=2.570(8), Yb(1)-N(2)=2.529(7), Yb(1)-N(7)=2.593(8), Yb(1)-O(1)=2.592(7), Yb(1)-N(8)_{centroid}=2.572(7), Yb(2)-N(1)=2.431(8), Yb(2)-N(2)_{centroid}=2.414(6), Yb(2)-O(1)=2.146(6), Yb(3)-O(1)=2.679(7), Yb(4)-O(1)=2.139(6), Yb(4)-N(6)_{centroid}=2.406(5), Yb(4)-N(8)=2.443(5), Yb(4)-N(5)=2.426(5), Yb(4)-N(7)_{centroid}=2.424(5), O(1)-Yb(1)-O(2)=1515.7(4), O(1)-Yb(1)-N(1)=71.0(2), O(1)-Yb(1)-N(2)=85.0(2), O(1)-Yb(1)-N(7)=78.8(2), Yb(4)-O(1)-Yb(2)=178.3(4), Yb(4)-O(1)-Yb(1)=92.2(2), Yb(2)-O(1)-Yb(1)=89.5(2), Yb(4)-O(1)-Yb(3)=90.1(2), Yb(2)-O(1)-Yb(3)=88.2(2), Yb(1)-O(1)-Yb(3)=177.7(2),

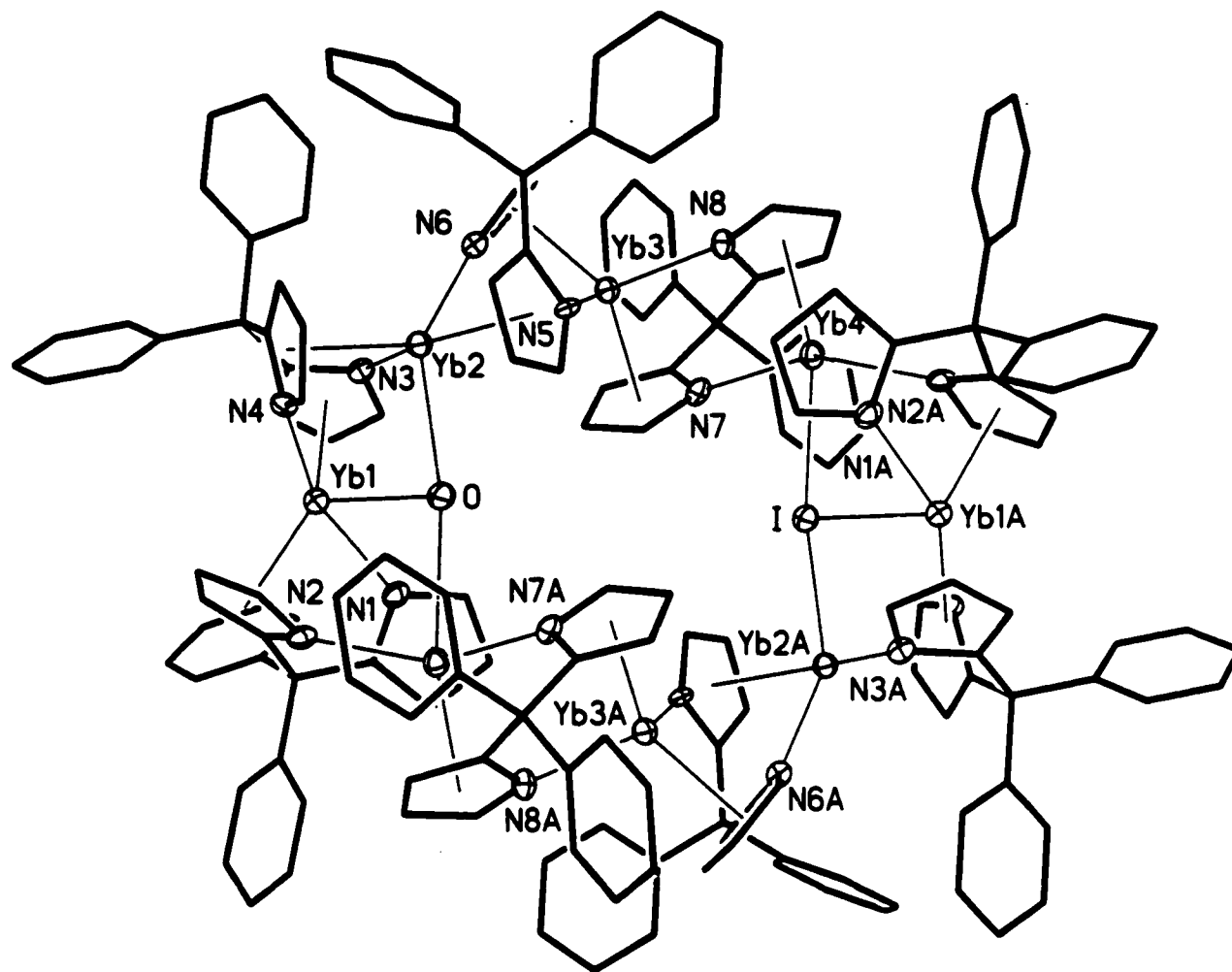


Figure 2.6: Thermal ellipsoid plot of $[(\text{diphenyldipyrrolylmethane-di-yl})_8\text{Yb}_8(\text{m-O})(\text{m-I})][\text{Li}(\text{THF})_4]_2 \cdot \text{THF}$ (**2.5**). Thermal ellipsoids are drawn at the 30% probability level. All carbon atoms were resolved anisotropically but are not shown as ellipsoids.

Selected Bond Distances (Å) and Angles (deg): Yb(1)-N(4)=2.535(17), Yb(1)-N(1)=2.588(17), Yb(1)-N(3)_{centroid}=2.502(17), Yb(1)-N(2)_{centroid}=2.509(17), Yb(1)-O=2.707(6), Yb(2)-O=2.797(6), Yb(2)-N(3)=1.6(16), Yb(2)-N(6)=1.9(19), Yb(3)-N(5)=1.2(2), Yb(3)-N(8)=1.9(19), Yb(4)-O=1.6(6), Yb(4)-N(2A)=1.2(2), Yb(4)-N(7)=1.2(2), N(4)-Yb(1)-N(1)=154.9(5), N(4)-Yb(1)-N(3)_{centroid}=85.7(5), N(4)-Yb(1)-N(2)_{centroid}=101.1(5), N(4)-Yb(1)-O=78.2(6), Yb(2)-O-Yb(4A)=169.8(6), Yb(1)-O-Yb(2)=86.9(6), Yb(1)-O-Yb(4A)=83.6(6),

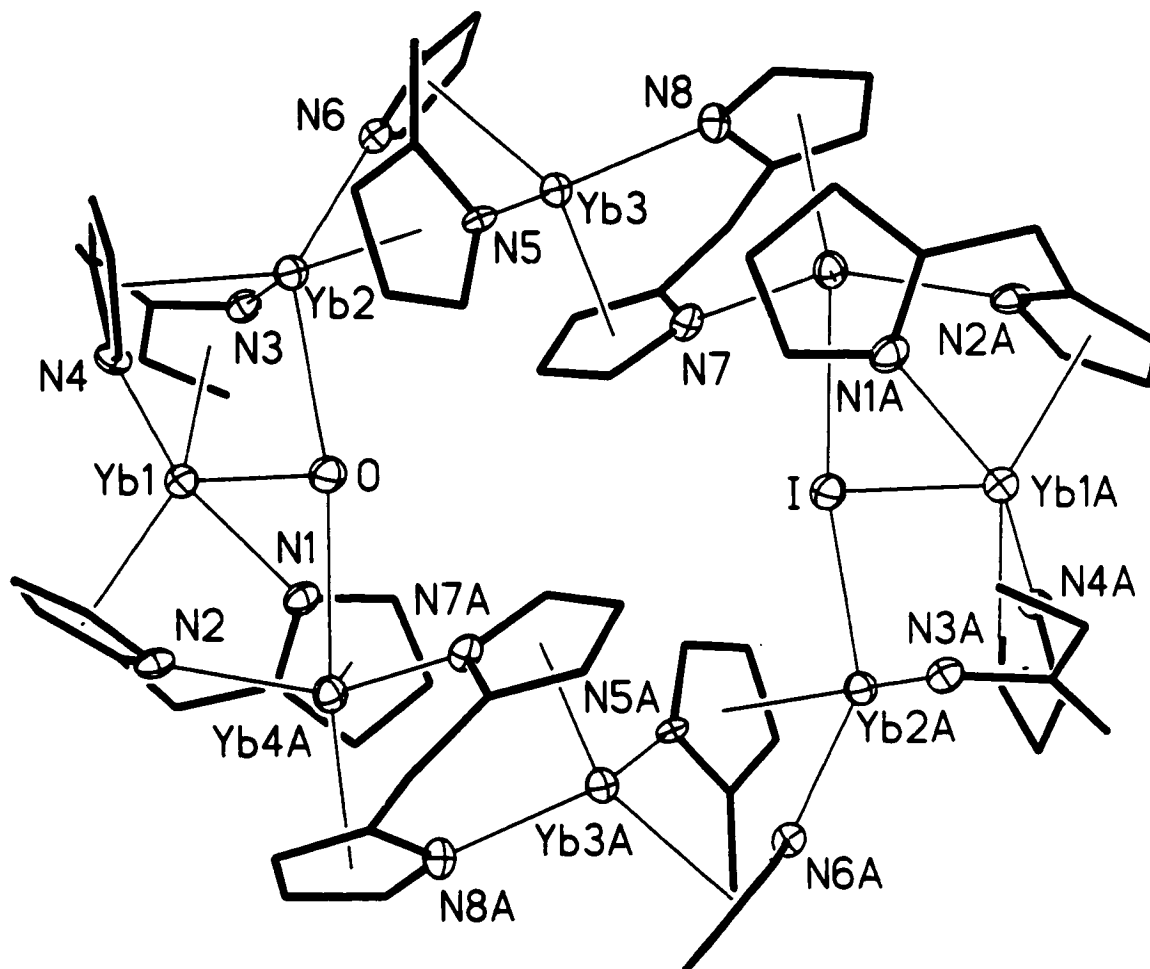


Figure 2.7: Thermal ellipsoid plot of $[(\text{diphenyldipyrrolylmethane-di-yl})_8\text{Yb}_8(\text{m-O})(\text{m-D})][\text{Li}(\text{THF})_4]_2 \cdot \text{THF}$ (**2.5**) displaying the elliptical arrangement of Yb atoms. Thermal ellipsoids are drawn at the 30% probability level. All carbon atoms were resolved anisotropically but are not shown as ellipsoids. Phenyl groups were omitted for clarity.

II.6: Conclusions

Attempts to form Yb(dipyrrolide) complexes have been revealed with the isolation of an attractive octameric structure with the eight metal centers organized in a ring. The particular octameric structure seems to play an important role in the stabilization of the Yb centers, since the same intermediate which is the building block of the octamer may also undergo different reaction leading to THF deoxygenation and disproportionation pathways. Finally, hosting small units may deform the large octameric structure. We are actively pursuing the possibility of using complex 2.1 for host-guest interactions and/or multi-electron redox processes.

References

- 1 W.J. Evans, T.A., Ulibarri, J.W. Ziller, *J. Am. Chem. Soc.* **1988**, 110, 6877
- 2 a) P. Girard, J.L. Namy, H.B. Kagan, *J. Am. Chem. Soc.* **1980**, 102, 2693; W. J.
- 3 b)W.J. Evans, I. Bloom, W. E. Hunter, and J. L. Atwood, *J. Am. Chem. Soc.* **1983**, 105, 140;
c)W. J. Evans, S. C. Engerer, P. A. Piliero, A. L. Wayda, *J. Chem. Soc. Chem. Commun.* **1979**, 1007;
d)W. J. Evans, S. C. Engerer, P. A. Piliero, A. L. Wayda, *Fundamentals of Homogeneous Catalysis*, Tsutsui, M. Ed., Plenum Press, New York, **1979**, 3;
e)W. J. Evans, M. A. Ansari, J. W. Ziller, S. I. Khan, *Organometallics*, **1995**, 14, 3;
f)W. J. Evans, T. A. Ulibarri, J. W. Ziller, *J. Am. Chem. Soc.* **1990**, 112, 219
g)W. J. Evans, L. A. Hughes, T. P. Hanusa, *J. Am. Chem. Soc.* **1984**, 106, 4270;
h)W. J. Evans, L. A. Hughes, T. P. Hanusa, *Organometallics*. **1986**, 5, 1285;
i)W. J. Evans, D. K. Drummond, S. G. Bott, J. L. Atwood, *Organometallics*, **1986**, 5, 2389;
j)W. J. Evans, R. A. Keyer, H. Zhang, J. L. Atwood, *J. Chem. Soc., Chem. Commun.* **1987**, 837;
k)W. J. Evans, D. K. Drummond, J. W. Grate, H. Zhang, J. L. Atwood, *J. Am. Chem. Soc.* **1987**, 109, 3928;
l)W. J. Evans, D. K. Drummond, *J. Am. Chem. Soc.* **1989**, 111, 3329;
m)W. J. Evans, R. A. Keyer, G. W. Rabe, D. K. Drummond, J. W. Ziller, *Organometallics*, **1993**, 12, 4664;
n)W. J. Evans, J. W. Grate, R. J. Doedens, *J. Am. Chem. Soc.* **1985**, 107, 1671;
o)W. J. Evans, T. A. Ulibarri, *J. Am. Chem. Soc.* **1987**, 109, 4292;

- p) W. J. Evans, J. W. Grate, L. A. Hughes, H. Zhang, J. L. Atwood, *J. Am. Chem. Soc.* **1985**, *107*, 3728;
- q) W. J. Evans, D. K. Drummond, *J. Am. Chem. Soc.* **1988**, *110*, 2772;
- r) W. J. Evans, D. K. Drummond, *Organometallics*, **1988**, *7*, 797;
- s) W. J. Evans, D. K. Drummond, L. R. Chamberlain, R. J. Doedens, S. G. Bott, H. Zhang, J. L. Atwood, *J. Am. Chem. Soc.* **1988**, *110*, 4983;
- t) W. J. Evans, D. K. Drummond, *J. Am. Chem. Soc.* **1986**, *108*, 7440;
- u) W. J. Evans, T. A. Ulibarri, J. W. Ziller, *J. Am. Chem. Soc.* **1990**, *112*, 2314;
- v) X. Zhang, G. R. Loppnow, R. McDonald, J. Takats, *J. Am. Chem. Soc.* **1995**, *117*, 7828;
- w) G. Desurmont, Y. Li, H. Yasuda, T. Maruo, N. Kanehisa, Y. Kai *Organometallics* **2000**, *19*, 1811.
- 4 a) W.J. Evans, J.W. Grate, W.E. Hughes, H. Zhang, J.L. Atwood, *J. Am. Chem. Soc.*, **1985**, *107*, 3728;
- b) W.J. Evans, I. Bloom, W.E. Hunter, J.L. Atwood, *J. Am. Chem. Soc.*, **1981**, *103*, 6507
- 5 W.J. Evans, T.A. Ulibarri, J.W. Ziller, *J. Am. Chem. Soc.*, **1990**, *112*, 219
- 6 W.J. Evans, T.A. Ulibarri, J.W. Ziller, *J. Am. Chem. Soc.*, **1988**, *110*, 6877
- 7 a) W.J. Evans, I. Bloom, J.W. Grate, L.A. Hughes, W.E. Hunter, J.L. Atwood., *Inorg. Chem.*, **1985**, *24*, 4630;
- b) W.J. Evans, I. Bloom, W.E. Hunter, J.L. Atwood, *Organometallics*, **1985**, *4*, 112;
- c) W.J. Evans, I. Bloom, W.E. Hunter, J.L. Atwood, *J. Am. Chem. Soc.*, **1983**, *105*, 1401;
- d) W.J. Evans, T.A. Ulibarri, J.W. Ziller., *J. Am. Chem. Soc.*, **1990**, *112*, 2314
- 8 W.J. Evans, R. Anwander, M.A. Ansari, J.W. Ziller, *Inorg. Chem.* **1995**, *34*, 5

- 9 G. Rabe, J. Riede, A. Schier, *Inorg. Chem.*, **1996**, 35, 2680
- 10 R. Minhas, J. Song, Y. Ma, S. Gambarotta, *Inorg. Chem.*, **1996**, 35, 1866
- 10 J. Jubb, S. Gambarotta, *J. Am. Chem. Soc.* **1994**, 117, 4477
- 11 a) T. Dube, S. Gambarotta, G.P.A. Yap, *Organometallics*, **2000**, 19, 115-117;
b) T. Dube, S. Conoci, S. Gambarotta, G.P.A. Yap, *Organometallics*, **2000**, 19, 1182-1185;
c) T. Dube, S. Conoci, S. Gambarotta, G.P.A. Yap, G. Vaspollo, *Angew. Chem. Int. Ed.*, **1999**, 38, 3657-3659;
d) T. Dube, M. Ganesan, S. Conoci, S. Gambarotta, G.P.A. Yap, *Organometallics*, **2000**, 19, 3716-3721;
e) M. Ganesan, S. Gambarotta, G.P.A. Yap, *Angew. Chem. Int. Ed.*, **2001**, 40, 766-769
- 12 R. J. Errington, Advanced practical inorganic and metalorganic chemistry, Blackie Academic & Professional, **1997**
- 13 *Organometallics*, Vol. 9, No7, **1990**, P.1999.
- 14 R.J. Angelici, *Inorganic Syntheses*, **1990**, Vol 27 P.136-140
- 15 T. Dube, D. Freckmann, S. Conoci, S. Gambarotta, G.P.A. Yap, *Organometallics*, **2000**, 19, 209-211
- 16 M. Ganesan, S. Gambarotta, G.P.A. Yap, *Angew. Chem. Int. Ed.*, **2001**, 40, 766-769

Chapter III:

Synthesis of Samarium and Ytterbium Complexes with 2,5-Dimethylpyrrole: The Effect of the Alkali Cation on the Bonding Mode of Divalent Lanthanide Centres

Summary

Introduction

Experimental Section

Results and Discussion

Structural Considerations

Conclusions

References

53

53

56

62

71

80

81

Mensis	☐
Mercur: fignat	☐
Mere: Saturn	☐
Mer.: Sublimat	☐
Nobis bou	NB
Nox	☐☐☐
Okum	☐☐☐☐☐☐☐☐
Piacituro	☐☐☐☐☐☐☐☐
Pulvis	☐☐☐☐☐☐☐☐
Pulvis Latriu	☐☐☐☐☐☐☐☐
Purificare	☐☐☐☐☐☐☐☐
Purificare	☐☐☐☐☐☐☐☐
Quida Essen	☐☐☐☐☐☐☐☐
Reaser.	☐☐☐☐☐☐☐☐
Requis	☐☐☐☐☐☐☐☐
Reverte	☐☐☐☐☐☐☐☐
Sal comune	☐☐☐☐☐☐☐☐
Sal Alkali	☐☐☐☐☐☐☐☐
Sal Ammoniac	☐☐☐☐☐☐☐☐
Sal Gypsum	☐☐☐☐☐☐☐☐
Sal petra	☐☐☐☐☐☐☐☐
Sapo	☐☐☐☐☐☐☐☐
Spiritus	☐☐☐☐☐☐☐☐
Spiritus Vin	☐☐☐☐☐☐☐☐
Sintheopatra	☐☐☐☐☐☐☐☐
Sivore	☐☐☐☐☐☐☐☐
Sublimare	☐☐☐☐☐☐☐☐
Sulphur	☐☐☐☐☐☐☐☐
Sulphur vitri	☐☐☐☐☐☐☐☐
Sulphur thionophan	☐☐☐☐☐☐☐☐
Sulphur nig	☐☐☐☐☐☐☐☐
Tartar	☐☐☐☐☐☐☐☐
Calc tartar	☐☐☐☐☐☐☐☐
Sal tartari	☐☐☐☐☐☐☐☐
Takum	☐☐☐☐☐☐☐☐
Terra	☐☐☐☐☐☐☐☐
Togham	☐☐☐☐☐☐☐☐
Tunc	☐☐☐☐☐☐☐☐
Vitriolum	☐☐☐☐☐☐☐☐
Vitrum	☐☐☐☐☐☐☐☐
Viride an	☐☐☐☐☐☐☐☐
Vrina	☐☐☐☐☐☐☐☐
Johannes	Worlidge

Synthesis of Samarium and Ytterbium Complexes with 2,5-Dimethylpyrrole: The Effect of the Alkali Cation on the Bonding Mode of Divalent Lanthanide Centres

III.1: Summary

The reactions of $\text{SmI}_2(\text{THF})_2$ and $\text{YbI}_2(\text{THF})_2$ with the alkali salts of 2,5-dimethylpyrrole, or the reaction of $\text{SmCl}_3(\text{THF})_3$ and $\text{YbCl}_3(\text{THF})_3$ with the same ligands followed by reduction with the appropriate alkali metals, led to the formation of divalent mono- and polynuclear complexes. Analysis of these complexes brings forth the observation that the bonding mode adopted by the ligand and the lanthanide metal is dependent on the nature of the alkali cation present in the structure.

III.2: Introduction

The field of organolanthanide chemistry has enjoyed a steady growth over the last two decades, a success that has been fuelled by the constant discoveries of new applications and the catalytic behaviour of Ln-C functionalities. Organolanthanides have been used to pursue catalytic reactions such as olefin hydrogenation,¹ dehydroamination,² hydrosilation,³ hydroboration,⁴ oligomerization⁵ and reductive cyclization.⁶ Undeniably, the most active and versatile ligands used with lanthanide metals to perform the aforementioned transformations have been based upon the cyclopentadienyl ligand system.⁷ This class of ligands has also shown great versatility when combined with low-valent lanthanide metals such as divalent samarium, leading to complexes that exhibit some activity as olefin polymerisation catalysts,⁸ display potent catalytic activity in metal-promoted organic synthesis,⁹ and perform the activation of dinitrogen molecules.¹⁰

In view of these processes and of the growing interest in the field, much work has been dedicated to find new ligand systems that can perform transformations similar to those observed with the Cp type ligands. Alternate ligands, such as alkoxides,¹¹ amides,¹² phosphides¹³ and pyrazolylborates¹⁴ were successfully used to stabilise low-valent samarium, but the calibre of the transformations displayed by the samarocenes was never reproduced.

One of the major features often recurring in lanthanide cyclopentadienyl chemistry is the rather systematic retention of alkali cations and their halide counteranions in the lanthanide primary coordination sphere. The presence of these formally inert units occasionally hampers the chemical reactivity of these species and often affords intractable products or complicates the reaction pathways. One of the major problems is that the halogen atom is usually not easily dislodged from the lanthanide coordination sphere.

Our recent studies on the polypyrrolide derivatives of low-valent samarium have highlighted a promising ability to stabilize highly reactive divalent samarium clusters. Even more important was the observation that the dipyrrolide systems closely reminiscent of an *ansa*-metallocene type of ligand is capable of substantially increasing the reactivity with respect to samarocene since a four electron reduction of dinitrogen was observed rather than a labile coordination.¹⁵ Therefore, since a pyrrolyl anion is closely reminiscent of the cyclopentadienyl moiety the obvious next step was to attempt the preparation of divalent (dipyrrolyl)₂Ln type of complexes for further reactivity studies. The use of 2,5-dimethylpyrrole was found to be advantageous over that of simple pyrrole, since the latter is prone to decomposition through the formation of polymeric

species. Herein, we describe the synthesis and characterisation of divalent lanthanide pyrrolide compounds and the role of the alkali cation in determining the type of M-ligand bonding mode.

III.3: Experimental Section

All operations were performed under an inert atmosphere of a nitrogen-filled dry box or by using Schlenk-type glassware in combination with a nitrogen-vacuum line.¹⁶ Solvents were dried by passing through a column of Al₂O₃ under an inert atmosphere prior to use, degassed *in vacuo* and transferred and stored under inert atmosphere. SmI₂(THF)₂,¹⁷ SmCl₃(THF)₃,¹⁸ YbI₂(THF)₂¹⁹ and YbCl₃(THF)₃²⁰ were prepared according to literature procedures. The NaH and KH suspensions in mineral oil (Aldrich) were washed with hexane, dried and stored under nitrogen in sealed ampoules. THF-d₈ was dried over Na/K alloy, vacuum transferred into ampoules, and stored under nitrogen prior to use. 2,5-dimethylpyrrole and the solutions of n-BuLi and CH₃Li were used as received from Aldrich. NMR spectra were recorded on a Varian Gemini 200 and on a Bruker AMX-500 spectrometer using vacuum sealed NMR tubes prepared inside a dry box. Infrared spectra were recorded on a Mattson 3000 FTIR instrument from Nujol mulls prepared inside a dry box. Samples for magnetic susceptibility measurements were carried out at room temperature using a Gouy balance (Johnson Matthey) and corrected for underlying diamagnetism. Elemental analyses were carried out using a Perkin-Elmer Series II CHN/O 2400 analyser.

Synthesis of $[(\mu-\eta^1, \eta^5\text{-Me}_2\text{C}_4\text{H}_2\text{N})_3\text{Sm}(\mu\text{-Cl})\{\text{Li}(\text{THF})_2\}_2]$ (3.1)

A solution of 2,5-dimethylpyrrole (1.3 mL, 12.8 mmol) in THF (40 mL) was stirred with n-BuLi (1.6 M, 8.5 mL, 13.6 mmol) at room temperature for 30 minutes. Subsequent addition of SmCl₃(THF)₃ (3.0 g, 6.4 mmol) in THF resulted in an immediate colour change to orange. After stirring 24 hours, metallic lithium (0.045 g, 6.4 mmol)

was added to the reaction mixture under argon atmosphere. Within an hour, the colour changed to dark brown and the mixture was stirred for additional 24 hours to ensure that all the lithium was consumed. The solvent was evaporated under vacuum and the residue was extracted with ether, after which the solution was centrifuged to remove insoluble precipitate. The ether was removed *in vacuo* to give a powder, which was solubilized in THF (10 mL). Hexane (20 mL) was added to the solution, which led to the crystallisation of **3.1** after 3 days at -36°C (2.8 g, 3.6 mmol, 57 % yield).

El. Anal. Calcd.(Found) for $\text{C}_{18}\text{ClH}_{24}\text{Li}_2\text{N}_3\text{O}_4\text{Sm}$: C 39.8(38.88); H 4.42(5.08); N 7.74(6.12).

IR (Nujol, cm^{-1}) ν : 3070(m), 2726(w), 1501(m), 1310(m), 1294(m), 1261(m), 1042(vs), 961(w), 914(s), 895(s), 757(vs), 723(w), 669(w), 601(m).

$\mu_{\text{eff}} = 3.3 \mu_{\text{B}}$

Synthesis of $[(\mu\text{-}\eta^1, \eta^5\text{-Me}_2\text{C}_4\text{H}_2\text{N})_3\text{Sm}(\mu\text{-I})\{\text{Li}(\text{TMEDA})_2\}\{\text{Li}(\text{OEt})_2\}]$ (**3.2**)

A solution of $\text{SmI}_2(\text{THF})_2$ (2.9 g, 4.4 mmol) in THF (100 mL) was treated with three equivalents of lithium 2,5-dimethylpyrrole (1.3 g, 13.3 mmol), which resulted in an instantaneous colour change to deep purple. The solution was stirred for 2 hours, after which the solvent was removed *in vacuo*, and the dark purple residue was redissolved in ether (75 mL). Upon addition of TMEDA (2.0 mL, 13.2 mmol) an appreciable amount of white solid precipitated. After standing at room temperature for 4 hours the solution was filtered and concentrated to 30 mL. Standing at room temperature overnight yielded purple plates of **3.2** (2.2 g, 2.88 mmol, 65 % yield). El. Anal. Calcd.(Found) for $\text{SmIN}_5\text{C}_{28}\text{Li}_2\text{H}_{50}\text{O}$: C 44.02(39.58), H 6.60(5.84), N 9.17(9.83). I.R.(Nujol mull, cm^{-1}) ν :

3087(w), 2724(w), 1501(w), 1459(vs), 1376(vs), 1288(m), 1266(m), 1159(m), 1129(m), 1031(s), 946(s), 792(s), 761(vs). $\mu_{\text{eff}} = 3.2 \mu_{\text{B}}$

Synthesis of $[(\text{Na}(\text{THF})_2)(\mu\text{-}\eta^1, \eta^5\text{-Me}_2\text{C}_4\text{H}_2\text{N})_2\text{Sm}]_2(\mu\text{-}\eta^1, \eta^5\text{-Me}_2\text{C}_4\text{H}_2\text{N})_2$ (3.3)

A solution of 2,5-dimethylpyrrole (1.1 mL, 1.1 g, 11.2 mmol) in THF (40 mL) was stirred with NaH (0.3 g, 11.6 mmol) at room temperature for 30 minutes. Subsequent addition of $\text{SmCl}_3(\text{THF})_3$ (1.8 g, 3.7 mmol) in THF and reflux for 20 hours resulted in a yellow coloured solution. Metallic sodium (0.09 g, 3.9 mmol) was added to the solution and was stirred for seven days to give a dark brown solution. The solution was centrifuged and concentrated to 20 mL. Red brown crystals of 3.3 were obtained upon cooling the solution to 4 °C (1.3 g, 1.2 mmol, 58 % yield).

El. Anal. Calcd.(Found) for $\text{C}_{60}\text{H}_{96}\text{N}_6\text{Na}_2\text{O}_6\text{Sm}_2$: C 53.57(51.62); H 7.14(7.02); N 6.25(6.11).

I.R. (Nujol, cm^{-1}) ν : 3084(m), 3066(m), 2729(w), 1500(w), 1308(w), 1290(w), 1258(s), 1171(w), 1096(w), 1051(vs), 1033(vs), 960(w), 892(w), 800(w), 763(vs), 739(s), 702(w).

$\mu_{\text{eff}} = 2.3 \mu_{\text{B}}$

Isolation of $[(\mu\text{-}\eta^1, \eta^5\text{-Me}_2\text{C}_4\text{H}_2\text{N})_2\text{Yb}(\mu\text{-Cl})\{\text{Li}(\text{OEt}_2)\}]_2$ (3.4) and $[(\mu\text{-}\eta^1, \eta^5\text{-Me}_2\text{C}_4\text{H}_2\text{N})_2\text{Yb}(\mu\text{-Cl})_2\{\text{Li}(\text{OEt}_2)\}\{\text{Li}(\text{THF})(\text{OEt}_2)\}]_2$ (3.5)

A solution of 2,5-dimethylpyrrole (0.9 g, 0.95 mL, 9.4 mmol) in THF (40 mL) was stirred with nBuLi (1.6 M, 5.9 mL, 9.4 mmol) at room temperature for 30 minutes. Subsequent addition of $\text{YbCl}_3(\text{THF})_3$ (2.3 g, 4.7 mmol) in THF caused the solution to become orange. After stirring 24 hours, metallic lithium (0.033 g, 4.7 mmol) was added

to the reaction mixture under an argon atmosphere and stirring continued for 4 days to give a yellow coloured solution. The solvent was evaporated *in vacuo* and the resultant residue was extracted with ether (40 ml) to give a red solution. The solution was centrifuged to remove insoluble LiCl and it was then concentrated to 20 ml and cooled to -36 °C for four days to give red crystals of **3.4** (0.9 g, 0.45 mmol, 40 % yield). The mother liquor was cooled again for four days to give yellow crystals of **3.5** along with red crystals of **3.4**. Characterization of **3.5** was therefore restricted to X-ray crystallography. El. Anal. Calcd.(Found) for $C_{32}H_{52}Cl_2Li_2N_4O_2Yb_2$ (**3.4**): C 40.21(38.61); H 5.44(5.14); N 5.86(5.81)

I.R. (Nujol, cm^{-1}) ν : 3090(m), 3075(m), 2729(m), 1309(m), 1255(m), 1195(w), 1154(m), 1089(m), 1057(m), 1033(s), 1002(m), 963(w), 905(w), 840(w), 791(w), 763(vs), 723(m), 669(w), 601(m).

1H NMR (200 MHz, THF- d_8 , 22 °C) δ : 1.11 (t, 12H, CH_3), 2.17 (br s, 24H, CH_3), 3.37 (q, 8H, CH_2), 5.80 (br s, CH).

^{13}C NMR (125.76 MHz, THF- d_8 , 22 °C) δ : 15.65 (CH_3), 16.68 (CH_3), 17.75 (CH_3), 66.30 (CH_2 -ether), 108.26 (CH-pyrrole), 110.06 (CH-pyrrole), 135.29 (quaternary C-pyrrole).

Synthesis of $[(\mu-\eta^1, \eta^5-Me_2C_4H_2N)_2Yb(\mu-I)_2\{Li(THF)\}_2]_n$ (**3.6**)

A solution of 2,5-dimethylpyrrole (0.4 g, 0.45 mL, 4.4 mmol) in THF (20 mL) was stirred with CH_3Li (1.4 M, 3.1 ml, 4.4 mmol) at room temperature for 30 minutes. Subsequent addition of $YbI_2(THF)_2$ (1.2 g, 2.2 mmol) in THF(30 ml) resulted in an immediate colour change to orange and the obtained mixture was stirred for 24 hours. The solvent was evaporated *in vacuo*, the residue was extracted with toluene (30 mL) and

the heterogeneous solution was centrifuged. Red crystals of **3.6** were formed upon standing the solution for 5 days at room temperature (1.0 g, 1.2 mmol, 55 % yield).

El. Anal. Calcd.(Found) for $C_{23.5}H_{36}I_2Li_2N_2O_2Yb$: C 34.42(30.42); H 4.39(4.15); N 3.41(3.69).

I.R. (Nujol, cm^{-1}) ν : 3084(w), 2736(w), 1634(w), 1603(w), 1548(w), 1342(s), 1312(s), 1294(s), 1259(vs), 1197(w), 1174(w), 1081(w), 1037(vs), 962(s), 915(vs), 890(vs), 783(vs), 734(vs), 696(s), 670(w), 636(w), 603(s).

1H NMR (200 MHz, THF- d_8 , 22 °C) δ : 1.73 (m, THF), 2.18 (br s, CH_3), 3.59 (m, THF), 5.77 (br s, CH).

^{13}C NMR (125.76 MHz, THF- d_8 , 22 °C) δ : 17.30 (CH_3 -pyrrole), 26.30 (CH_2 -THF), 68.32 (CH_2 -THF), 108.52 (CH-pyrrole), 135.50 (quaternary C-pyrrole).

Synthesis of $[(\mu-\eta^1, \eta^5-Me_2C_4H_2N)_4\{K(THF)\}_2Yb]_n$ (**3.7**)

A solution of 2,5-dimethylpyrrole (0.4 g, 4.6 mmol) in THF (25 mL) was stirred with KH (0.2g, 4.7 mmol) at room temperature for 30 minutes. Subsequent addition of $YbI_2(THF)_2$ (1.3g, 2.3 mmol) in THF (30 mL) resulted in a colour change to yellow-orange while the solution was stirred for 20 hours. The solution was centrifuged to remove KI and then concentrated to lower volume (15 mL). Yellow crystals of **3.7** were obtained upon layering hexane over the solution (0.8 g, 1.1 mmole, 38 % yield).

I.R. (Nujol, cm^{-1}) ν : 3064(w), 2729(w), 2360(w), 2342(w), 1307(w), 1257(s), 1096(w), 1036(s), 955(w), 913(w), 801(w), 754(s), 739(s).

1H NMR (200 MHz, THF- d_8 , 22 °C) δ : 1.68 (br s, THF), 2.42 (br s, CH_3), 3.54 (br s, THF), 5.53 (br s, CH).

^{13}C NMR (125.76 MHz, THF- d_8 , 22 °C) δ : 16.70 (CH_3 -pyrrole), 26.40 (CH_2 -THF), 68.20 (CH_2 -THF), 105.70 (CH-pyrrole), 133.20 (quaternary C-pyrrole).

III.4: Results and Discussion

Treatment of $\text{SmCl}_3(\text{THF})_3$ with two equivalents of the lithium salt of 2,5-dimethylpyrrole followed by reduction using metallic lithium under argon atmosphere in THF afforded complex **3.1** in a 57% yield. The dark colour observed for this compound is indicative of a divalent samarium atom, observation which was further validated by the measurement of the magnetic moment. The composition of **3.1** was conclusively determined by elemental analysis and confirmed by X-ray crystal determination.

The complex (Figure 3.1) consists of a divalent Sm center surrounded by three π -bonded 2,5-dimethylpyrrole fragments [$\text{Sm-N}(1)_{\text{centroid}} = 2.733(14)\text{\AA}$; $\text{Sm-N}(2)_{\text{centroid}} = 2.701(14)\text{\AA}$; $\text{Sm-N}(3)_{\text{centroid}} = 2.707(14)\text{\AA}$] and by a chlorine atom [$\text{Sm-Cl} = 2.891(4)\text{\AA}$]. If each pyrrole ring centroid is regarded as occupying a single coordination site the coordination geometry around the Sm atom can be considered as distorted tetrahedral [$\text{Cl-Sm-N}(1)_{\text{centroid}} = 97.1(7)^\circ$; $\text{Cl-Sm-N}(2)_{\text{centroid}} = 100.5(7)^\circ$; $\text{Cl-Sm-N}(3)_{\text{centroid}} = 101.6(7)^\circ$]. The structure also contains two lithium atoms. The first is σ -bonded to two pyrrolide ligand N atoms [$\text{Li}(2)\text{-N}(2) = 2.116(3)\text{\AA}$; $\text{Li}(2)\text{-N}(3) = 2.047(4)\text{\AA}$] while the second is attached to a single pyrrolide ligand N atom [$\text{Li}(1)\text{-N}(1)_{\text{centroid}} = 2.064(3)\text{\AA}$] and to the chlorine [$\text{Li}(1)\text{-Cl} = 2.327(3)\text{\AA}$]. Each lithium atom is also co-ordinated to two THF molecules [$\text{Li}(1)\text{-O}(1) = 1.964(3)\text{\AA}$]. Like the Sm centre, the lithium atoms adopt a distorted tetrahedral geometry [$\text{Cl-Li}(1)\text{-N}(1) = 104.0(17)^\circ$; $\text{Cl-Li}(1)\text{-O}(1) = 109.4(17)^\circ$; $\text{Cl-Li}(1)\text{-O}(2) = 107.8(17)^\circ$].

The bonding mode adopted by the pyrrolide ligands is consistent with that observed in the dipyrrolide complexes of divalent samarium. However, in these particular

derivatives the metal usually sustains two π -bonds and two σ -bonds, as opposed to three π -bonds observed in the present case. It is important to note that these cyclopentadienyl analogues do not form the expected Cp_2Sm type of complexes, and the -ate anionic type of structure is possibly the result of the presence of the additional coordinating nitrogen atoms in the pyrrole ring.

In order to evaluate the role of the chloride atom in determining the structure of the complex, a similar reaction was carried out with $\text{SmI}_2(\text{THF})_2$ and three equivalents of the lithium salt of 2,5-dimethylpyrrole. The reaction was carried out at room temperature, in THF and in the presence of TMEDA yielding crystalline material which was identified by X-ray crystallography as $(\mu\text{-}\eta^1, \eta^5\text{-Me}_2\text{C}_4\text{H}_2\text{N})_3\text{Sm}(\mu\text{-I})\{\text{Li}(\text{TMEDA})_2\}\{\text{Li}(\text{OEt})_2\}$ (3.2) (Figure 3.2). The formulation was in accordance with the characterisation analytical and magnetic data. Besides the solvation of the Li atom [$\text{Li}(1)\text{-N}(4) = 2.518(9)\text{\AA}$; $\text{Li}(1)\text{-N}(5) = 2.179(10)\text{\AA}$], the structure of 3.2 is very similar to that of 3.1 except for the replacement of chlorine by iodine [$\text{Sm-I} = 3.246(5)\text{\AA}$; $\text{I-Sm-N}(1)_{\text{centroid}} = 98.0(14)\text{\AA}$; $\text{I-Sm-N}(2)_{\text{centroid}} = 103.7(14)\text{\AA}$; $\text{I-Sm-N}(3)_{\text{centroid}} = 101.0(14)\text{\AA}$]. The samarium atom still adopts a similarly distorted tetrahedral geometry, and it seems that changing the halide does not cause a substantial structural modification.

In contrast to the apparent lack of role played by the halogen, the nature of the alkali cation can have a large impact on the structure of the product. Treatment of $\text{SmCl}_3(\text{THF})_3$ with three equivalents of the sodium salt of 2,5-dimethylpyrrole followed by reduction with metallic sodium in THF afforded a new complex [$\{(\text{Na}(\text{THF})_2)(\mu\text{-}\eta^1, \eta^5\text{-Me}_2\text{C}_4\text{H}_2\text{N})_2\text{Sm}\}_2(\mu\text{-}\eta^1, \eta^5\text{-Me}_2\text{C}_4\text{H}_2\text{N})_2$] (3.3) in 58% yield. Again, the dark red-brown colour of the crystals indicates the presence of divalent samarium atoms.

Analytical data and magnetic moment calculations were consistent with the structural formulation as elucidated by an X-ray crystal structure (Figure 3.3). The complex is a symmetry-generated dimer where two samarium atoms are bridged by two π -bonded pyrrolide rings. Each samarium atom is co-ordinated to four 2,5-dimethylpyrrolyle units, two of which being σ -bonded [Sm(1)-N(3)=2.602(9)Å; Sm(1)-N(1A)=2.623(8)Å], and two π -coordinated [Sm(1)-N(1)_{centroid}=2.675(12)Å; Sm(1)-N(2)_{centroid}=2.651(12)Å]. Two sodium atoms, both σ and π -bonded to 2,5-dimethylpyrrole ligands [Na(1)-N(2) = 2.385(11)Å; Na(1)-N(3)_{centroid} = 2.543(14)Å] are located to the exterior of the molecule and complete the structure. Each Na atom is also coordinated to two THF molecules [Na(1)-O(1) = 2.347(11)Å; Na(1)-O(2) = 2.307(10)Å]. The bonding observed around each samarium is basically identical to that observed in complexes containing dipyrrolide-based ligands, the only difference consisting of the absence of linking carbon backbone. It is at least surprising that this complex does not react with N₂ given the very close resemblance with a bent metallocene and the identical coordination environment to that of a dipyrrolide. This behavior demonstrates once again that the nature of the alkali cation used to pursue the reaction has a substantial impact on the reaction pathway. It is possible in this case that the larger ionic radius of sodium prevents it from binding the samarium directly, as was done by the smaller lithium atoms in the complexes 3.1 and 3.2.

Reaction of YbCl₃(THF)₃ with two equivalents of the lithium salt of 2,5-dimethylpyrrole and the subsequent reduction with metallic lithium afforded a mixture of two compounds: the orange [(μ - η^1, η^5 -Me₂C₄H₂N)₂Yb(μ -Cl){Li(OEt₂)}]₂ (3.4) and the yellow [(μ - η^1, η^5 -Me₂C₄H₂ N)₂Yb(μ -Cl)₂{Li(OEt₂)} {Li(THF)(OEt₂)}]₂ (3.5). Complex

3.4 was characterised through elemental analysis, ^1H NMR, and ^{13}C NMR, all of which support the structure determination yielded by X-ray crystallography (Figure 3.4). The complex is dimeric with two divalent ytterbium centers bridged by two chlorine atoms [$\text{Yb-Cl} = 2.711(3)\text{\AA}$; $\text{Yb-Cl(A)} = 2.688(3)\text{\AA}$]. Each ytterbium is also π -bonded to two 2,5-dimethylpyrrole ligands [$\text{Yb-N(1)}_{\text{centroid}} = 2.459(15)\text{\AA}$; $\text{Yb-N(2)}_{\text{centroid}} = 2.456(15)\text{\AA}$]. The structure also contains two lithium atoms that are σ -bonded to two pyrrolide ligands [$\text{Li-N(1)} = 2.020(2)\text{\AA}$; $\text{Li-N(2A)} = 1.980(2)\text{\AA}$] and bearing each one molecule of ether [$\text{Li-O(1)} = 1.870(2)\text{\AA}$].

While complex 3.4 was isolated from the reaction mixture as an analytically pure crystalline solid, complex 3.5 was obtained as a minor product of a second crop of crystalline material from the reaction mother liquor where 3.4 was the major component. Since physical separation of the crystalline mass proved unfeasible for analytical purposes, X-ray structure determination was the only possibility to identify complex 3.5. Complex 3.5 also has a dimeric structure that contains two divalent Yb atoms. Each unit contains an ytterbium atom that is π -bonded to two 2,5-dimethylpyrrole ligands [$\text{Yb-N(1)}_{\text{centroid}} = 2.469(10)\text{\AA}$; $\text{Yb-N(2)}_{\text{centroid}} = 2.54(10)\text{\AA}$] and σ -bonded to two chlorine atoms [$\text{Yb-Cl(1)} = 2.682(3)\text{\AA}$; $\text{Yb-Cl(2)} = 2.744(2)\text{\AA}$] providing a distorted tetrahedral geometry to the metal centre. Each unit also contains two lithium atoms that are σ -bonded to a pyrrolide ligand [$\text{Li(1)-N(1)} = 2.066(2)\text{\AA}$] and to a chlorine atom [$\text{Li(1)-Cl(1)} = 2.403(17)\text{\AA}$]. One of these lithium atoms is coordinated to two solvent molecules (one being THF and the other ether) while the second lithium atom is coordinated to an ether molecule [$\text{Li(2)-O(4)} = 1.985(19)\text{\AA}$] and a chloride atom from the second [$\text{Li(2)-Cl(2A)} = 2.452(16)\text{\AA}$] unit to form the dimeric structure. In its composition, complex 3.5

is very similar to complex 3.4, except that it contains two extra LiCl molecules and four extra solvent molecules.

Comparing the previous reaction to its chloride free counterpart, we proceeded with the reaction of $\text{SmI}_2(\text{THF})_2$ with two equivalents of the lithium salt of 2,5-dimethylpyrrole in THF at room temperature. Red crystals of $[(\mu\text{-}\eta^1, \eta^5\text{-Me}_2\text{C}_4\text{H}_2\text{N})_2\text{Yb}(\mu\text{-I})_2\{\text{Li}(\text{THF})\}_2]_n$ (3.6) were obtained from toluene after work-up of the reaction mixture. Elemental analysis, ^1H -NMR and ^{13}C -NMR were in agreement with the structure elucidated by X-ray diffraction analysis (Figure 3.6). Complex 3.6 is very similar to 3.5, the only difference arising from the nature of the halogen atom (iodine versus chlorine). The divalent ytterbium atoms are still π -bonded by the pyrrolide ligands [$\text{Yb-N}(1)_{\text{centroid}} = 2.440(7)\text{\AA}$; $\text{Yb-N}(2)_{\text{centroid}} = 2.450(7)\text{\AA}$], and also σ -ligated to two iodine atoms [$\text{Yb-I}(1) = 3.1203(5)\text{\AA}$; $\text{Yb-I}(2) = 3.1174(5)\text{\AA}$] thus adopting a distorted tetrahedral geometry. The only other noticeable difference between complex 3.5 and 3.6 is that in the latter the ether molecules are partially replaced by THF. The central lithium atoms bears two THF molecules [$\text{Li}(1)\text{-O}(1) = 1.922(12)\text{\AA}$] while the terminal lithium is bonded to only one solvent molecule [$\text{Li}(2)\text{-O}(2) = 1.908(13)\text{\AA}$]. The presence of resulting empty coordination sites is responsible for the aggregation of these units leading to polymeric aggregation.

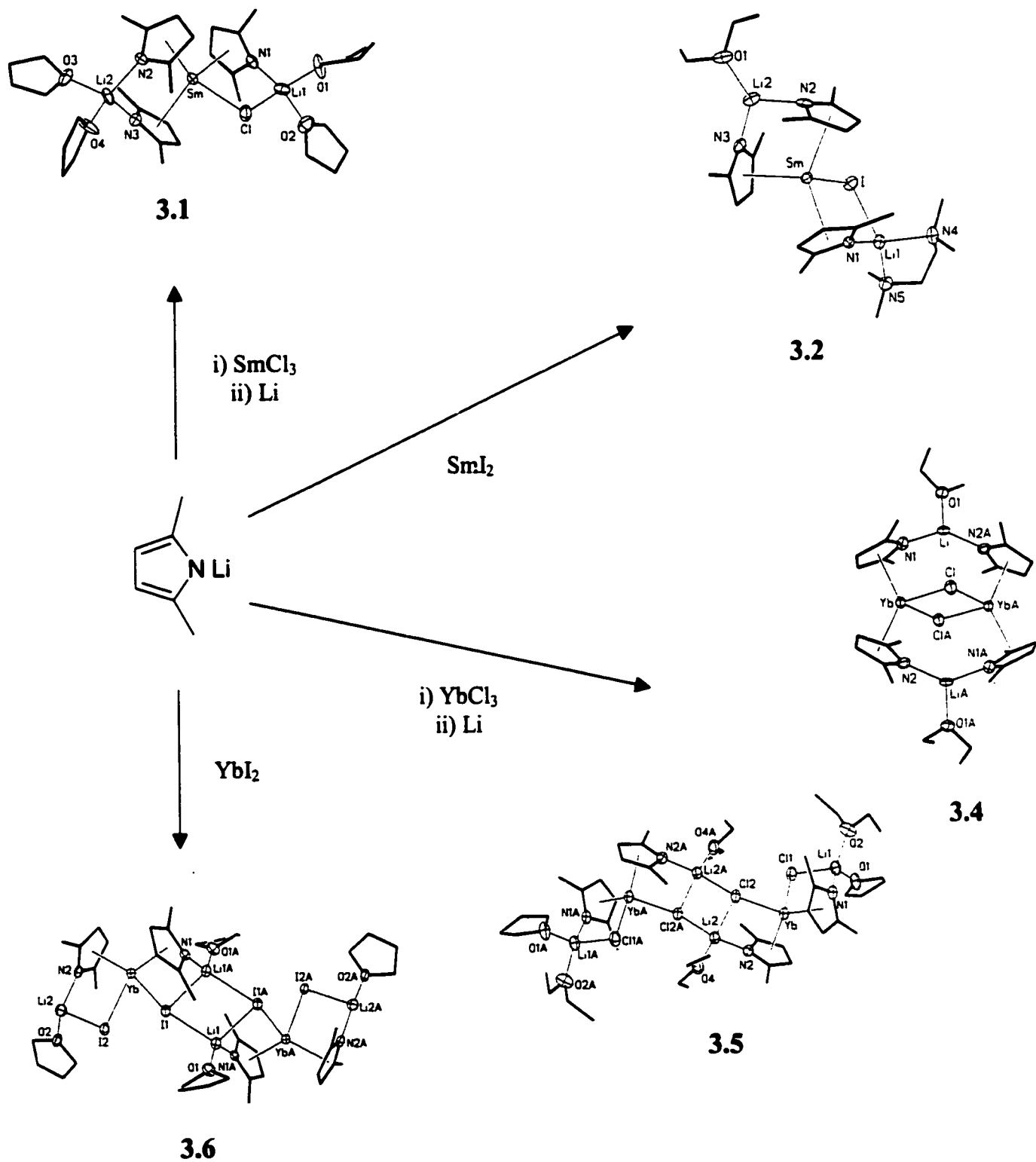
In order to complete the series of experiments aimed to assess the role of the alkali cation in determining the structure and nuclearity of these complexes, we carried out the reaction of $\text{YbI}_2(\text{THF})_2$ with two equivalents of the potassium salt of 2,5-dimethylpyrrole in THF at room temperature. Yellow crystals of $[(\mu\text{-}\eta^1, \eta^5\text{-Me}_2\text{C}_4\text{H}_2\text{N})_4\{\text{K}(\text{THF})\}_2\text{Yb}]_n$ (3.7) were obtained from the reaction that were

characterised as usual by elemental analysis, $^1\text{H-NMR}$ and $^{13}\text{C-NMR}$. The structure of **3.7** was clarified by X-ray structural determination (Figure 3.7). Complex **3.7** has a polymeric structure consisting of units that contain a single divalent ytterbium atom. Each of these lanthanide metals is σ -bonded to four pyrrolide ligands [$\text{Yb-N}(1) = 2.378(4)$; $\text{Yb-N}(1\text{C}) = 2.378(4)$; $\text{Yb-N}(2) = 2.409(4)$; $\text{Yb-N}(2\text{C}) = 2.409(4)$], which causes the metal to adopt a pseudo-tetrahedral geometry [$\text{N}(1)\text{-Yb-N}(2) = 93.4(2)^\circ$; $\text{N}(1)\text{-Yb-N}(2\text{C}) = 115.0(2)^\circ$; $\text{N}(1)\text{-Yb-N}(1\text{C}) = 117.8(2)^\circ$]. The structure also contains two potassium atoms that are π -bonded to two pyrrolide ligands [$\text{K}(\text{OB})\text{-N}(1)_{\text{centroid}} = 2.910(8)\text{\AA}$; $\text{K}(\text{OB})\text{-N}(2)_{\text{centroid}} = 2.675(8)\text{\AA}$], and also coordinated to a THF molecule [$\text{K}(\text{OB})\text{-O}(1\text{B}) = 2.675(5)\text{\AA}$]. These potassium atoms are responsible for the polymeric structure of this compound, as each atom is coordinated by a 2,5-dimethylpyrrole fragment, leading to an array where every unit is linked to four others. This structure of **3.7** is a significant departure from the structures observed previously for reactions involving the lithium salt of 2,5-dimethylpyrrole and ytterbium, once again emphasising the central role the alkali cation on both the structure and molecular aggregation. It is interesting to note that, in contrast to most of the structures described earlier, the pyrrolide ligands in complex **3.7** prefer to coordinate the Yb centre through σ -bonds instead of π -bonds.

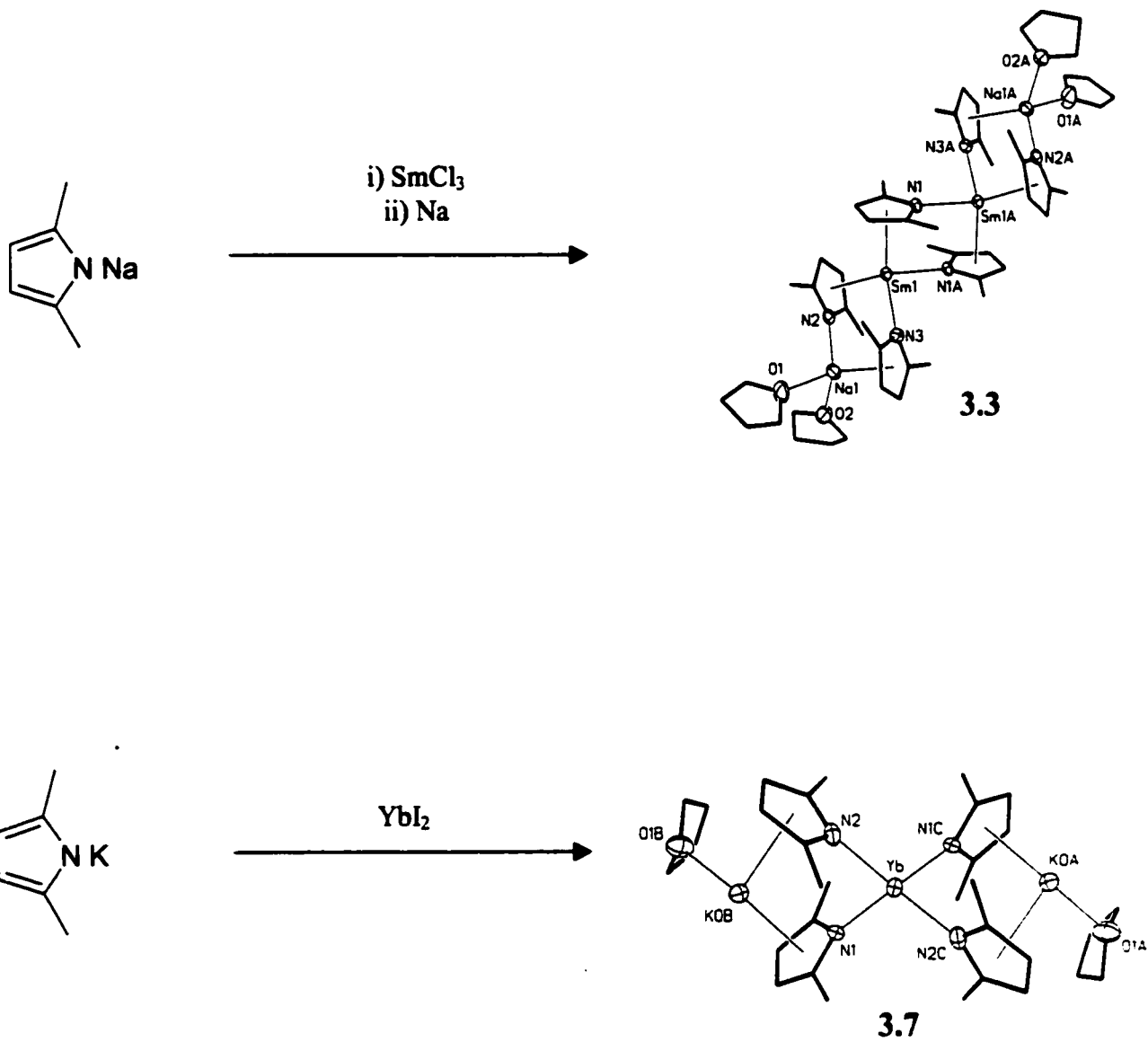
From the structures reported in this chapter, it seems likely that the bonding mode adopted by 2,5-dimethylpyrrole is directed, not by the lanthanide metal or the solvent used, but by the choice of alkali metal. All the structures that include lithium atoms (complexes **3.1**, **3.2**, **3.4**, **3.5** and **3.6**) have pyrrolide fragments that exclusively form π -bonds to the Sm or Yb centers while the pyrrole nitrogen is σ -bonded to the lithium atom.

The utilisation of Na instead of Li such as in complex 3.3, causes samarium to be both π and σ -bonded to the 2,5-dimethylpyrrolide ligands since the sodium atom is also bonded in a similar fashion. Finally, replacement by potassium as observed in complex 3.7 produces lanthanide centers that form σ interactions exclusively, as the potassium cations feature only π -interactions to the pyrrolide rings. Thus, it appears that the bonding mode enjoyed by the lanthanide metal is wholly dependent on the nature of the bonding between the pyrrolide ligand and the alkali metal. A hard alkali cation such as lithium is better stabilised by σ -bonding the ligand which in turn confers π -bonding to the lanthanide centre, while a softer alkali metal such as potassium prefers to interact with the π electrons, which leads to a σ -bonded Sm or Yb centre.

Scheme 3.1



Scheme 3.2



III.5: Structural Considerations

Suitable crystals were selected, mounted on thin glass fibres using viscous oil and cooled to the data collection temperature. Data was collected on a Bruker AX SMART 1k CCD diffractometer using 0.3° ω -scans at 0, 90, and 180° in ϕ . Unit-cell parameters were determined from 60 data frames collected at different sections of the Ewald sphere. Semi-empirical absorption corrections based on equivalent reflections were applied (Blessing, R., *Acta Cryst.*, 1995, A51, 33-38).

No symmetry higher than triclinic was evident from the diffraction data of 3.1, 3.2·2(thf), and 3.6·0.5(toluene). Solution in the centric option yielded chemically reasonable and computationally stable results of refinement. Systematic absences in the diffraction data and unit-cell parameters were uniquely consistent for the reported space groups for 3.3·0.5(diethyl ether), 3.4, 3.5, and 3.7. The structures were solved by direct methods, completed with difference Fourier syntheses and refined with full-matrix least-squares procedures based on F^2 . The absolute configuration parameter in 3.7 refined to nil indicating that the true hand of the data has been determined.

Two symmetry unique but chemically identical molecules of 3.2 are located each at an inversion center. The compound molecule for 3.5 is located at an inversion center. Compounds 3.6 and 3.7 are infinite polymers propagated by inversion and by two-fold rotation, respectively. A coordinated solvent in 3.5 was resolved to be diethyl ether/thf with a site occupancy distribution of 60/40. A toluene solvent molecule was located cocrystallized at half-occupancy at an inversion center of 3.6·0.5(toluene). Two molecules of tetrahydrofuran (thf) solvent were found in the asymmetric unit of 3.2·2(thf). A molecule of diethyl ether solvent was found rotationally disordered along its

molecular axis at half-occupancy at an inversion center in 3.3·0.5(diethyl ether). All non-coordinated, cocrystallized molecules were refined isotropically with cyclic molecules refined as flat polygons. All other non-hydrogen atoms were refined with anisotropic displacement parameters. All hydrogen atoms were treated as idealised contributions. All scattering factors and anomalous dispersion factors are contained in the SHEXTL 5.10 program library (Sheldrick, G. M., Bruker AXS, Madison, WI, 1997).

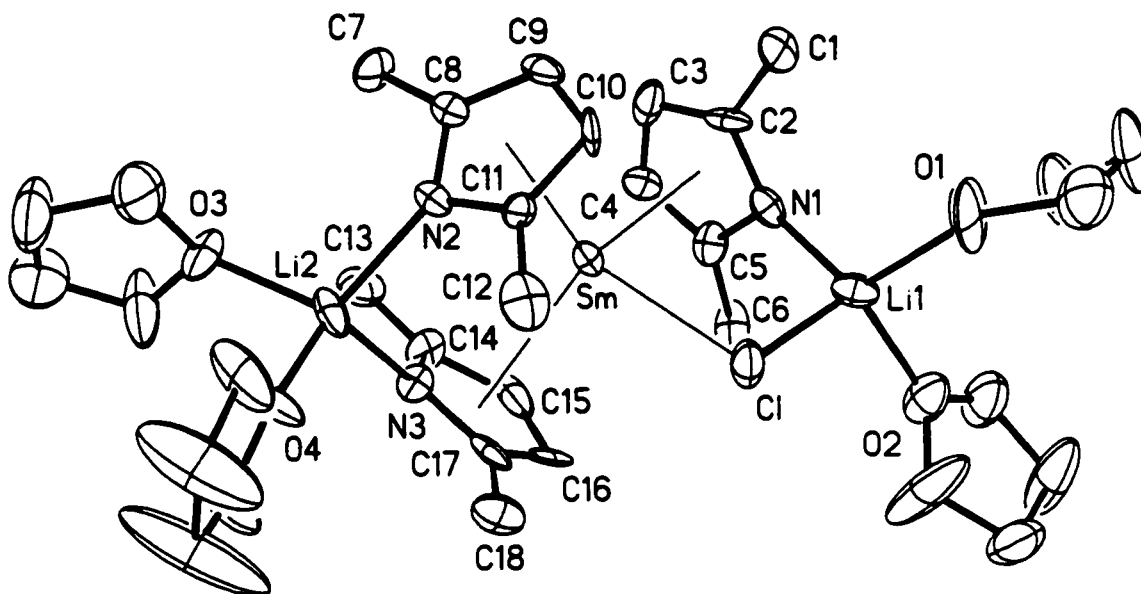


Figure 3.1: Thermal ellipsoid plot of $[(\mu\text{-}\eta^1, \eta^5\text{-Me}_2\text{C}_4\text{H}_2\text{N})_3\text{Sm}(\mu\text{-Cl})\{\text{Li}(\text{THF})_2\}_2]$.

Thermal ellipsoids are drawn at the 30% probability level.

Selected Bond Distances (Å) and Angles (deg): $\text{Sm-N}(1)_{\text{centroid}}=2.733(14)$,

$\text{Sm}(1)\text{N}(1\text{A})=2.623(8)$, $\text{Sm-N}(3)_{\text{centroid}}=2.707(14)$, $\text{Sm-Cl}=2.891(4)$, $\text{L}(1)\text{-N}(1)=2.064(3)$,

$\text{L}(1)\text{-C}(1)=2.327(3)$, $\text{L}(1)\text{-O}(1)=1.964(3)$, $\text{L}(1)\text{-O}(2)=2.026(3)$, $\text{L}(2)\text{-N}(2)=2.116(3)$, $\text{L}(2)\text{-}$

$\text{N}(3)=2.047(4)$, $\text{Cl-Sm-N}(1)_{\text{centroid}}=97.1(7)$, $\text{Cl-Sm-N}(2)_{\text{centroid}}=100.5(7)$, Cl-Sm-

$\text{N}(3)_{\text{centroid}}=101.6(7)$, $\text{Cl-Li}(1)\text{-N}(1)=104.0(17)$, $\text{Cl-Li}(1)\text{-O}(1)=109.4(17)$, $\text{Cl-Li}(1)\text{-}$

$\text{O}(2)=107.8(17)$,

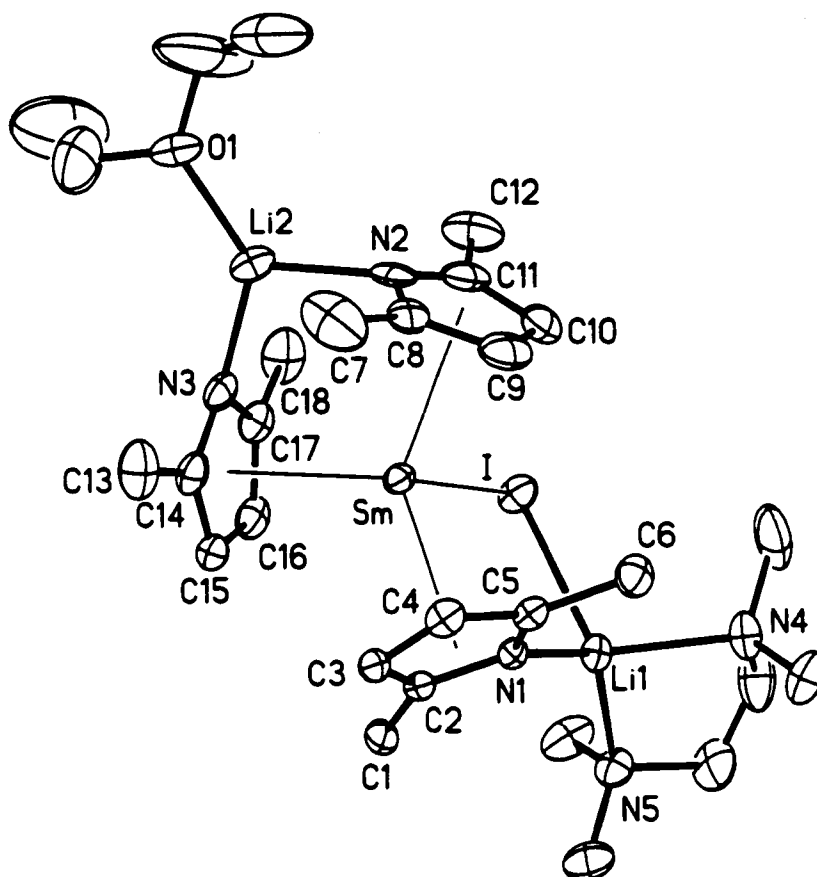


Figure 3.2: Thermal ellipsoid plot of $[(\mu\text{-}\eta^1, \eta^5\text{-Me}_2\text{C}_4\text{H}_2\text{N})_3\text{Sm}(\mu\text{-I})\{\text{Li}(\text{TMEDA})_2\}\{\text{Li}(\text{OEt}_2)_2\}]$. Thermal ellipsoids are drawn at the 30% probability level.

Selected Bond Distances (Å) and Angles (deg): $\text{Sm-N}(1)_{\text{centroid}}=2.656(5)$, $\text{Sm-N}(2)_{\text{centroid}}=2.705(5)$, $\text{Sm-N}(3)_{\text{centroid}}=2.678(5)$, $\text{Sm-I}=3.246(5)$, $\text{Li}(1)\text{-I}=2.873(9)$, $\text{Li}(1)\text{-N}(1)=2.016(9)$, $\text{Li}(1)\text{-N}(4)=2.158(9)$, $\text{Li}(1)\text{-N}(5)=2.179(10)$, $\text{Li}(2)\text{-N}(2)=2.095(13)$, $\text{Li}(2)\text{-N}(3)=1.966(13)$, $\text{Li}(2)\text{-O}(1)=1.901(12)$, $\text{I-Sm-N}(1)_{\text{centroid}}=98.0(14)$, $\text{I-Sm-N}(2)_{\text{centroid}}=103.7(14)$, $\text{I-Sm-N}(3)_{\text{centroid}}=101.0(14)$, $\text{I-Li}(1)\text{-N}(1)=96.3(3)$, $\text{I-Li}(1)\text{-N}(4)=105.5(4)$, $\text{I-Li}(1)\text{-N}(5)=114.4(3)$, $\text{O}(1)\text{-Li}(2)\text{-N}(2)=126.9(7)$, $\text{O}(1)\text{-Li}(2)\text{-N}(3)=126.0(7)$,

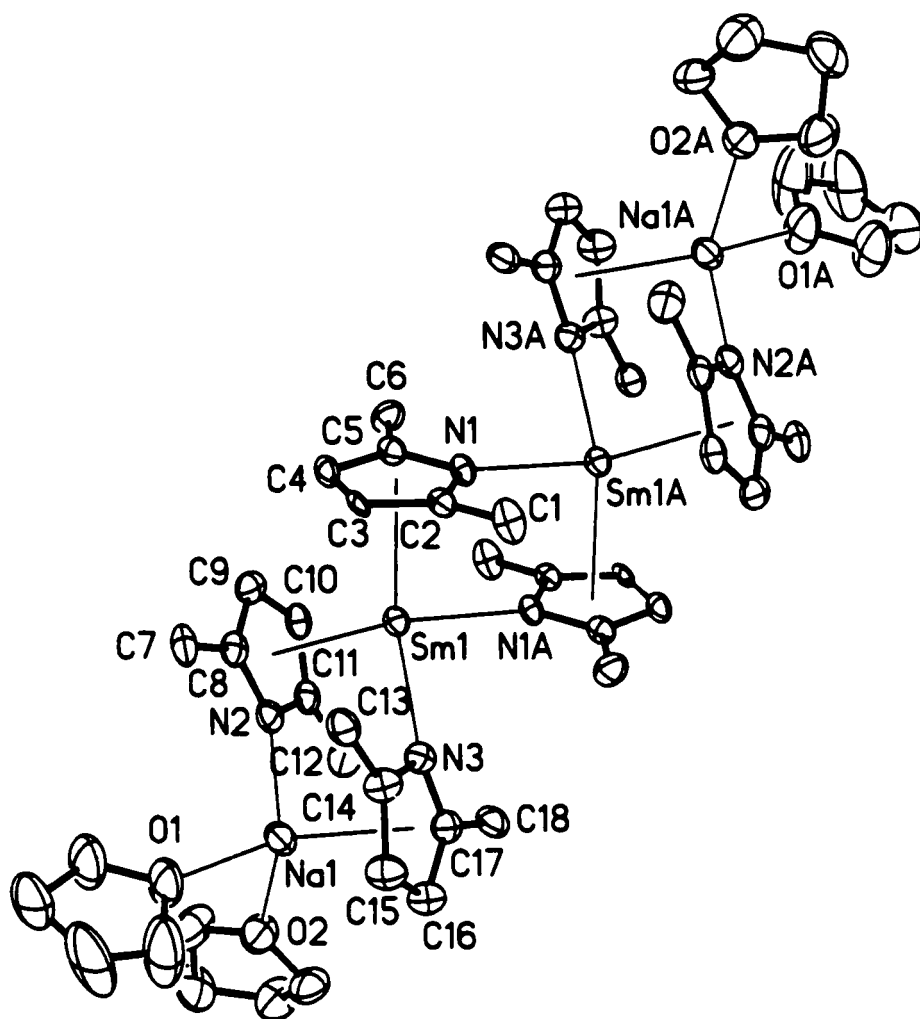


Figure 3.3: Thermal ellipsoid plot of $[\{(\text{Na}(\text{THF})_2)(\mu\text{-}\eta^1, \eta^5\text{-Me}_2\text{C}_4\text{H}_2\text{N})_2\text{Sm}\}_2(\mu\text{-}\eta^1, \eta^5\text{-Me}_2\text{C}_4\text{H}_2\text{N})_2]$. Thermal ellipsoids are drawn at the 30% probability level.

Selected Bond Distances (Å) and Angles (deg): Sm(1)-N(1A)=2.623(8), Sm(1)-N(1)_{centroid}=2.675(12), Sm(1)-N(2)_{centroid}=2.651(12), Sm(1)-N(3)=2.602(9), Na(1)-O(1)=2.347(11), Na(1)-O(2)=2.307(10), Na(1)-N(1)=2.385(11), Na(1)-N(3)=2.543(14), N(3)-Sm(1)-N(1A)=98.7(3), N(3)-Sm(1)-N(1)_{centroid}=119.6(4), N(3)-Sm(1)-N(2)_{centroid}=102.2(4), O(1)-Na(1)-O(2)=91.0(4), O(1)-Na(1)-N(2)=117.0(4), O(1)-Na(1)-N(3)_{centroid}=115.4(4),

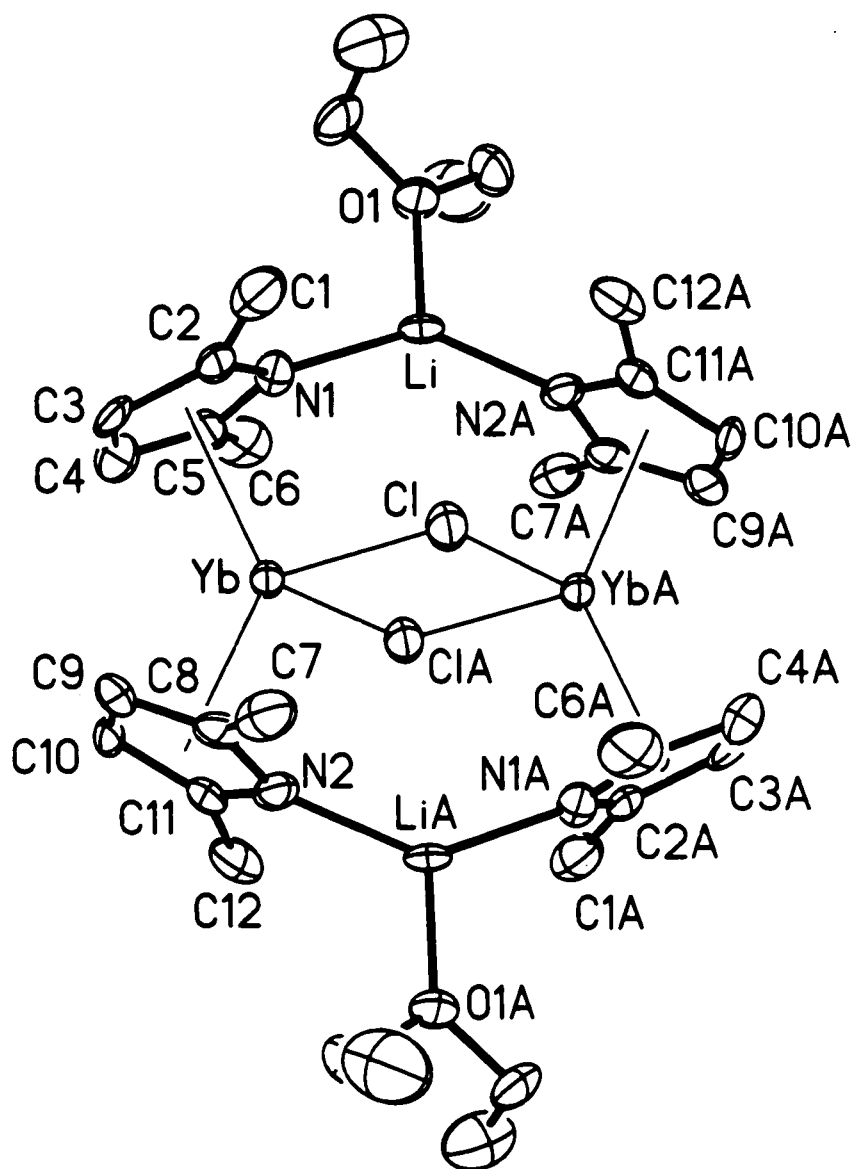


Figure 3.4: Thermal ellipsoid plot of $[(\mu\text{-}\eta^1, \eta^5\text{-Me}_2\text{C}_4\text{H}_2\text{N})_2\text{Yb}(\mu\text{-Cl})\{\text{Li}(\text{OEt}_2)\}]_2$.

Thermal ellipsoids are drawn at the 30% probability level.

Selected Bond Distances (Å) and Angles (deg): Yb-Cl=2.711(3), Yb-Cl(A)=2.688(3),
 Yb-N(1)_{centroid}=2.459(15), Yb-N(2)_{centroid}=2.456(15), Li-O(1)=1.870(2), Li-
 N(1)=2.020(2), Li-N(2A)=1.980(2), Cl-Yb-N(1)_{centroid}=107.3(11), Cl-Yb-
 N(2)_{centroid}=106.5(11), Cl-Yb-Cl(A)=87.63(11), N(1)-Li-O(1)=110.4(11), N(1)-Li-
 N(2A)=136.4(11)

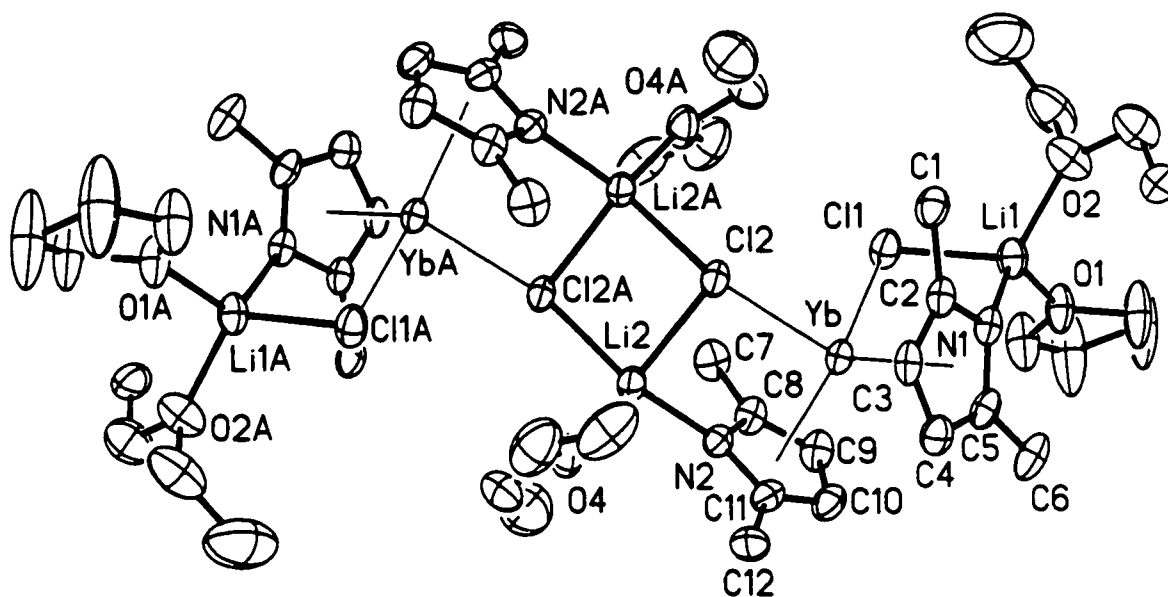


Figure 3.5: Thermal ellipsoid plot of $[(\mu\text{-}\eta^1, \eta^5\text{-Me}_2\text{C}_4\text{H}_2\text{N})_2\text{Yb}(\mu\text{-Cl})_2\{\text{Li}(\text{OEt}_2)\}\{\text{Li}(\text{THF})(\text{OEt}_2)\}]_2$. Thermal ellipsoids are drawn at the 30% probability level.

Selected Bond Distances (Å) and Angles (deg): Yb-N(1)_{centroid}=2.469(10), Yb-N(2)_{centroid}=2.454(10), Yb-Cl(1)=2.682(3), Yb-Cl(2)=2.744(2), Li(1)-Cl(1)=2.403(17), Li(1)-N(1)=2.066(2), Li(1)-O(1)=1.958(18), Li(1)-O(2)=2.010(4), Li(2)-N(2)=2.074(17), Li(2)-O(4)=1.985(19), Li(2)-Cl(2)=2.452(16), Li(2)-Cl(2A)=2.457(16), Cl(1)-Yb-Cl(2)=99.5(8), Cl(1)-Yb-N(1)_{centroid}=103.3(8), Cl(1)-Yb-N(2)_{centroid}=110.9(8), Cl(1)-Li(1)-N(1)=97.3(7), Cl(1)-Li(1)-O(1)=101.0(8), Cl(1)-Li(1)-O(2)=116.3(19), Cl(1)-Li(2)-Cl(2A)=94.1(6), Cl(1)-Li(2)-N(2)=96.5(6), Cl(1)-Li(2)-O(4)=121.6(8)

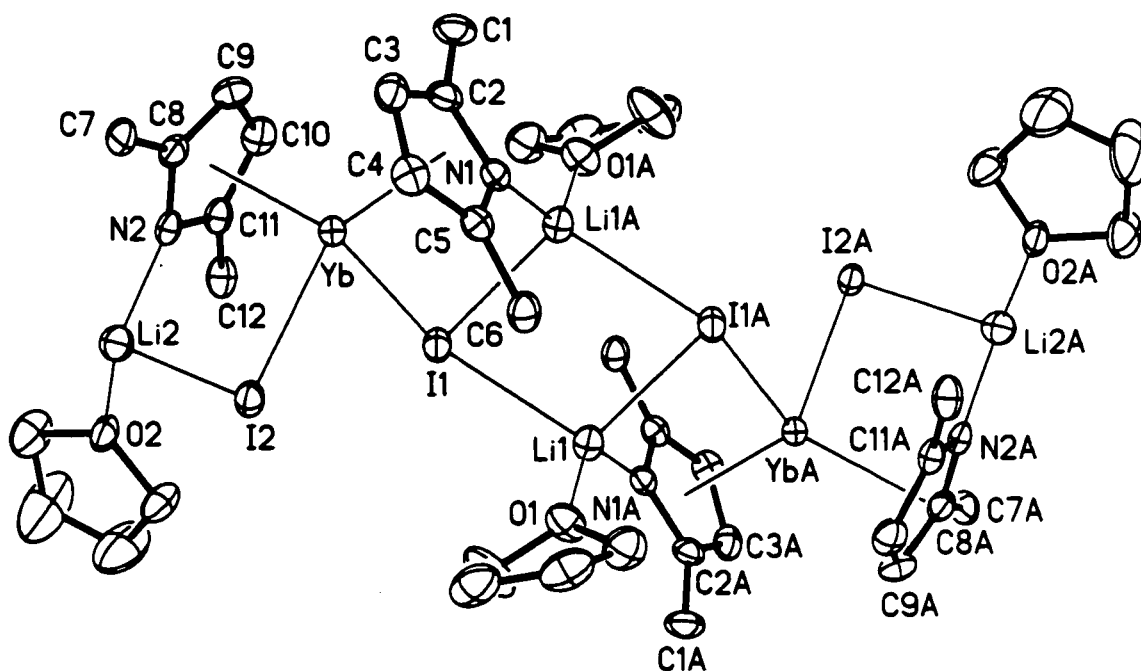


Figure 3.6: Thermal ellipsoid plot of $[(\mu\text{-}\eta^1, \eta^5\text{-Me}_2\text{C}_4\text{H}_2\text{N})_2\text{Yb}(\mu\text{-I})_2\{\text{Li}(\text{THF})\}_2]_n$.

Thermal ellipsoids are drawn at the 30% probability level.

Selected Bond Distances (Å) and Angles (deg): Yb-N(1)_{centroid}=2.440(7), Yb-N(2)_{centroid}=2.450(7), Yb-I(1)=3.1203(5), Yb-I(2)=3.1174(5), Li(2)-N(2)=2.007(13), Li(2)-I(2)=2.851(12), Li(2)-O(2)=1.908(13), Li(1A)-N(1)=2.011(12), Li(1A)-O(1A)=1.922(12), Li(1A)-I(1)=2.835(12), Li(1A)-I(1A)=2.872(12), I(1)-Yb-N(1)_{centroid}=105.3(19), I(1)-Yb-N(2)_{centroid}=109.8(19), I(1)-Yb-I(2)=92.9(15), I(2)-Li(2)-N(2)=98.2(5), I(2)-Li(2)-O(2)=108.5(5), O(2)-Li(2)-N(2)=122.2(6), I(1)-Li(1A)-N(1)=98.6(5), I(1)-Li(1A)-O(1A)=106.9(5), I(1)-Li(1A)-I(1A)=103.8(4),

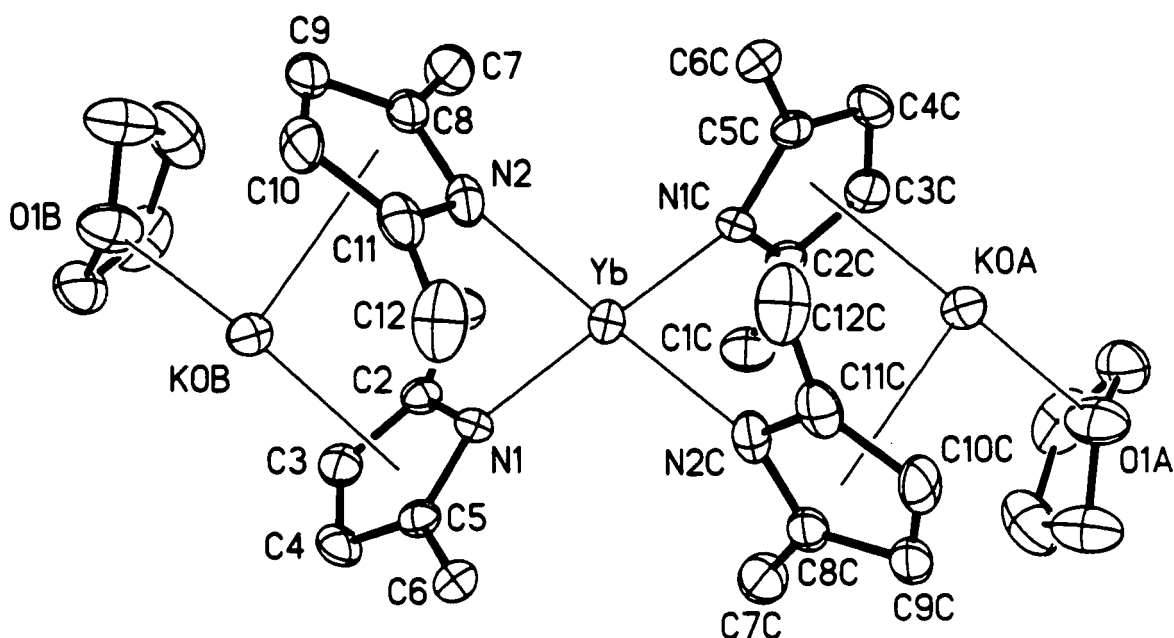


Figure 3.7: Thermal ellipsoid plot of $[(\mu\text{-}\eta^1, \eta^5\text{-Me}_2\text{C}_4\text{H}_2\text{N})_4\{\text{K}(\text{THF})\}_2\text{Yb}]_n$. Thermal ellipsoids are drawn at the 30% probability level.

Selected Bond Distances (Å) and Angles (deg): Yb-N(1)=2.378(4), Yb-N(2)=2.409(4), Yb-N(1C)=2.378(4), Yb-N(2C)=2.409(4), K(OB)-N(1)_{centroid}=2.910(8), K(OB)-N(2)_{centroid}=2.983(8), K(OB)-O(1B)=2.675(8), N(1)-Yb-N(2)=93.4(2), N(1)-Yb-N(1C)=117.8(2), N(1)-Yb-N(2C)=115.0(2), O(1B)-K(OB)-N(1)_{centroid}=110.5(17), O(1B)-K(OB)-N(2)_{centroid}=106.8(17),

III.6: Conclusion

By using the monopyrroldie ligand of 2,5-dimethylpyrrole, it was possible to synthesise and isolate several divalent lanthanide complexes. In spite of the close similarity of the monopyrrole with the Cp ligands, complexes of divalent samarium and ytterbium did not resemble the expected Cp_2Ln type of structure. The polynuclearity of the structures stems from the presence of the deprotonated nitrogen atom on the pyrrole ring, which also provides the opportunity for the σ coordination mode not found in cyclopentadienyl systems. When the halide used in the lanthanide starting material was changed from chloride to iodide, no significant structural variation was observed in the molecular structures. Alternately, upon varying the salt used to prepare the ligand led to very different bonding modes for the lanthanide centers. Hard alkali cations, such as lithium, encourage the π coordination of the Sm or Yb centres by binding the pyrrolide fragments in a σ fashion, while softer alkali cations such as potassium interact with the ligands through π interactions, leading to ligand-metal σ -bonds. The ability of the alkali cation to remain attached to the ligand system of divalent lanthanide and to determine the type of Ln-ligand bonding mode is fascinating, since it provides a tool to tune the metal redox potential

References

- 1 a) Molander, G.A., Hoberg, J.O., *J. Org. Chem.*, **1992**, 57, 3266;
 b) Jeske, G., Jauke, H., Mauermann, H., Shumann, H., Marks, T.J., *J. Am. Chem. Soc.*, **1985**, 107, 8111.
 c) Evans, W.J., Bloom, I., Hunter, W.E., Atwood, J.L., *J. Am. Chem. Soc.*, **1983**, 105,1401.
- 2 a) Li, Y., Marks, T.J., *J. Am., Chem. Soc.*, **1996**, 118, 9295;
 b) Li, Y., Marks, T.J., *Organometallics*, **1996**, 15, 3770;
 c) Li, Y., Marks, T.J., *J. Am., Chem. Soc.*, **1996**, 118,707;
 d) Gagné, M.R., Nolan, S.P., Marks, T.J., *Organometallics*, **1990**, 9,1716.
- 3 a) Takahashi, T., Hasegawa, M., Suzuki, N., Saburi, M., Rousset, C.J., Fanwick, P.E., Nagishi, E.J., *J. Am. Chem. Soc.*, **1991**, 113, 8564;
 b) Fu, P.F., Brard, L., Li, Y., Marks, T.J., *J. Am. Chem. Soc.*, **1995**, 117, 7157;
 c) Molander, G.A., Julius, M., *J. Org. Chem.*, **1992**, 57, 6347.
- 4 a) Bijpost, E.A., Duchateau, R., Teuben, J.H., *J. Mol. Catal.*, **1995**, 95, 121;
 b) Harrison, K.N., Marks, T.J., *J. Am. Chem. Soc.*, **1992**, 114, 9220.
- 5 a) Thompson, M.E., Bercaw, J.E., *Pure Applied Chemistry*, **1984**, 56, 1.

- b) Burger, B.J., Thompson, M.E., Bercaw, J.E., Cotton, W.D., *J. Am. Chem. Soc.*, **1990**, 112, 1566;
- c) Parkin, G., Bunel, E., Burger, B.J., Trimmer, M.S., van Asselt, A., Bercaw, J.E., *J. Mol. Cat.*, **1987**, 41, 21.
- 6 a) Molander, G.A., Nichols, P.J., *J. Am. Chem. Soc.*, **1995**, 117, 4415;
- b) Molander, G.A., Hoberg, J.O., *J. Am. Chem. Soc.*, **1992**, 114, 3123.
- 7 a) Marks, T.J., Fragala, I.L., Reidel, D., *Fundamental and Technological Aspects of Organo-f-Element Chemistry*, Dordrecht, 1985;
- b) Schumann, H., *Angew. Chem. Int. Ed. Engl.*, **1984**, 23, 474;
- c) Evans, W.J., *Polyhedron*, **1987**, 6, 803; d) Evans, W.J., *J. Organomet. Chem.*, **1983**, 250, 217.
- 8 a) Jeske, G., Lauke, H., Mauermann, H., Swepston, P.N., Schumann, H., Marks, T.J., *J. Am. Chem. Soc.*, **1985**, 107 8091;
- b) Jeske, G., Schock, L.E., Swepston, P.N., Schumann, H., Marks, T.J., *J. Am. Chem. Soc.*, **1985**, 107, 8103;
- c) Watson, P.L., Parshall, G.W., *Acc. Chem. Res.*, **1985**, 18, 51.
- 9 a) Schumann, H., Meese-Marktscheffel, J.A., Esser, L. *Chem. Rev.*, **1995**, 95, 865;

- b) Edelmann, F.T., in *Comprehensive Organometallic Chemistry II*; Abel, E.W., Stone, R.G.S., Wilkinson, G.; Pergamon Press: Oxford, U.K., 1995; Vol. 4, Chapter 2 and references therein.;
- c) Schaverien, C.J., *Adv. Organomet. Chem.*, **1994**, 36, 283 and references therein.;
- d) Evans, W.J., *Adv. Organomet. Chem.*, **1985**, 24, 31 and references therein.;
- e) Kagan, H.B.; Namy, J.L., in *Handbook on the Physics and Chemistry of Rare Earths*; Gschneider, K.A., Eyring, L.; Elsevier: Amsterdam, 1984; Chapter 50;
- f) Marks, T.J., Ernst, R.D., in *Comprehensive Organometallic Chemistry*, Wilkinson, G., Stone, F.G.S., Abel, E.W.; Pergamon Press: Oxford, U.K., 1982; Chapter 21 and references therein.
- 10 Evans, W.J., Ulibarri, T.A., Ziller, J.M., *J. Sm. Chem. Soc.*, **1988**, 110, 6877
- 11 (a) Sen, A., Chebolu, V., Rheingold, A. L. *Inorg. Chem.*, **1987**, 26, 1821
- (b) Evans, W. J., Anwander, R., Ansari, M. A., Ziller, J. W. *Inorg. Chem.*, **1995**, 34, 5.
- (c) Hitchcock, P. B., Holmes, S. A., Lappert, M. F., Tian, S. *J. Chem. Soc., Chem. Commun.*, **1994**, 2691
- (d) Biagini, P.; Lugli, G.; Abis, L.; Millini, R. *J. Organomet. Chem.*, **1994**, 474.
- 12 (a) Dubé, T.; Conoci, S.; Gambarotta, S.; Yap, G. P. A.; Vasapollo, G. *Angew. Chem. Int. Ed.* **1999**, 38, 3657,

- (b) Jubb, J.; Gambarotta, S. *J. Am. Chem. Soc.*, **1994**, 116, 4477.
- 13 (a) Piers, W. E., Shapiro, P. J., Bunel, E. E., Bercaw, J. E., *Syn. lett.*, **1990**, 74;
(b) Qian, C., Ge, Y., Deng, D., Gu, Y., Zhang, C., *J. Organomet. Chem.*, **1988**, 344, 175;
(c) Qian, C., Zhu, D.; Li, D., *J. Organomet. Chem.*, **1992**, 430, 175;
(d) Piers, W. E., Bercaw, J.E., *J. Am. Chem. Soc.*, **1990**, 112, 9406
- 14 Evans, W. J., Grate, J. W., Hughes, L. A., Zhang, H., Atwood, J. L., *J. Am. Chem. Soc.*, **1985**, 107, 3728
- 15 (a) J. Jubb, S. Gambarotta, *J. Am. Chem. Soc.*, **1994**, 117, 4477
(b) Dube, T., Gambarotta, S., Yap, G.P.A., *Angew. Chem. Int. Ed.*, **1999**, 38, 1432-1435;
(c) Guan, J., Dube, T., Gambarotta, S., Yap, G.P.A., *Organometallics*, **2000**, 19, 4820-4827;
(d) Dube, T., Ganesan, M., Conoci, S., Gambarotta, S., Yap, G.P.A., *Organometallics*, **2000**, 19, 3716-3721;
- 16 R. J. Errington, Advanced practical inorganic and metalorganic chemistry, Blackie Academic & Professional, **1997**
- 17 (a) Takats, J. J. *Alloys Compd.*, **1997**, 249, 52;
(b) Hasinoff, L., Takats, J., Zhang, X. W., Bond, A. H., Rogers, R. D., *J. Am. Chem. Soc.*, **1994**, 116, 8833.;
(c) Ferrence, G. M., McDonald, R., Takats, J., *Angew. Chem., Int. Ed.*, **1999**, 38, 2233
- 18 (a) Nief, F., Ricard, L., *J. Organomet. Chem.*, **1994**, 464, 149.;

- (b) Rabe, G., Riede, J., Schier, A., *Inorg. Chem.*, **1996**, 35, 2680.;
- (c) Gosink, H. J., Nief, F., Ricard, L., Mathey, F., *Inorg. Chem.*, **1995**, 34, 1306;
- (d) Fryzuk, M. D., Haddad, T. S., Rettig, S. J., *Organometallics*, **1992**, 11, 2967
- 19 *Organometallics*, Vol. 9, No7, **1990**, P.1999.
- 20 R.J. Angelici, *Inorganic Syntheses*, **1990**, Vol 27 P.136-140

Synthesis of Pyrrole Supporting Schiff-Base Samarium Dinuclear Complexes

IV.1: Summary

The reaction of $[Sm\{N(SiMe_3)_2\}_2(THF)_2]$ with highly delocalized pyrrole supporting schiff base ligands yields three distinct complexes. In two of these complexes the samarium atom has undergone oxidation to the trivalent state at the expenses of the ligand. Conversely, X-ray characterization of the third complex clearly indicated the presence of divalent samarium centers.

IV.2: Introduction

Over the last 20 years, the field of lanthanide organometallic chemistry has grown in importance with the realisation that many of these metals display unique chemical properties such as restricted oxidation states and enhanced ionic character.¹ The use of cyclopentadienyl-based ligand systems was instrumental in the growth of the field, since they offered the versatility needed to meet the electronic and steric requirements to stabilise a wide variety of complexes.² Over the last few years, headway has been made in using auxiliary ligand systems that, while preserving the salient characteristics of the Cp systems, offer distinctive reactivity features. One class of such ligand systems is based on polypyrrolides, which has shown great promise for increasing even further the reactivity of divalent lanthanides.³⁻⁶ These ligands have been used with a few lanthanides, but the most influential impact was felt in the chemistry of divalent samarium, where the already highly reactive metal is activated even further by the ligand system. The clusters resulting from these reactions are typically so reactive that attack to

the ligand system,⁴ solvent,⁵ or even dinitrogen⁶ is commonly observed. Pyrroles often mimic the cyclopentadienyl functions because of their ability to form π -bonds with metals offering great steric stabilisation. On the other hand, they also offer the possibility of forming σ -bonds through the nitrogen atom offering a versatility of bonding modes and an increased stability. A direct consequence of this behavior is the ability of forming cluster structures and retaining alkali cation in the molecular structures. By favoring polynuclear aggregation, polypyrrolide ligands make possible multi-electron redox processes via co-operative attack of several metals on the same substrate.⁶

Another class of ligand that has lately been shown to form interesting complexes with lanthanides is the Salen-type Schiff-base ligands. Recent results have shown that this type of ligand, when coordinating yttrium, is able to perform catalytic asymmetric aldol-Tishchenko reactions, which are used to couple carbonyl compounds.⁷ Salen type Schiff bases have previously been used with divalent samarium,⁴ but in this case there was reduction of both the ligand and the solvent, yielding trivalent samarium species.

Therefore, we became interested in using ligand systems capable of combining the characteristics of both pyrrole-based ligands with those of the tetradentate Schiff bases. The aim was to stabilize low-valent samarium and take advantage of the denticity to use these complexes for further reactivity studies. Herein we describe our preliminary results.

IV.3: Experimental Section

All operations were performed under an inert atmosphere of a nitrogen-filled dry box or by using Schlenk-type glassware in combination with a nitrogen-vacuum line.⁸ Solvents were dried by passing through a column of Al₂O₃ under an inert atmosphere prior to use, degassed *in vacuo* and transferred and stored under inert atmosphere. [Sm{N(SiMe₃)₂}₂(THF)₂].⁹ was prepared according to literature procedures, and the ligands were prepared through variations of literature procedures.^{10,11,12} NMR spectra were recorded on a Varian Gemini 200 and on a Bruker AMX-500 spectrometer. Infrared spectra were recorded on a Mattson 3000 FTIR instrument from Nujol mulls prepared inside a dry box. Samples for magnetic susceptibility measurements were carried out at room temperature using a Gouy balance (Johnson Matthey) and corrected for underlying diamagnetism. Elemental analyses were carried out using a Perkin-Elmer Series II CHN/O 2400 analyser.

Preparation of 1,2-Benzenediamine, N,N'-bis(1H-pyrrol-2-ylmethylene)

A 250 mL flask fitted with a magnetic stirrer was charged with phenylene diamine (3.9 g., 36.3 mmols) and 2-pyrrole carboxaldehyde (6.9 g., 72.6 mmols) and dissolved in ethanol (70 mL). While under nitrogen flow, the solution was slightly heated to solubilize both reactants after which a catalytic amount of acetic acid was added (0.5 mL). The solution was allowed to react over a 12-hour period during which a fine white power precipitated out of the solution. The powder was filtered and recrystallized from a minimum amount of boiling methanol to obtain the white crystals of the desired di-imino (6.9 g., 26.3 mmols, 72 % yield).

M.S.- E.I. m/e+ : 262.

$^1\text{H-NMR}$ (200 MHz, CDCl_3 , 298 K) δ : 7.70 (s, 2H, C-H imine), 7.24 (mult, 2H, C-H phenyl), 7.05 (mult, 2H, C-H phenyl), 6.40 (q, 2H, C-H pyrrole), 6.25 (q, 2H, C-H pyrrole) 6.02 (q, 2H, C-H pyrrole).

$^{13}\text{C NMR}$ (benzene- D_6 , 200 MHz, 25°C) δ : 150.7 (CH-imino), 145.8 (quaternary C-phenyl), 126.4 (CH-pyrrole), 118.9 (CH-phenyl), 117.4 (CH-pyrrole), 109.9 (CH-pyrrole).

Preparation of 3,4-Dimethyl 1,2-Benzenediamine,N,N'-bis(1H-pyrrol-2-ylmethylene)

A 250 mL flask fitted with a magnetic stirrer was charged under nitrogen atmosphere with 3,4-dimethylphenyldiamine (5.6 g., 41.0 mmoles) and 2-pyrrole carboxaldehyde (7.8 g., 82.0 mmoles) in ethanol (70 mL). A catalytic amount of acetic acid (0.5mL) was added and the solution was allowed to react over a 12-hour period during which a bright yellow fine powder precipitated out of the solution. The solid was filtered and washed with small portions of chilled ethanol (-38°C) affording the product (6.2 g, 21.4 mmoles, 52 % yield).

M.S.- E.I. m/e+ : 290.

$^1\text{H-NMR}$ (200 MHz, CDCl_3 , 298 K) δ : 7.75 (s, 2H, C-H imine), 6.85 (s, 2H, C-H phenyl), 6.36 (q, 2H, C-H pyrrole), 6.27 (q, 2H, C-H pyrrole), 6.00 (q, 2H, C-H pyrrole), 2.25 (s, 6H, CH_3).

^{13}C NMR (Benzene- D_6 , 200 MHz, 25°C) δ : 150.0 (CH-imino), 143.6 (quaternary C-phenyl), 134.4 (quaternary C-phenyl), 131.3 (CH-phenyl), 123.7 (CH-pyrrole), 116.9 (CH-pyrrole), 109.8 (CH-pyrrole), 19.1 (CH_3 -methyl).

Preparation of 1,2-Ethanediamine, N,N'-bis[1-(1H-pyrrol-2-yl)ethylidene]

Ethylene diamine (1.4 g, 22.5 mmoles) was transferred via syringe into a 250 mL flask containing a magnetic stirrer and a solution of acetylpyrrole (4.9 g, 45 mmoles) in ethanol (40 mL). A catalytic amount of acetic acid (0.5 mL) was added to the mixture, which was subsequently fitted with a reflux column and a drying tube and then refluxed for 48 hours. The resulting orange solution was evaporated to dryness yielding a slightly oily orange solid. The crude product was recrystallized from a minimum amount of hot methanol. The resulting off-white crystalline product was rinsed with 3 portions of ether (30 mL) to remove possible traces of unreacted acetylpyrrole (2.6 g, 10.7 mmoles, 48 % yield).

M.S.- E.I. m/e⁺ : 242.

^1H -NMR (200 MHz, CDCl_3 , 298 K) δ : 6.75 (q, 2H, C-H pyr), 6.43 (q, 2H, C-H pyr), 6.12 (q, 2H, C-H pyr), 6.58 (s, 4H, C-H ethylene), 1.79 (s, 6H, C-H CH_3).

^{13}C NMR (Benzene- D_6 , 200 MHz, 25°C) δ : 160.2 (quaternary C-imino), 133.4 (quaternary C-pyrrole), 121.4 (CH-pyrrole), 110.9 (CH-pyrrole), 108.5 (CH-pyrrole), 51.0 (CH_2 -ethylene), 15.1 (CH_3 -methyl).

Synthesis of [(SB-SB)Sm₂(THF)₄] (4.1) [SB-SB = C-C Bonded 1,2-Benzenediamine, N,N'-bis(pyrrol-2-ylmethylene) Dimer]

A solution of [Sm{N(SiMe₃)₂}(THF)₂] (1.1 g., 1.7 mmoles) in anhydrous THF (30 mL) was treated with 1,2-benzenediamine, N,N'-bis(1H-pyrrol-2-ylmethylene) (0.5 g., 1.7 mmoles) at room temperature and under argon atmosphere. After standing for 3 days at room temperature, the reaction mixture separated thin red crystalline plates of 4.1. (0.65 g, 1.1 mmoles, 64 % yield).

I.R. (Nujol mull, cm⁻¹) ν : 3083(w), 3051(w), 1646(w), 1576(s), 1542(m), 1505(m), 1465(s), 1435(s), 1389(s), 1329(s), 1301(m), 1261(m), 1261(s), 1220(w), 1183(m), 1169(m), 1155(m), 1097(m), 1088(m) 1062(s), 1027(s), 969(m), 991(w), 867(m), 803(m), 779(m), 733(s), 701(w), 687(w), 670(w), 629(w), 608(w), 571(w), 562(w).

μ_{eff} : 2.45 μ_B

Synthesis of [Sm(3,4-Dimethyl 1,2-Benzenediamine,N,N'-bis(pyrrol-2-ylmethylene) (THF)₄] [Sm (3,4-Dimethyl 1,2-Benzenediamine,N,N'-bis(pyrrol-2-ylmethylene)₂] (4.2)

A solution of [Sm{N(SiMe₃)₂}(THF)₂] (1.0 g., 1.6 mmoles) in anhydrous THF (30 mL) was treated with 3,4-dimethyl 1,2-benzenediamine,N,N'-bis(1H-pyrrol-2-ylmethylene) (0.5 g., 1.6 mmoles) at room temperature and under argon atmosphere. After 2 days at room temperature yellow rectangular prisms of 4.2 separated. (0.27 g, 0.3 mmoles, 38 % yield).

I.R. (Nujol mull, cm⁻¹) ν : 3090(w), 3072(w), 1725(w), 1696(w), 1591(s), 1554(s), 1516(s), 1493(s), 1459(s), 1459(s), 1436(s), 1393(s), 1384(s), 1340(s), 1295(s), 1259(s), 1227(m), 1188(m), 1174(s), 1093(s), 1063(s), 1029(s), 975(s), 954(m), 899(s), 888(s), 872(s), 865(s), 811(s), 795(s), 749(s), 713(s), 688(m), 674(w), 665(w), 645(w), 615(s).

μ_{eff} : 2.16 μ_B

Synthesis of (Sm[1,2-Ethylenediamine,N,N'-bis(1-(pyrrol-2-yl)ethylidene)]) \cdot 2 \cdot 4THF(4.3)

A solution of [Sm{N(SiMe₃)₂}₂(THF)₂] (2.2 g., 3.6 mmoles) in anhydrous THF (50 mL) was treated with 1,2-ethylenediamine,N,N'-bis[1-(1H-pyrrol-2-yl)ethylidene] (0.9 g., 3.6 mmoles) at room temperature and under nitrogen atmosphere. After 15 minutes a light colored precipitate separated while the colour of the solution changed from deep red to greenish brown. The reaction was allowed to react for 12 hours after which the unreacted ligand was removed by centrifugation. The brown supernatant was reduced to a small volume (15 mL) and allowed to stand at room temperature for 1 day, upon which yellow crystals of 4.3 separated (0.36 g, 0.6 mmoles, 16 % yield).

I.R. (Nujol mull, cm⁻¹) ν 3084(w), 2727(w), 2659(w), 1574(s), 1504(s), 1462(s), 1378(s), 1340(s), 1313(m), 1291(m), 1260(s), 1210(m), 1180(m), 1147(s), 1093(s), 1039(s), 939(s), 891(m), 873(m), 840(m), 818(s), 803(s), 772(s), 734(s), 695(w), 684(w), 668(w), 617(w).

μ_{eff} : 2.62 μ_B

IV.4: Results and Discussion

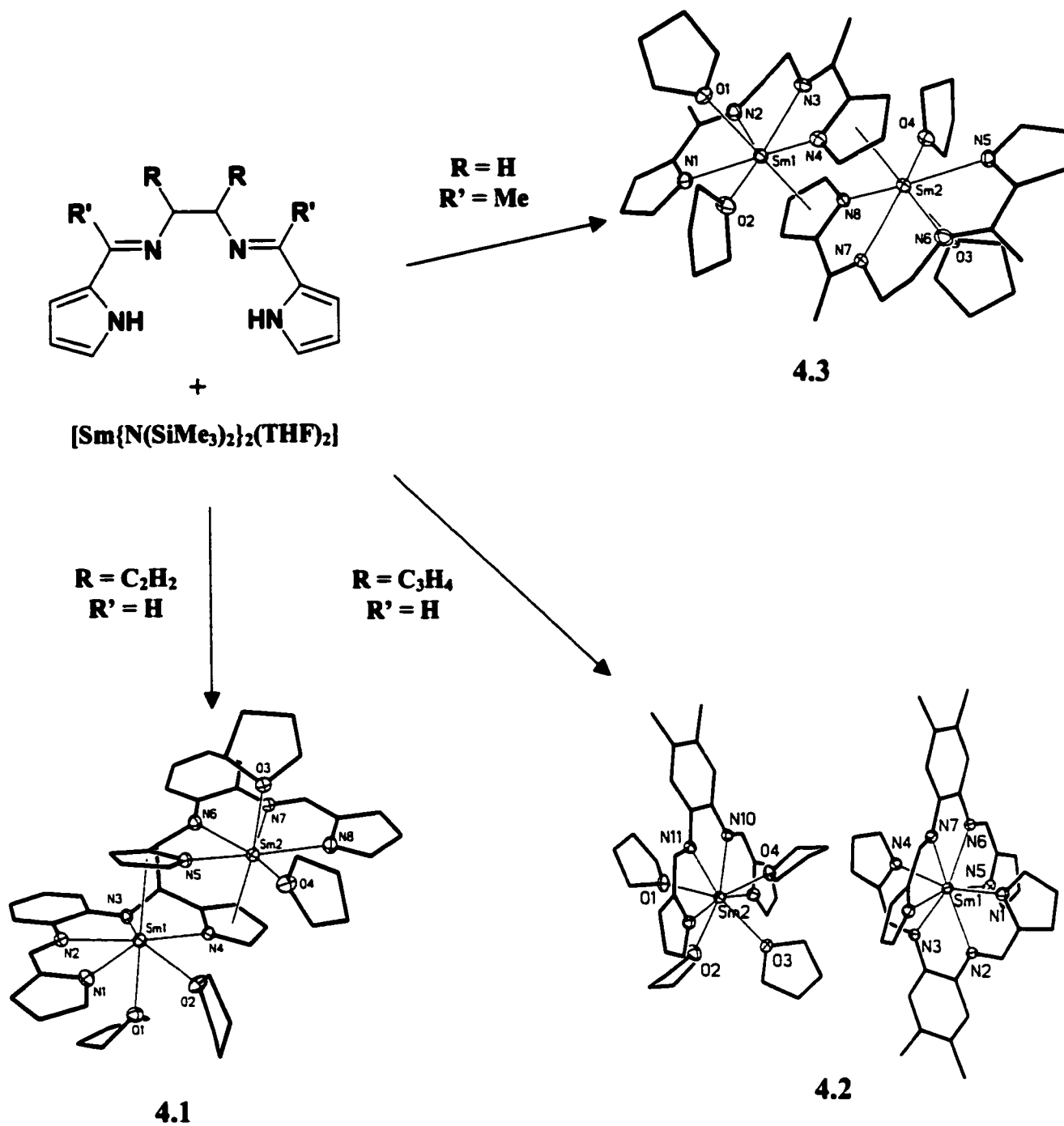
The reaction of 1,2-benzenediamine,N,N'-bis(1H-pyrrol-2-ylmethylene) with $[\text{Sm}\{\text{N}(\text{SiMe}_3)_2\}_2(\text{THF})_2]$ in THF afforded a bright-red solution from which a large mass of bright-red air-sensitive crystals precipitated. The light colour of the crystals suggested that the samarium atoms were in the trivalent state. This observation was substantiated by the magnetic moment, which is consistent with trivalent compounds of this type and by the connectivity yielded by the X-ray crystal structure (Figure 4.1). The oxidation of the metal center in this case is realized at the expense of the one imino moiety of the ligand, which was reductively coupled with an identical moiety of another molecule. The C-C bond generated in the process is thus holding together the dimetallic structure. This type of reductive coupling promoted by strongly reducing metals, including divalent samarium, has precedent in the chemistry of the salicylidenedi-iminate tetradentate Schiff bases (salen-type). The process may be envisioned by assuming a substantial transfer of charge from the samarium center towards the imino moiety. The resulting radical character developed by the carbon atom is the driving force for the formation of the C-C bond and irreversible oxidation of the metal center to the trivalent state. However, the fact that the ligand contains two pyrrolide rings, whose ability to stabilize the divalent samarium center has been exhaustively documented, makes this behavior somewhat unexpected. In fact, there is no steric constraint within the ligand to prevent the two pyrrolyl rings from π -ligating the samarium which in turn could adopt the bent samarocene type of structure already observed with di- and polypyrrolide and even simple pyrrolides. Thus, in order to assess

the generality of the ability of samarium to reduce the imino functions, we have performed the same reaction with other ligands of this type carrying small modification and substituents in the backbone.

A very minor ligand modification such as the presence of two methyl groups in the ligand phenyl ring and in 3,4 positions pointing well away from the metal center was sufficient to drive the reaction in a surprisingly different direction. The reaction of 3,4-dimethyl-1,2-benzenediamine, N,N'-bis(1H-pyrrol-2-ylmethylene) with $[\text{Sm}\{\text{N}(\text{SiMe}_3)_2\}_2(\text{THF})_2]$ afforded a trivalent samarium compound and also dinuclear $[\text{Sm}(3,4\text{-dimethyl}, 1,2\text{-benzenediamine}, \text{N}, \text{N}'\text{-bis}(\text{pyrrol-2-ylmethylene})(\text{THF})_4)]_2[\text{Sm}(3,4\text{-dimethyl}, 1,2\text{-benzenediamine}, \text{N}, \text{N}'\text{-bis}(\text{pyrrol-2-ylmethylene})_2]$ (4.2). The very light red colour was diagnostic for the presence of trivalent samarium which, once again, was supported by the value of the magnetic moment. As indicated by the crystal structure, the complex is ionic and contains one cationic trivalent samarium surrounded by the ligand and solvent molecules. The counteranion consists of another samarium surrounded by two ligands. This ionic structure is a complete departure from the ligand dimerization previously observed since the ligand system, being untouched, was not involved in the oxidation of the metal center. In addition, three ligand molecule have been consumed by two metal centers. Therefore, the formation of trivalent samarium is ascribed to a disproportionation mechanism producing a small amount of colloidal metallic Sm. No evidence could be found for the presence of different products in the reaction mother liquor in spite of the moderate yield. Regardless, this result is in line with the formation of 4.1 in the sense that it also emphasizes the instability of divalent samarium center while in combination with tetradentate Schiff bases.

The next step was to introduce alkyl groups directly on the imino function in an attempt to prevent the reductive coupling and formation of C-C bond. Unfortunately, acetylpyrrole proved very unreactive towards condensation with 1,2-phenylenediamine, and we were forced to use the more active 1,2-ethylenediamine. This modification of the ligand backbone was not very desirable given that charge delocalization throughout the ligand was no longer possible. The reaction of $[\text{Sm}\{\text{N}(\text{SiMe}_3)_2\}_2(\text{THF})_2]$ with 1,2-ethanediamine, $\text{N,N}'\text{-bis}[1\text{-}(1\text{H-pyrrol-2-yl)ethylidene}]$ was carried out in THF at room temperature for three days affording yellow cuboid crystals of $(\text{Sm}[1,2\text{-Ethylenediamine,N,N}'\text{-bis}(1\text{-pyrrol-2-yl)ethylidene}])_2 \cdot 4\text{THF}$ (**4.3**). In sharp contrast to the light colour and the value of the magnetic moment in line with those of the other two trivalent complexes, the X-ray crystal structure clearly indicated that the metal centers are in the divalent state. The structure of the complex is rather close to that of complex **4.1** in both the way the ligand binds the samarium center and the dinuclear aggregation realized via the π -interaction of the samarium center with the pyrrolyl ring of the second unit. The only significant difference appears to be that the two units are staggered with respect to each other and therefore by preventing the two imino functions from coming to close proximity the reduction of the imino function was prevented. It is conceivable that the pyrrole rings bridging the two metal centers permit the metal-metal coupling of both samarium atoms, accounting for the unexpectedly light colour and the low paramagnetism. Complex **4.3** provides the first case of stabilization of a divalent samarium center by a tetradentate Schiff base. We still find surprising the apparent lack of reactivity with dinitrogen given that what appeared to be the prerequisite for its coordination appear to be satisfied.

Scheme 4.1



IV.5: Structural Considerations

Suitable crystals were selected, mounted on thin, glass fibres using paraffin oil and cooled to the data collection temperature. Data were collected on a Bruker AX SMART 1k CCD diffractometer using 0.3° ω -scans at 0, 90, and 180° in ϕ . Unit-cell parameters were determined from 60 data frames collected at different sections of the Ewald sphere. Semi-empirical absorption corrections based on equivalent reflections were applied (Blessing, R., *Acta Cryst.*, 1995, A51, 33-38).

No symmetry higher than triclinic was observed for 4.2·2(thf) and refinement in the centrosymmetric space group option yielded computationally stable and chemically reasonable results of refinement. Systematic absences in the diffraction data and unit-cell parameters were uniquely consistent with the reported space groups for 4.1·(thf), and 4.3·2(thf). The structures were solved by direct methods, completed with difference Fourier syntheses and refined with full-matrix least-squares procedures based on F^2 .

One, three (one at half-occupancy), and two molecules of tetrahydrofuran (thf) solvent were located cocrystallized in the asymmetric units 4.1·(thf), 4.2·2.5(thf), and 4.3·2(thf), respectively. The cocrystallized thf molecules in 4.2·2.5(thf), and 4.3·2(thf) were found to be severely disordered and were treated as rigid, flat, pentagons with the atoms having smallest isotropic parameter per ring assigned oxygen atom identities. All non-hydrogen atoms were refined with anisotropic displacement parameters. All hydrogen atoms were treated as idealized contributions. All scattering factors are contained in the SHEXTL 5.10 program library (Sheldrick, G. M., Bruker AXS, Madison, WI, 1997).

1. Complex 4.1 is a dimer formed by two identical units where an imino function from each ligand has been reduced to form a carbon-carbon bond between the two moieties. Each metal center is σ -bonded to 4 nitrogen atoms from the dianionic 1,2-Benzenediamine, N,N'-bis(pyrrol-2-ylmethylene and to two THF molecules [Sm(1)-O(1) = 2.491(5)Å; Sm(1)-O(2) = 2.554(4)Å; Sm(2)-O(3) = 2.473(5)Å; [Sm(2)-O(4) = 2.618(5)Å], one coplanar with the ligand and the other in a perpendicular position. A pyrrole ring of a second tetradentate unit surrounding the second samarium atom is π -bonded to samarium with the ring centroid placed in the second axial position in *trans* to the THF molecule of the distorted octahedron centered on each samarium [Sm(1)-N(5)_{centroid} = 2.524(5)Å; Sm(2)-N(4)_{centroid} = 2.563(5)Å]. The link between the two units is realized via reduced imino carbon atoms present on each original ligand [C(12)-C(21) = 1.598(9)Å]. The length of the carbon-nitrogen bonds of the reduced imino functions is as expected for single bonds [C(21)-N(6) = 1.446(8)Å; C(12)-N(3) = 1.460(8)Å], while the intact imino functions display significantly shorter C-N bond distances thus indicating the presence of a substantial multiple bond character [C(5)-N(2) = 1.288(8)Å; C(28)-N(7) = 1.283(8)Å]. The N atoms of the reducing imino functions form with Sm rather short bond distances [Sm(1)-N(3) = 2.373(5)Å; Sm(2)-N(6) = 2.365(5)Å]. The pyrrole moieties neighbor to the reduced imino functions form fairly long Sm-N distances probably as a result of the a π -bonding with the second Sm center [Sm(1)-N(4) = 2.561(5)Å; Sm(2)-N(5) = 2.525(5)Å]. The other two nitrogen atoms in each unit have similar Sm-N bond lengths [Sm(1)-N(1) = 2.502(5)Å; Sm(1)-N(2) = 2.516(5)Å; Sm(2)-N(7) = 2.531(6)Å; Sm(2)-N(8) = 2.519(6)Å].

2. Complex 4.2 is ionic in nature, with both the anion and the cation containing a single Sm(III) atom. In the cationic unit, the metal center is 8-coordinate, being σ -bonded to the dianionic tetradentate 3,4-dimethyl 1,2-benzenediamine,N,N'-bis(pyrrol-2-ylmethylene) ligand and coordinatively bound to four molecules of THF [Sm(2)-O(1) = 2.479(4)Å; Sm(2)-O(2) = 2.523(4)Å; Sm(2)-O(3) = 2.517(4)Å; Sm(2)-O(4) = 2.441(3)Å]. The ligand maintains a planar arrangement of the three rings and the metal center with the four nitrogen donor atoms forming comparable Sm-N distances [Sm(2)-N(9) = 2.478(4)Å; Sm(2)-N(10) = 2.519(4)Å; Sm(2)-N(11) = 2.529(4)Å; Sm(2)-N(12) = 2.507(4)Å]. The Sm center in the counteranion is also eight-coordinate, but with the coordination environment defined by two tetradentate ligands and without solvent molecules. Despite their similarities, both ligands in the anion are not identically bound to the metal center. The ligand containing the nitrogens labeled 1 through 4 is planar and very similar to the ligand observed in the cation [Sm(1)-N(1) = 2.491(4)Å; [Sm(1)-N(2) = 2.545(4)Å; Sm(1)-N(3) = 2.536(4)Å; Sm(1)-N(4) = 2.487(4)Å], while the second ligand, which contains the nitrogen atoms labeled 5 through 8, is not planar but slightly twisted along the N(7)-C(32) and the N(6)-C(23) bonds. Other than this spatial arrangement difference, the Sm-N distances [Sm(1)-N(5) = 2.504(4)Å; Sm(1)-N(6) = 2.561(4)Å; Sm(1)-N(7) = 2.526(4)Å; Sm(1)-N(8) = 2.504(4)Å] and the imino carbon-nitrogen distances [C(23)-N(6) = 1.302(6)Å; C(32)-N(7) = 1.304(6)Å] are the same as in the planar ligand [C(5)-N(2) = 1.297(6)Å; C(14)-N(3) = 1.310(6)Å].

3. Complex 4.3 is dimeric and is formed by two identical units linked by two Sm-pyrrole π interactions. Each unit is composed of a Sm (II) atom σ -bonded to a tetradentate 1,2-ethylenediamine,N,N'-bis[1-(pyrrol-2-yl)ethylidene] ligand, which define

the equatorial plane of the pentagonal bipyramid centered on samarium. The four nitrogen donor atoms are basically coplanar with the metal center. One molecule of THF occupies the fifth position of the equatorial plane [Sm(1)-O(2) = 2.547(6)], while the two axial positions are respectively occupied by the second THF molecule [Sm(1)-O(1) = 2.534(6)]; and the centroid of the π -bonded pyrrolyl ring of the second unit [Sm(1)-N(8)_{centroid} = 2.578(6)Å, Sm(2)-N(4)_{centroid} = 2.565(6)Å]. The pyrrole nitrogen not involved in π -bonding and its adjacent imino nitrogen form comparable Sm-N bond distances [Sm(1)-N(1) = 2.474(8)Å; Sm(1)-N(2) = 2.477(8)Å; Sm(2)-N(5) = 2.478(7)Å; Sm(2)-N(6) = 2.471(8)Å]. The nitrogen-Sm σ -bond formed with the pyrrole engaged in π -bonding with the second metal center is somewhat longer [Sm(1)-N(4) = 2.502(8)Å; Sm(2)-N(8) = 2.484(8)Å]. This π interaction also slightly perturbs the adjacent imino function [C(9)-N(3) = 1.364(12)Å; C(23)-N(7) = 1.368(12)Å] with respect to the others [C(5)-N(2) = 1.302(12)Å; C(19)-N(6) = 1.293(12)Å].

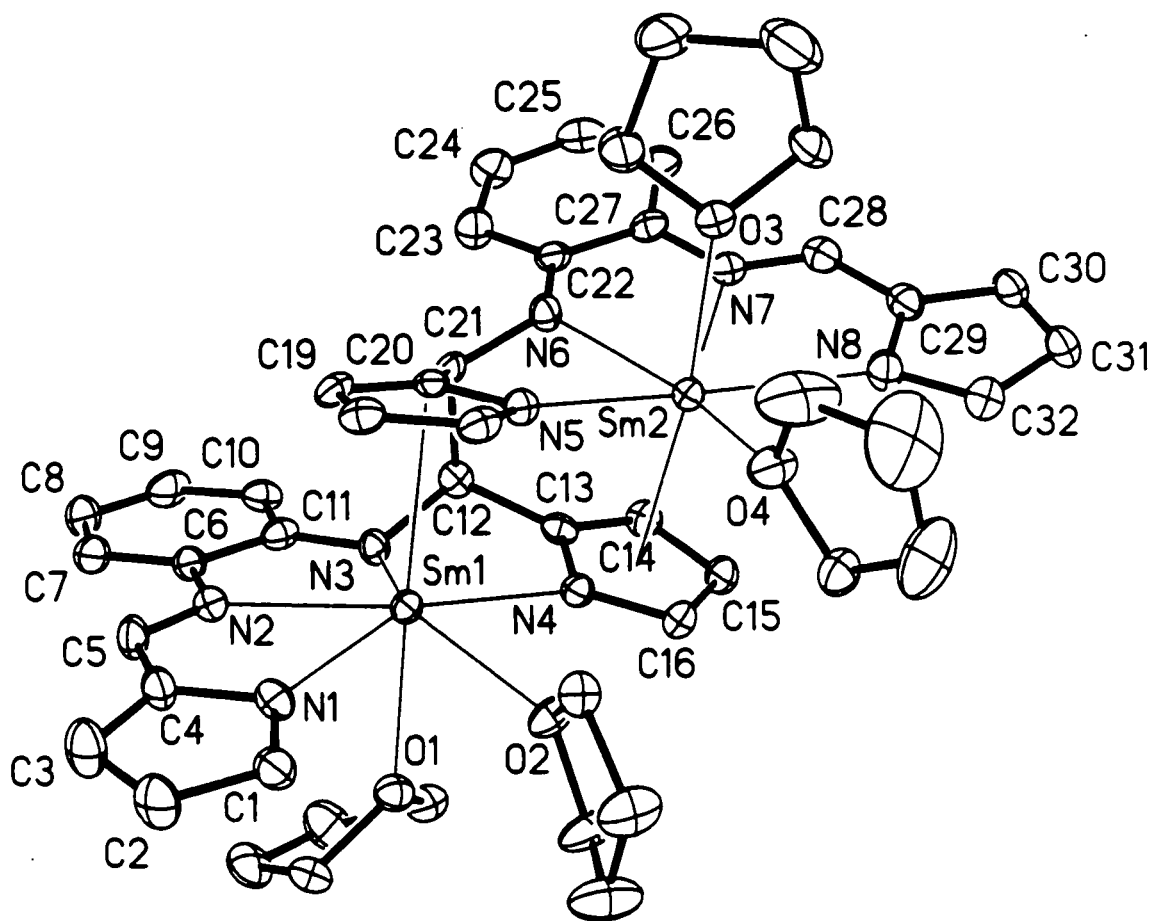


Figure 4.1: Thermal ellipsoid plot of $[\text{Sm}(\text{SB-SB})(\text{THF})_4]$ (4.1). Thermal ellipsoids are drawn at the 30% probability level.

Selected Bond Distances (Å) and Angles (deg): Sm(1)-N(1) = 2.502(5), Sm(1)-N(2) = 2.516(5), Sm(1)-N(3) = 2.373(5), Sm(1)-N(4) = 2.561(5), Sm(1)-O(1) = 2.491(5), Sm(1)-N(5)_{centroid} = 2.424(5), C(5)-N(2) = 1.288(8), C(12)-N(3) = 1.460(8), O(1)-Sm(1)-O(2) = 78.31(15), N(1)-Sm(1)-O(2) = 79.57(17), N(1)-Sm(1)-N(2) = 60.30(18), N(3)-Sm(1)-N(4) = 68.42(17), N(1)-Sm(1)-N(4) = 154.49(17), N(3)-C(12)-C(13) = 110.3(5), N(2)-C(5)-N(4) = 120.6(6), O(1)-Sm(1)-N(5)_{centroid} = 174.5(17),

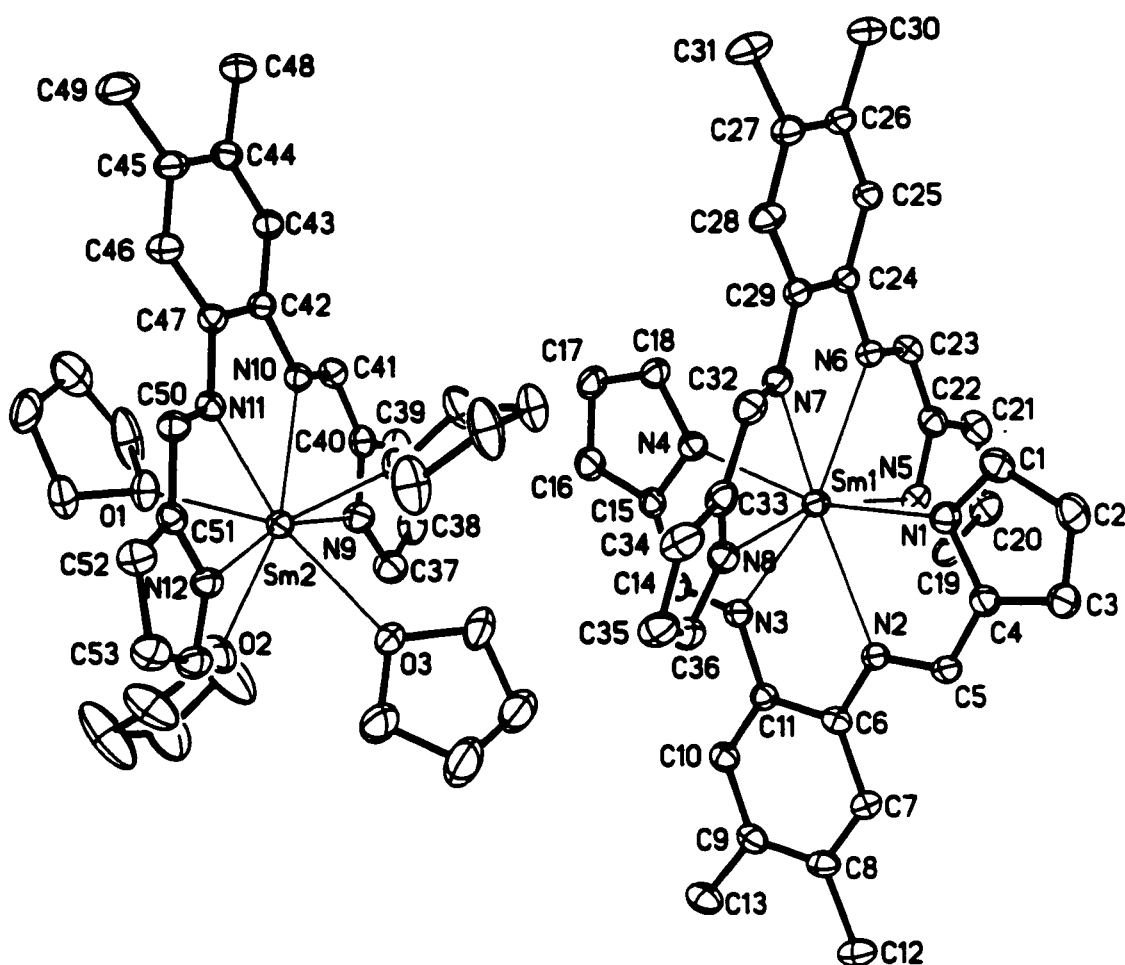


Figure 4.2: Thermal ellipsoid plot of $[\text{Sm}(3,4\text{-Dimethyl } 1,2\text{-Benzenediamine}, \text{N}, \text{N}'\text{-bis(pyrrol-2-ylmethylene)})(\text{THF})_4][\text{Sm}(3,4\text{-Dimethyl } 1,2\text{-Benzenediamine}, \text{N}, \text{N}'\text{-bis(pyrrol-2-ylmethylene)}_2)]$ (4.2). Thermal ellipsoids are drawn at the 30% probability level.

Selected Bond Distances (Å) and Angles (deg): $\text{Sm}(2)\text{-N}(12)=2.507(4)$, $\text{Sm}(2)\text{-N}(11)=2.529(4)$, $\text{Sm}(2)\text{-O}(1)=2.479(4)$, $\text{Sm}(2)\text{-O}(3)=2.517(4)$, $\text{Sm}(1)\text{-N}(1)=2.491(4)$, $\text{Sm}(1)\text{-N}(4)=2.478(4)$, $\text{Sm}(1)\text{-N}(2)=2.545(4)$, $\text{N}(11)\text{-Sm}(2)\text{-N}(12)=66.88(13)$, $\text{N}(9)\text{-Sm}(2)\text{-N}(12)=161.80(15)$, $\text{O}(2)\text{-Sm}(2)\text{-O}(3)=74.55(15)$, $\text{O}(3)\text{-Sm}(2)\text{-O}(4)=70.86(14)$, $\text{N}(1)\text{-Sm}(1)\text{-N}(4)=161.72(15)$, $\text{N}(5)\text{-Sm}(1)\text{-N}(8)=162.51(14)$, $\text{N}(1)\text{-Sm}(1)\text{-N}(2)=67.36(13)$, $\text{N}(1)\text{-Sm}(1)\text{-N}(8)=85.71(13)$,

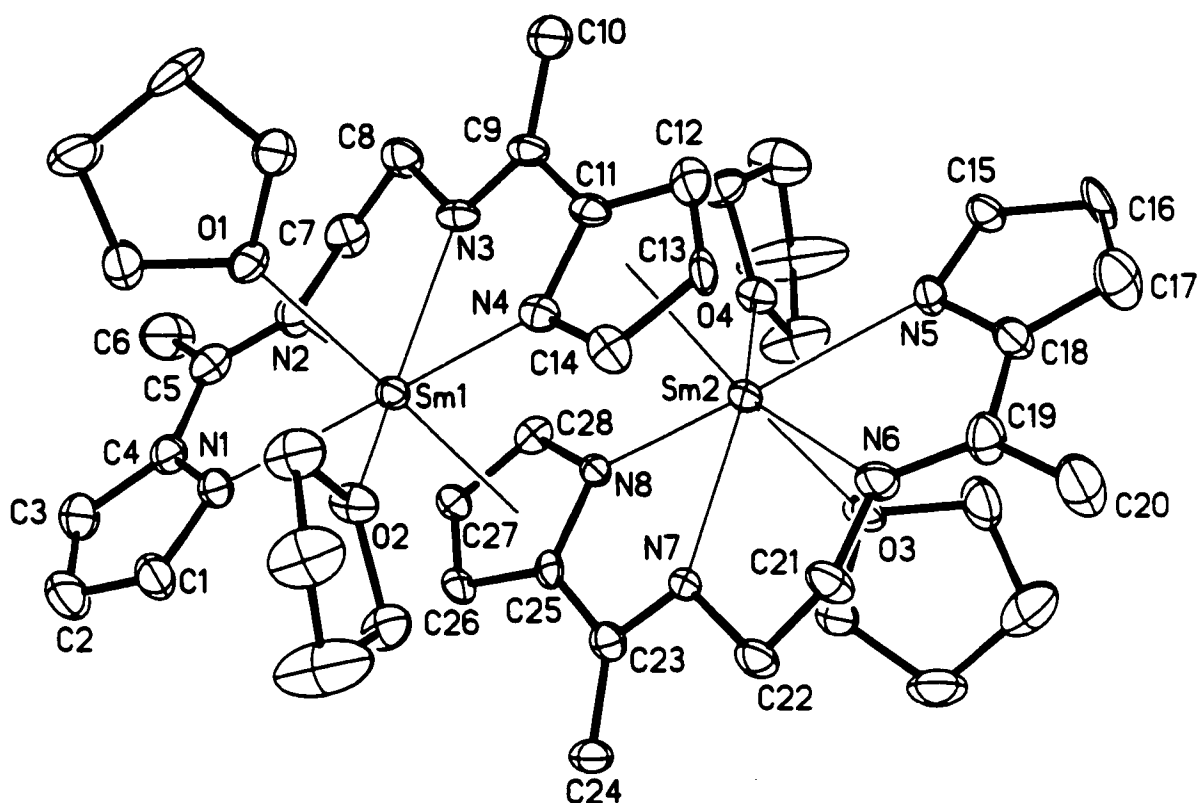


Figure 4.3: Thermal ellipsoid plot of (Sm[1,2-Ethanediamine,N,N'-bis(1-(pyrrol-2-yl)ethylidene))₂•4THF (4.3). Thermal ellipsoids are drawn at the 30% probability level.

Selected Bond Distances (Å) and Angles (deg): Sm(1)-N(1) = 2.474(8), Sm(1)-N(2) = 2.477(8), Sm(1)-N(3) = 2.391(9), Sm(1)-N(4) = 2.502(8), N(2)-C(5) = 1.302(12), N(3)-C(9) = 1.364(12), Sm(1)-O(1) = 2.534(6), Sm(1)-O(2) = 2.547(6), Sm(1)-N(8)_{centroid} = 2.578(6), Sm(1)-N(4)-Sm(2) = 105.2(3), N(4)-Sm(1)-N(8) = 74.4(2), N(1)-Sm(1)-N(4) = 150.8(3), N(4)-Sm(1)-O(2) = 75.0(2), O(1)-Sm(1)-O(2) = 76.8(2), O(1)-Sm(1)-N(8)_{centroid} = 174.6(3),

IV.6: Conclusion

We have successfully carried out the transamination reaction between $[\text{Sm}\{\text{N}(\text{SiMe}_3)_2\}_2(\text{THF})_2]$ and three dipyrrolide supporting schiff bases in an attempt to obtain divalent samarium complexes free of alkali cation and hopefully capable of interacting with N_2 . Two of the complexes obtained sustain trivalent samarium centers, while the third was able to stabilize a divalent samarium species. The presence of an imino-methyl group instead of an imino-hydrogen in the third complex discourages the formation of stabilized radical centers, which are part of the main decomposition pathway for the ligand. The pyrrole supporting schiff base ligand does not activate divalent samarium as much as the di- and tetrapyrrolide ligands previously seen, since there is no indication of solvent cleavage or dinitrogen activation by the third complex.

References

- 1
 - a) Evans, W. J.; Hozbor, M. A. *J. Organomet. Chem.*, **1987**, 326, 299, and references cited therein.
 - b) Schaverien, C. *J. Adv. Organomet. Chem.*, **1994**, 36, 283, and references cited therein.
 - c) Marks, T. J.; Ernst, R. D. In Comprehensive Organometallic Chemistry; Pergamon: Oxford, 1982; Chapter 21.
 - d) Evans, W. *Adv. Organomet. Chem.*, **1985**, 24, 131;
 - e) Wainwright, K. P. *Coord. Chem. Rev.*, **1977**, 166, 35.
 - f) Cotton, S. A. *Coord. Chem. Rev.*, **1997**, 160, 993.
 - g) Pikramenou, Z. *Coord. Chem. Rev.*, **1997**, 1644, 189.
 - h) Gunko, Y. K.; Edelman F. T. *Commun. Inorg. Chem.*, **1997**, 19, 153.
 - i) Gunko, Y. K.; Edelman F. T. *Coord. Chem. Rev.*, **1996**, 156, 1;
 - j) Parker D.; Williams J. A. *J. Chem. Soc., Dalton Trans.*, **1996**, 3613;
 - k) Edelman, F. T. *Angew. Chem., Int. Ed. Engl.*, **1995**, 34, 2466
- 2
 - a) Evans, W. J.; Bloom, I.; Hunter, W. E.; Atwood, J. L., *J. Am. Chem. Soc.*, **1983**, 105, 1401.
 - b) Evans, W. J.; Engerer, S. C.; Neville, A. C. *J. Am. Chem. Soc.*, **1978**, 100, 331.
 - c) Evans, W. J.; Engerer, S. C.; Piliero, P. A.; Wayda, A. L. *J. Am. Chem. Soc., Chem. Commun.*, **1979**, 101, 1007.

- d) Evans, W. J.; Engerer, S. C.; Piliero, P. A.; Wayda, A. L. Fundamentals of Homogeneous Catalysis; Tsutsui, M., Ed.; Plenum Press: New York, 1979, Vol. 3.
- e) Evans, W. J.; Ansari, M. A.; Ziller, J. W. *Organometallics*, 1995, 14, 3;
- f) Evans, W. J.; Ulibarri, T. A.; Ziller, J. W. *J. Am. Chem. Soc.*, 1990, 112, 219.
- g) Evans, W. J.; Hughes, L. A.; Hanusa, T. P. *Organometallics*, 1986, 5, 1285.
- h) Evans, W. J.; Hughes, L. A.; Hanusa, T. P. *J. Am. Chem. Soc.*, 1984, 106, 4270.
- i) Evans, W. J.; Drummond, D. K.; Bott, S. G.; Atwood, J. L. *Organometallics*, 1986, 5, 2389.
- j) Evans, W. J.; Ulibarri, T. A.; Ziller, J. W. *J. Am. Chem. Soc.*, 1988, 110, 6877.
- k) Evans, W. J.; Keyer, R. K.; Zhang, H.; Atwood, J. L. *J. Chem. Soc., Chem. Commun.*, 1987, 837.
- l) Evans, W. J.; Drummond, D. K.; Grate, J. W.; Zhang, H.; Atwood, J. L. *J. Am. Chem. Soc.*, 1987, 109, 3928.
- m) Evans, W. J.; Drummond, D. K. *J. Am. Chem. Soc.* 1989, 111, 3329;
- n) Evans, W. J.; Keyer, R. A.; Rabe, G. W.; Drummond, D. K.; Ziller, J. W. *Organometallics*, 1993, 12, 4664.
- o) Evans, W. J.; Grate, J. W.; Doedens, R. J. *J. Am. Chem. Soc.* 1985, 107, 1671.
- p) Evans, W. J.; Ulibarri, T. A. *J. Am. Chem. Soc.*, 1987, 109, 4292.
- q) Evans, W. J.; Grate, J. W.; Hughes, L. A.; Zhang, H.; Atwood, J. L. *J. Am. Chem. Soc.*, 1985, 107, 3728.
- r) Evans, W. J.; Drummond, D. K. *J. Am. Chem. Soc.*, 1988, 110, 2772.

- s) Evans, W. J.; Drummond, D. K. *Organometallics*, **1988**, 7, 797.
- t) Evans, W. J.; Drummond, D. K.; Chamberlain, L. R.; Doedens, R. J.; Bott, S. G.; Zhang, H.; Atwood, J. L. *J. Am. Chem. Soc.*, **1988**, 110, 4983.
- u) Evans, W. J.; Drummond, D. K. *J. Am. Chem. Soc.*, **1986**, 108, 7440.
- v) Evans, W. J.; Ulibarri, T. A.; Ziller, J. W. *J. Am. Chem. Soc.*, **1990**, 112, 2314.
- w) Evans, W. J.; Leman, J. T.; Ziller, J. W. *Inorg. Chem.*, **1996**, 35, 4283;
- x) Desurmont, G., Li, Y., Yasuda, H., Maruo, T., Kanehisa, N., Kai, Y.,
Organometallics, **2000**, 19, 1811;
- 3 a) C. H. Lee, S. Lindsey, *Tetrahedron*, **1994**, 50, 11 427;
- b) B. Y. Liu, C. Bruckner, D. Dolphin, *Chem. Commun.*, **1996**, 2141, references therein;
- c) J. Jubb, S. Gambarotta, *J. Am. Chem. Soc.*, **1994**, 117, 4477;
- d) Dube, T., Gambarotta, S., Yap, G.P.A., *Organometallics*, **1998**, 17, 3967-3973;
- e) Dube, T., Conoci, S., Gambarotta, S., Yap, G.P.A., Vaspollo, G., *Angew. Chem. Int. Ed.*, **1999**, 38, 3657-3659;
- f) Dube, T., Gambarotta, S., Yap, G.P.A., *Organometallics*, **2000**, 19, 115-117;
- g) Dube, T., Gambarotta, S., Yap, G.P.A., *Organometallics*, **2000**, 19, 121-126
- 4 Dube, T., Freckmann, D., T., Conoci, S., Gambarotta, S., Yap, G.P.A.,
Organometallics, **2000**, 19, 209-211
- 5 a) Guan, J., Dube, T., Gambarotta, S., Yap, G.P.A., *Organometallics*, **2000**, 19, 4820-4827;
- b) Dube, T., Gambarotta, S., Yap, G.P.A., *Organometallics*, **2000**, 19, 817-823;

- c) Dube, T., Conoci, S., Gambarotta, S., Yap, G.P.A., *Organometallics*, **2000**, 19, 1182-1185;
- 6 a) Dube, T., Gambarotta, S., Yap, G.P.A., *Angew. Chem. Int. Ed.*, **1999**, 38, 1432-1435;
- b) Guan, J., Dube, T., Gambarotta, S., Yap, G.P.A., *Organometallics*, **2000**, 19, 4820-4827;
- c) Dube, T., Ganesan, M., Conoci, S., Gambarotta, S., Yap, G.P.A., *Organometallics*, **2000**, 19, 3716-3721;
- 7 Mascarenhas, C.M., Miller, S.P., White, P.S., Morken, J.P., *Angew. Chem. Int. Ed.*, **2001**, 40, 601
- 8 R. J. Errington, Advanced practical inorganic and metalorganic chemistry, Blackie Academic & Professional, **1997**
- 9 Evans, W.J., Drummond, D.K., Zhang, H., Atwood, J.L., *Inorg. Chem.*, **1988**, 27, 575
- 10 Weber, J.H. *Inorg. Chem.* **1967**, 6, 258-262.
- 11 Franceschi, F., Guillemot, G., Solari, E., Floriani, C., Re, N., Birkedal, H., Pattison, P., *Chem. Eur. J.* **2001**, 7, 1468-1478.
- 12 a) Srivastava, S., Mishra, R., *J. Indian Chem. Soc.*, **1995**, 72, 719-720;
- b) Srivastava, S., Singh, D., *Asian J. Chem.*, **1999**, 11, 1511-1513.

Chapter V:

Dinitrogen Activation by Diethyl- and Methylphenyl- Dipyrrolide Divalent Samarium Complexes

Summary

111

Introduction

111

Experimental Section

113

Results and Discussion

118

Structural Considerations

122

Conclusions

131

References

132

Balneu Mure	MB
Balneu Viperis	VB
Bene	bn
Borax	W W
Calmare	C
Calc	VE T
Calc vive	W r 20
Calc osium	*
Caput martis	⊙ ⊙
Canthare	⊙
Cera	⊙
Christallum	⊙
Cinis	E C
Cinres clovelli	⊙
Cinlar	⊙
Congular	⊙
Cochoto	⊙
Cruciatum	⊙
Crucis Vini	⊙
Crucis	⊙
Crucibulum	⊙
Cucurbitum	⊙
Dies	⊙
Digerere	⊙
Dilabere	⊙
Distillar	⊙
Elixir	⊙
Emus Equi	⊙
Ferros	⊙
Flegma	⊙
Fleuro	⊙
Gumma	⊙
Hora	⊙
Ignis	⊙
Ignis rotis	⊙
Lapis calumina	⊙
Lapis	⊙
Lutare	⊙
Lutum Symplicis	⊙
Magnes	⊙
Marchaite	⊙
Materia	⊙
Melissum	⊙

Dinitrogen Activation by Diethyl- and Methylphenyl- Dipyrrolide Divalent Samarium Complexes

V.1: Summary

The reaction of $[Sm\{N(SiMe_3)_2\}_2(THF)_2]$ with two dipyrrolide ligands of formula $[(R_2C(\alpha-C_4H_3N)_2)]$ ($R = Et$ or Me, Ph) has been examined. The reactions, in THF and under N_2 gave two new dinitrogen complexes, where the dinitrogen molecule has undergone a four electron reduction via the cooperative attack of four samarium atoms. The same reactions carried out under an argon atmosphere offered a divalent samarium macrocyclic cluster, in the case of the diethyldipyrrolide ligand. A similar reaction carried out under argon with the methylphenyl derivative offered the isolation of the unprecedented tripyrrole derivative, which formed a trinuclear mixed-valent Sm^{II}/Sm^{III} linear cluster.

V.2: Introduction

Even though recent results have described the availability of new, highly reactive divalent lanthanides such as thulium (II),¹ neodymium (II) and dysprosium (II),² divalent samarium still offers the best combination of high reactivity and availability of a well characterised system. Much of this characterisation stems from the interesting chemical transformations displayed by the cyclopentadienyl divalent samarium derivatives,³ which have provided a uniquely various and rich chemistry with a large series of diversified substrates.^{4,5} Reversible dinitrogen fixation was obtained with Cp^*_2Sm featuring a side-on bonding mode but without apparent N-N triple bond reduction given that the N-N

distance remained surprisingly short. The use of ancillary ligands such as calix-tetrapyrrole produced novel dinitrogen complexes that, albeit displaying the same π -bonding modes, clearly indicated that dinitrogen had undergone an irreversible four electron reduction.⁶ Attempts to prevent the involvement of alkali cations, unavoidable with calix-tetra pyrroles, by using dipyrrole ligands also provided a variety of complexes including the dinitrogen complexes as macrocyclic clusters. Different from the tetrapyrroles, the dipyrrole ligand systems have allowed the isolation of tetranuclear clusters containing dinitrogen thus demonstrating the simultaneous co-operative interaction of four metal centers.⁷ These systems have also been used successfully to characterise the Sm (II) precursors to dinitrogen activation through reactions carried out under argon atmosphere, producing large polynuclear clusters where the nuclearity seems to be controlled by the dipyrrole ligand substituents.⁸

The observations prompted us to extend this study to other dipyrrolide dianions bearing different substituents. The aims was twofold: 1) Firstly we wish to understand if different substituents could modify the metal redox potential thus pushing the reduction till complete N-N cleavage; 2) Secondly, to gather further information about the ability of ligand substituents to control the nuclearity of large clusters. Herein we describe our findings.

V.3: Experimental Section

All operations were performed under an inert atmosphere of a nitrogen-filled dry box or by using Schlenk-type glassware in combination with a nitrogen-vacuum line.⁹ Tetrahydrofuran and hexanes were dried by passing through a column of Al₂O₃ under an inert atmosphere prior to use, degassed *in vacuo* and transferred and stored under inert atmosphere. Dimethyl ethylene glycol was dried by distillation over LiAlH₄. [Sm{N(SiMe₃)₂}(THF)₂] was prepared according to literature procedures¹⁰ and methylphenyldipyrromethane was prepared from a variation of the literature procedures.¹¹ NMR spectra were recorded on a Varian Gemini 200 and on a Bruker AMX-500 spectrometer. Infrared spectra were recorded on a Mattson 3000 FTIR instrument from Nujol mulls prepared inside a dry box. Samples for magnetic susceptibility measurements were carried out at room temperature using a Gouy balance (Johnson Matthey) and corrected for underlying diamagnetism. Elemental analyses were carried out using a Perkin-Elmer Series II CHN/O 2400 analyser.

Preparation of Diethyldipyrrolylmethane

A catalytic amount of methyl sulfonic acid (0.5 mL) was added to a stirred mixture of 2-pentanone (7.6 mL, 0.07 moles) and pyrrole (20 mL, 0.3 moles). After stirring for 30 minutes under nitrogen flow, the colour of the solution changed from clear yellow to dark-green. The removal of excess pyrrole *in vacuo* afforded a green paste which was dissolved in a small volume of ethanol (25 mL). A small quantity of water was added to the solution until it became cloudy. The heterogeneous mixture was placed

at 4°C for 24 hours, upon which white crystalline needles of diethyldipyrrolylmethane needles were recovered (3.6 g, 17.8 mmoles, 25 % yield).

M.S.- E.I. m/e+ : 202

¹H-NMR (200 MHz, CDCl₃, 298 K) δ: 6.84 (br, 2H, N-H pyrrole), 6.22 (mult, 4H, C-H pyrrole), 6.12 (q, 2H, C-H pyr), 1.75 (q, 4H, CH₂ ethyl), 0.615 (t, 6H, CH₃ ethyl)

¹³C NMR (Benzene-D₆, 200 MHz, 25°C) δ: 116.9 (CH-pyrrole), 107. CH-pyrrole), 106.1 (CH-pyrrole), 29.3 (CH₂-ethyl), 8.01 (CH₃-ethyl)

El. Anal. Calcd (found) for C₁₃H₁₈N₂: C 77.18 (76.91); H 8.97 (8.85); N 13.84 (13.54)

Preparation of Methylphenyldipyrrolylmethane

Neat pyrrole (25 mL, 0.36 mol) was placed into a 250 mL flask under nitrogen atmosphere, fitted with a magnetic stirrer and a dropping funnel, and then cooled with an ice bath. While stirring, a solution of acetophenone (8.4 mL, 0.07 mol), a catalytic amount of methyl sulfonic acid (0.5 mL), and ethanol (30 mL) was added over a period of 20 minutes. The solution was allowed to react overnight, after which the ethanol and the excess pyrrole were removed *in vacuo*. The crude residual solid was solubilized in methylene chloride (20 mL) and filtered over a short column of silica to remove poly-pyrrole contaminants. Methylene chloride was removed *in vacuo* to give a white solid which was further purified by sublimation (110°C, 50 mtorr) to yield a white crystalline solid (5.2 g, 22.0 mmoles, 30 % yield).

M.S.- E.I. m/e+ : 236

$^1\text{H-NMR}$ (500 MHz, Benzene- D_6 , 298 K) δ : 7.05 (mult, 5H, C-H phenyl), 6.25 (q, 4H, C-H pyr), 6.02 (q, 2H, C-H pyrrole), 1.79 (s, 3H, CH_3)

^{13}C NMR (Benzene- D_6 , 125.76 MHz, 25°C) δ : 148.1 (quaternary C-phenyl), 137.4 (quaternary C-pyrrole), 128.4 (CH-phenyl), 128.0 (CH-phenyl), 126.7 (CH-phenyl), 117.2 (CH-pyrrole), 108.4 (CH-pyrrole), 106.9 (CH-pyrrole), 45.0 (quaternary C), 29.0 (CH_3 methyl)

128.4 128.3 128.1 127.9 126.7 117.2 108.4 106.9 44.9 29.0

Synthesis of $\{[(\text{C}_2\text{H}_5)_2\text{C}(\alpha\text{-C}_4\text{H}_3\text{N})_2]\text{Sm}\}_4(\text{THF})_2(\mu\text{-N}_2)$ (5.1)

A solution of $[\text{Sm}\{\text{N}(\text{SiMe}_3)_2\}_2(\text{THF})_2]$ (1.1 g., 1.9 mmol) in anhydrous THF (75 mL) was treated with diethyldipyrromethane (0.4g., 1.9 mmol) at room temperature and under a nitrogen atmosphere. After 3 days at room temperature, large dark-red crystals of 5.1 separated. (0.72 g, 0.42 mmol, 90% yield)

I.R. (Nujol mull, cm^{-1}) ν : 3092(w), 2729(w), 2207(w), 2057(w), 1698(w), 1627(w), 1562(w), 1460(s), 1428(s), 1406(m), 1376(s), 1338(m), 1326(m), 1306(m), 1272(s), 1254(s), 1172(s), 1133(s), 1069(s), 1035(s), 961(s), 927(s), 877(s), 835(s), 756(s), 726(s), 670(w), 632(s), 568(s);

μ_{eff} : 3.6 μB

Synthesis of $\{[1,1'\text{-diethyl}(\alpha\text{-C}_4\text{H}_3\text{N})_2\text{Sm}]_8(\text{THF})_4\}$ (5.2)

A solution of $[\text{Sm}\{\text{N}(\text{SiMe}_3)_2\}_2(\text{THF})_2]$ (2.0 g., 3.3 mmoles) in anhydrous THF (300 mL) was treated with diethyldipyrromethane (0.7 g., 3.3 mmoles) at room temperature and under an argon atmosphere. After 5 days at room temperature red needles were formed. (1.1 g, 0.32 mmoles, 78 % yield)

I.R. (Nujol mull, cm^{-1}) ν : 3082(m), 3064(m), 2722(w), 2503(w), 2394(w), 1685(w), 1639(w), 1594(w), 1543(m), 1459(s), 1423(s), 1377(s), 1341(m), 1325(m), 1284(m), 1260(s), 1172(s), 1132(s), 1086(s) 1038(s), 951(s), 925(m), 883(s), 831(s), 799(s), 751(s), 665(w), 632(m);

μ_{eff} : 10.6 μ_B

Synthesis of $\{[(\text{C}_6\text{H}_5)(\text{CH}_3)\text{C}(\alpha\text{-C}_4\text{H}_3\text{N})_2\text{Sm}]_4(\text{DME})_2(\mu\text{-N}_2)\}$ (5.3)

A solution of $[\text{Sm}\{\text{N}(\text{SiMe}_3)_2\}_2(\text{THF})_2]$ (1.2 g., 2.0mmoles) in anhydrous DME (175 mL) was treated with methyphenyldipyrromethane (0.5 g., 2.0 mmoles) at room temperature and under nitrogen atmosphere. After standing 2 days at room temperature small red crystals of 5.3 separated (0.6 g, 0.3 mmoles, 68 % yield).

I.R. (Nujol mull, cm^{-1}) ν : 3090(w), 3058(w), 1599(m), 1491(s), 1464(s), 1426(m), 1411(m), 1378(m), 1363(m), 1315(w), 1280(w), 1260(m), 1230(w), 1192(w), 1180(m), 1145(m), 1104(s), 1079(s), 1062(s) 1032(s), 971(w), 946(m), 936(w), 916(w), 866(s),

838(m), 795(s), 773(s), 730(m), 725(m), 705(m), 700(m), 640(m), 635(m), 622(w),
569(s), 554(s), 529(s);

μ_{eff} : 3.4 μ_B

Synthesis of $\{[(\text{C}_6\text{H}_5)(\text{CH}_3)\text{C}(\alpha\text{-C}_4\text{H}_3\text{N})_2] [(\text{C}_6\text{H}_5)(\text{CH}_3)\text{C}(\alpha\text{-C}_4\text{H}_3\text{N})(\beta\text{-C}_4\text{H}_3\text{N})] [(\text{C}_6\text{H}_5)(\text{CH}_3)\text{C})_2(\alpha\text{-C}_4\text{H}_3\text{N})_2(\alpha,\alpha\text{-C}_4\text{H}_2\text{N})] \text{Sm}_3\} \text{THF}_2$ (5.4)

A solution of $[\text{Sm}\{\text{N}(\text{SiMe}_3)_2\}_2(\text{THF})_2]$ (1.0 g., 1.7 mmoles) in anhydrous THF (50 mL) was treated with non-sublimed methyphenyldipyrromethane (0.39 g., 1.7 mmoles) at room temperature and under an argon atmosphere. After standing 4 days at room temperature, the solution volume was reduced (25 mL) and layered with anhydrous hexane (20 mL). Once the layering was complete, the solid mass obtained was examined with a polarized optical microscope and found to consist of two different crystalline products. Red crystals of complex 5.3 were the major component of the mixture, and their identity was clarified by isolating the crystals and comparing the I.R. spectra with an analytically pure sample. Complex 5.4 was the minor compound and it was isolated as dark red hexagonal prisms. While the crystals were suitable for X-ray analysis, the physical separation for other analytical determinations proved to be unfeasible thus preventing further spectroscopic characterization.

V.4: Results and Discussion

The transamination reaction performed with the alkali and halogen-free $[\text{Sm}\{\text{N}(\text{SiMe}_3)_2\}_2(\text{THF})_2]$ and diethylmethylpyrrolide in a small volume of THF at room temperature gave large red crystals of the dinitrogen complex **5.1** in good yield. The short N-N distance indicated by the crystal structure (Figure 5.1) showed that the dinitrogen molecule underwent a four electron reduction $[\text{N}(1)-\text{N}(1\text{A})=1.415(4)\text{\AA}]$, implying that each metal center was oxidized to the trivalent state. Accordingly, the coordination of dinitrogen is irreversible, with the complex remaining unchanged when exposed to vacuum and high temperature. As a common feature to the other dinitrogen complexes of similar ligand systems previously reported, complex **5.1** displays a very poor solubility in the most common solvents

The same reaction carried out under an argon atmosphere gave a quick precipitation of divalent **5.2** as a dark-red microcrystalline powder. Crystals of suitable size for x-ray analysis (Figure 5.2) were grown upon carrying out reactions in diluted solutions and allowing the reaction flasks to rest in a vibration free environment for 5 days. Compound **5.2** is an octameric macrocycle formed by an aggregation of divalent samarium monomers. This compound is a good representative candidate of the reactive precursor that performs dinitrogen activation to yield compound **5.1**. Each macrocycle can collapse in the presence of two dinitrogen molecules to form four-Sm subunits that can co-operatively reduce the guest molecule and form a tetrameric complex.

Use of the methylphenyl-methyldipyrrolide ligand and the usual reaction conditions offered neither the dinitrogen nor the macrocyclic complexes but instead yielded intractable compounds. However, the reaction of samarium (II) and

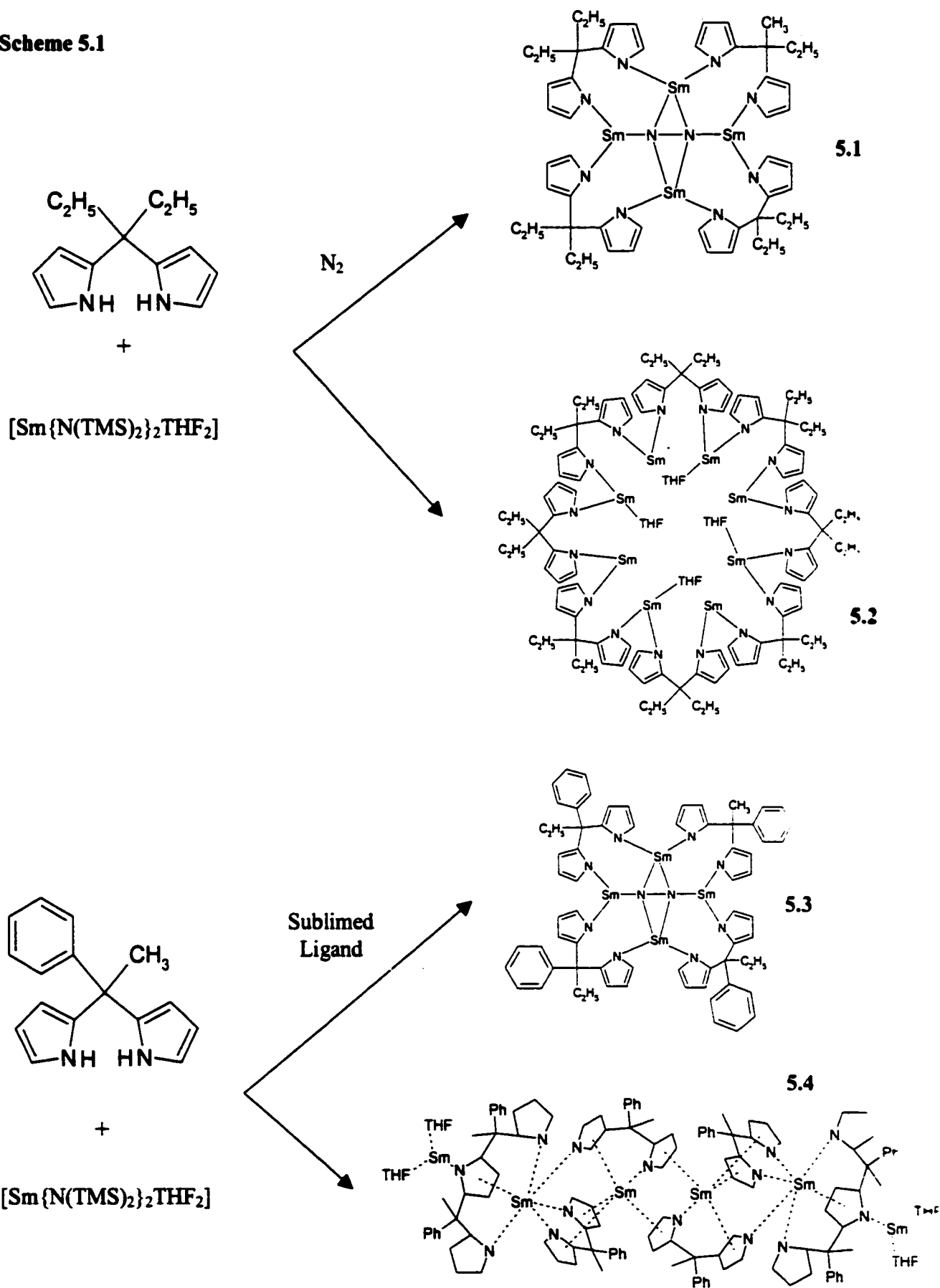
methylphenyl-methyldipyrrolide in small volumes of anhydrous DME gave compound **5.3** as red crystals (Figure 5.3). This compound is very similar to compound **5.1**, but there are slight variations in the bonding mode of the ligands. Whether these variations are due to the change in the solvent or to the asymmetry of the ligand backbone remains unclear. Attempts to reproduce the divalent samarium precursor from an argon atmosphere with the analogous ligand system were also unsuccessful from DME.

Compound **5.4** was obtained from the reaction of recrystallised (but not sublimed) methylphenyl-methyldipyrrolide and $[\text{Sm}\{\text{N}(\text{SiMe}_3)_2\}_2(\text{THF})_2]$ at room temperature in THF. When the solution was reduced in volume and layered with hexanes, crystalline material was obtained after a few days. Two distinct types of crystals were observed, the major component consisting of very small ~~redish~~reddish brown crystals which were identified as compound **5.3** by comparison of the IR spectra with that of an analytically pure sample. The minor component was composed of large red hexagonal prisms which could not be manually separated from the smaller crystals, although single crystals were successfully analyzed by X-ray crystallography (Figure 5.4). The structure clearly shows the presence of three methylphenyl-methyldipyrrolide derivatives, one being an N-confused dipyrrolide and the other being a tripyrrole moiety, in addition to the regular dipyrrole. Analysis of the ligand by mass spectrometry only showed the peaks for the expected dipyrrole. Such a result was inconclusive since a minor product which is less volatile than a major one is usually masked from ~~anaysis~~analysis in mass spectroscopy. Also, it is possible that the tripyrrane would not survive the ionisation intact to be analysed, especially if it was present in low concentrations. Close inspection of the 500 MHz ^1H -NMR finally identified the presence of the two unexpected ligands in

the starting material. Two small peaks between 1.77 and 1.78 ppm were found to integrate to approximately 10% of the methyl peak at 1.79 ppm. Because of the resemblance of all the methylphenyl-polypyrrolide ligands, this was found to be the only sign-method to detect the presence of unwanted analogues. Sublimation of the ligand proved successful in the separation of analytically pure methylphenyldipyrromethane, from which complex 5.3 was obtained.

Although the isolation of 5.4 is purely serendipitous, this species provides the first example of a tripyrrolide-metal complex. Also unclear is the mixed-valent status of the metals since the redox partner of the metal oxidation has not been identified. Work is underway to synthesise rational complexes of samarium with tripyrrolide ligands.

Scheme 5.1



V.5: Structural Considerations

Suitable crystals were selected, mounted on thin, glass fibres using paraffin oil and cooled to the data collection temperature. Data were collected on a Bruker AX SMART 1k CCD diffractometer using 0.3° ω -scans at 0, 90, and 180° in ϕ . Unit-cell parameters were determined from 60 data frames collected at different sections of the Ewald sphere. Semi-empirical absorption corrections based on equivalent reflections were applied (Blessing, R., *Acta Cryst.*, 1995, A51, 33-38).

No symmetry higher than triclinic was observed for 5.1·2(thf) and refinement in the centrosymmetric space group option yielded computationally stable and chemically reasonable results of refinement. Systematic absences in the diffraction data and unit-cell parameters were uniquely consistent with the reported space groups for 5.2·4(thf), 5.3 and 5.4·3(thf). The structures were solved by direct methods, completed with difference Fourier syntheses and refined with full-matrix least-squares procedures based on F^2 .

The compound molecules of 5.1·2(thf), 5.3, and 5.4·3(thf) reside on an inversion center. One, eight (half-occupancy), and three (half-occupancy) molecules of tetrahydrofuran (thf) solvent were located cocrystallized in the asymmetric units of 5.1·2(thf), 5.2·4(thf), and 5.4·3(thf), respectively. The half-occupied, cocrystallized, thf molecules were found to be severely disordered and were treated as rigid, flat, pentagons with the atoms having smallest isotropic parameter per ring assigned oxygen atom identities. All non-hydrogen atoms were refined with anisotropic displacement parameters. All hydrogen atoms were treated as idealized contributions. All scattering factors are contained in the SHEXTL 5.10 program library (Sheldrick, G. M., Bruker AXS, Madison, WI, 1997).

1. Complex 5.1 is comprised of four samarium atoms, bridged by four diethyldipyrromethane ligands and surrounding a dinitrogen molecule [N(1)-N(1A)=1.415(4)Å (Figure 5.1). Each ligand is dianionic, with each pyrrole ring σ -bonded to one samarium [Sm(1)-N(2)=2.698(4)Å], and at the same time π -bonded to another adjacent metal [Sm(1)-N(3)_{centroid}=2.693(4)Å]. Two of the samarium atoms have an end-on bonding mode with respect to the dinitrogen molecule [Sm(1)-N(1)=2.145(3)Å] and are also coordinated to a molecule of THF [Sm(1)-O(1)=2.525(3)Å]. These metal atoms display a distorted octahedral geometry [O(1)-Sm(1)-N(1)=145.56(13)°, [N(4)-Sm(1)-N(3)_{centroid}=170.5(14)°, [N(2)-Sm(1)-N(5)_{centroid}=170.3(14)]. The second pair of samarium atoms are bound in a side-on fashion to the dinitrogen molecule and have slightly longer Sm-N bond lengths [Sm(2)-N(1)=2.328(3)Å].

2. Complex 5.2 (Figure 5.2) is formed by 8 samarium atoms bridged by eight diethyldipyrromethane ligands to form a large and planar ring. Each samarium atom is σ -bonded to two pyrrole moieties from two different ligands [Sm(1)-N(1)=2.617(10)Å] and π -bonded to two other pyrrole rings from the same ligands [Sm(1)-N(2)_{centroid}=2.582(10)Å]. The presence of four THF molecules gives rise to two sets of differentiable samarium atoms with every second metal atom complexed to a solvent molecule [Sm(2)-O(1)=2.599(10)Å]. The samarium atoms that bear the coordinate THF adopt a distorted trigonal bipyramidal conformation with THF oxygen atom and two π -bonded pyrrole centroids placed in the equatorial positions, and with the 2 σ -bonded

pyrrole nitrogen atoms occupying the axial positions {[N(2)-Sm(2)-N(3)=162.7(3)°], [O(1)-Sm(2)-N(2)=77.3(3)°], [N(4)_{centroid}-Sm(2)-N(2)=101.8(3)°], [N(1)_{centroid}-Sm(2)-N(2)=85.1(3)°]}. The other samarium atoms, which do not bear the coordinated solvent molecules, adopt a highly distorted tetrahedral conformation {[N(2)_{centroid}-Sm(1)-N(1)=84.9(3)°], [N(2)_{centroid}-Sm(1)-N(16)=111.9(3)°], [N(2)_{centroid}-Sm(1)-N(15)_{centroid}=126.8(3)°]}.

3. Complex 5.3 (Figure 5.3) is very similar to complex 5.1, as it is formed by four methylphenyldipyrromethane samarium units and two DME molecules organized in a 4 membered ring around the centrally located molecule of N₂. The nitrogen-nitrogen distance [N(1)-N(1A)=1.42(2)] indicates a four electron reduction of N₂ and compares well with that of 5.1. However, a closer observation does bring up a discrepancy with the previous complex. While the Sm atoms side on bind to the N₂ unit, both are both π -bonded and σ -bonded to two pyrrole rings from two different ligands, the other two terminally bonded metals are π -bonded to only one ring and σ bonded to the other three. The bridging σ -bonded nitrogen atom from the pyrrolide ring doesn't equally interact with the two metal atoms [Sm(1)-N(2)=2.585(12)Å], [Sm(2)-N(2)=2.828(12)Å], forming a stronger σ -bond to one samarium than to the other.

4. The unit cell of 5.4 is composed by two crystallographically independent but chemically equivalent units (Figure 5.4). Each molecule is composed by six samarium atoms forming a symmetry generated zig-zag type of array. The three independent samarium atoms are bridged by three different pyrrole based ligands. The first ligand is an N-confused methylphenyldipyrromethane, where one of the pyrrole rings has the attachment to the central carbon shifted to the ring β position. The two pyrrole rings

form σ -bonds with two different Sm atoms [Sm(1)-N(1)=2.583(6)Å]; [Sm(2)-N(2)=2.464(6)Å], and one of these rings provides the π -bond used to bridge the two units of the [Sm(1A)-N(1)_{centroid}=4.042Å]. The second ligand is a normal methylphenyldipyrromethane, and it adopts the same bonding mode observed with 5.3, with both pyrrole rings σ -bonding the same samarium [Sm(2)-N(3)=2.481(6)Å]; [Sm(2)-N(4)=2.392(6)Å], and forming π -bonds to the next samarium atom [Sm(1)-N(3)_{centroid}=2.708(6)Å]. The third ligand is an unprecedented 5-10-di(phenylmethyl)tripyrane which acts as a trianionic and hexadentate ligand, wrapping around the terminal Sm atom with the pyrrole rings σ -bonded to the same samarium [Sm(2)-N(5)=2.544(6)Å]; [Sm(2)-N(7)=2.495(6)Å], and the third π -bonded to the central Sm atom [Sm(3)-N(5)_{centroid}=2.581(6)Å]. The central pyrrole ring of each tripyrane ligand forms a σ -bond to the third samarium atom [Sm(3)-N(6)=2.602(6)Å], while π -bonding to the Sm(2) atom [Sm(2)-N(6)_{centroid}=2.514(6)Å]. It is interesting to observe that the observed tripyrrolide moiety only crystallized as the R,S stereo-isomer as both bridging carbons that link the pyrrole rings are chiral.

Observing the metal atoms, we see that the Sm(1) metal adopts a highly distorted trigonal bis-pyramidal geometry where the nitrogen atoms of the σ -bonded rings occupy the axial position and the other 4 positions are taken up by the centroids of the four pyrrole rings π -bonding the metal {[N(1)-Sm(1)-N(4)_{centroid}=167.0(2)°], [N(1)-Sm(1)-N(1A)_{centroid}=94.8(2)°], [N(1)-Sm(1)-N(2)_{centroid}=83.4(2)°], [N(1)-Sm(1)-N(3)_{centroid}=103.9(2)°]}. Scrutinizing the Sm(2) atom we observe that it is σ -bonded to 5 pyrrole nitrogens and π -bonded by a sixth pyrrole ring to afford a highly distorted octahedral geometry at the metal center [N(2)-Sm(2)-N(6)_{centroid}=164.1(2)°], [N(4)-

$\text{Sm}(2)\text{-N}(5)=159.5(2)^\circ$; $[\text{N}(3)\text{-Sm}(2)\text{-N}(7)]=155.2(2)^\circ$. Finally, the $\text{Sm}(3)$ atom is σ -bonded to a single pyrrole nitrogen, π -bonded to two pyrrole rings and coordinatively bound by two THF molecules [$\text{Sm}(3)\text{-O}(1)=2.575(6)\text{\AA}$]; [$\text{Sm}(3)\text{-O}(2)=2.574(5)\text{\AA}$] which confers a distorted trigonal bis-pyramidal geometry to the metal center $\{[\text{N}(6)\text{-Sm}(1)\text{-O}(1)_{\text{centroid}}]=174.2(2)^\circ$, $[\text{N}(6)\text{-Sm}(1)\text{-O}(2)_{\text{centroid}}]=99.9(2)^\circ$, $[\text{N}(6)\text{-Sm}(3)\text{-N}(5)_{\text{centroid}}]=83.4(2)^\circ$, $[\text{N}(6)\text{-Sm}(3)\text{-N}(7)_{\text{centroid}}]=81.1(2)^\circ\}$. As complex **5.4** is a mixed-valent compound arising from a trivalent and two divalent Sm atoms, the electronic character of the metal atoms is interesting. For example, as the $\text{Sm}(1)$ atom is π -bonded to four pyrrole rings and σ -bonded to a fifth, the formal electron count is made at 32 if we consider that particular Sm as a divalent one.

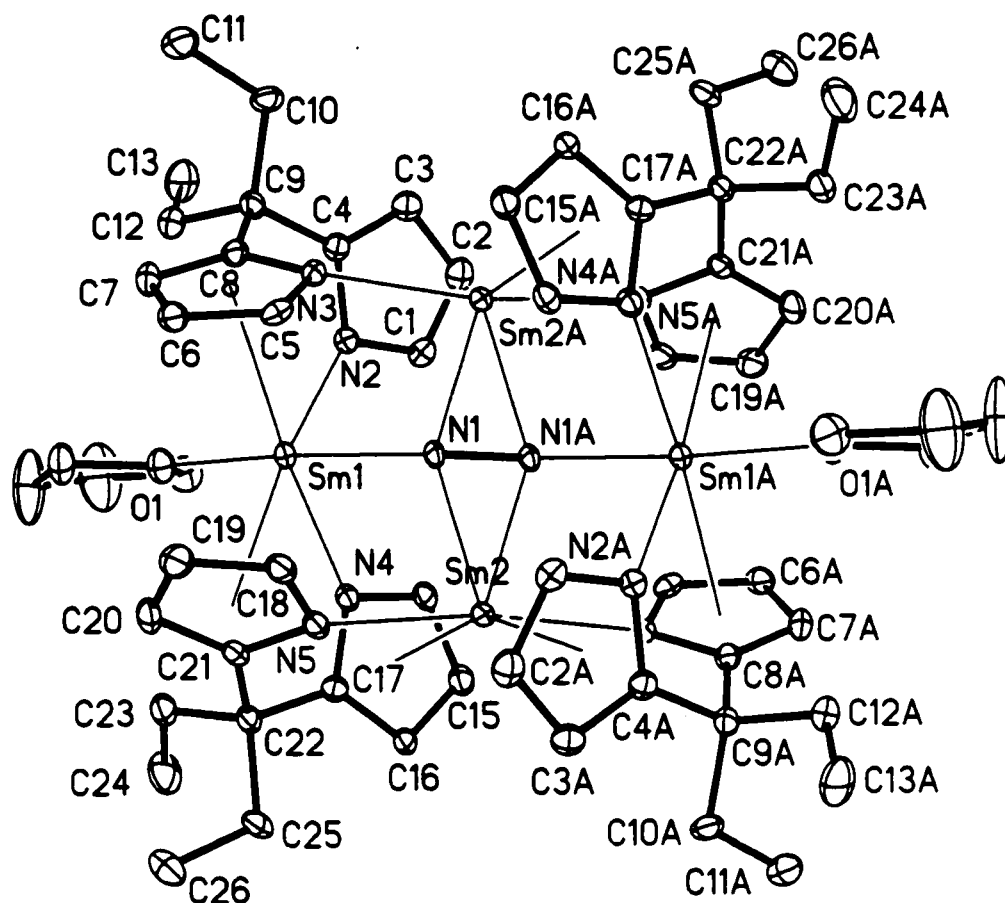


Figure 5.1: Thermal ellipsoid plot of $[4((\text{C}_2\text{H}_5)_2\text{C}(\alpha\text{-C}_4\text{H}_3\text{N})_2)\text{Sm}](\text{THF})_2(\mu\text{-N}_2)$ (5.1).

Thermal ellipsoids are drawn at the 30% probability level.

Selected Bond Distances (Å) and Angles (deg): N(1)-N(1A)=1.415(6), Sm(1)-N(1)=2.145(3), Sm(2)-N(1)=2.342(3), Sm(2)-N(1A)=2.342(3), Sm(1)-O(1)=2.525(3), Sm(1)-N(2)=2.698(4), Sm(1)-N(3)_{centroid}=2.693(4), Sm(2)-N(5)=2.579(4), N(4)-Sm(1)-N(3)_{centroid}=170.5(13), N(2)-Sm(1)-N(5)_{centroid}=170.3(13), Sm(1)-N(1)-N(1A) = 156.64(13), O(1)-Sm(1)-N(1) = 145.56(13), N(1)-Sm(1)-N(2) = 77.16(13), N(2)-Sm(1)-N(4) = 76.83(13),

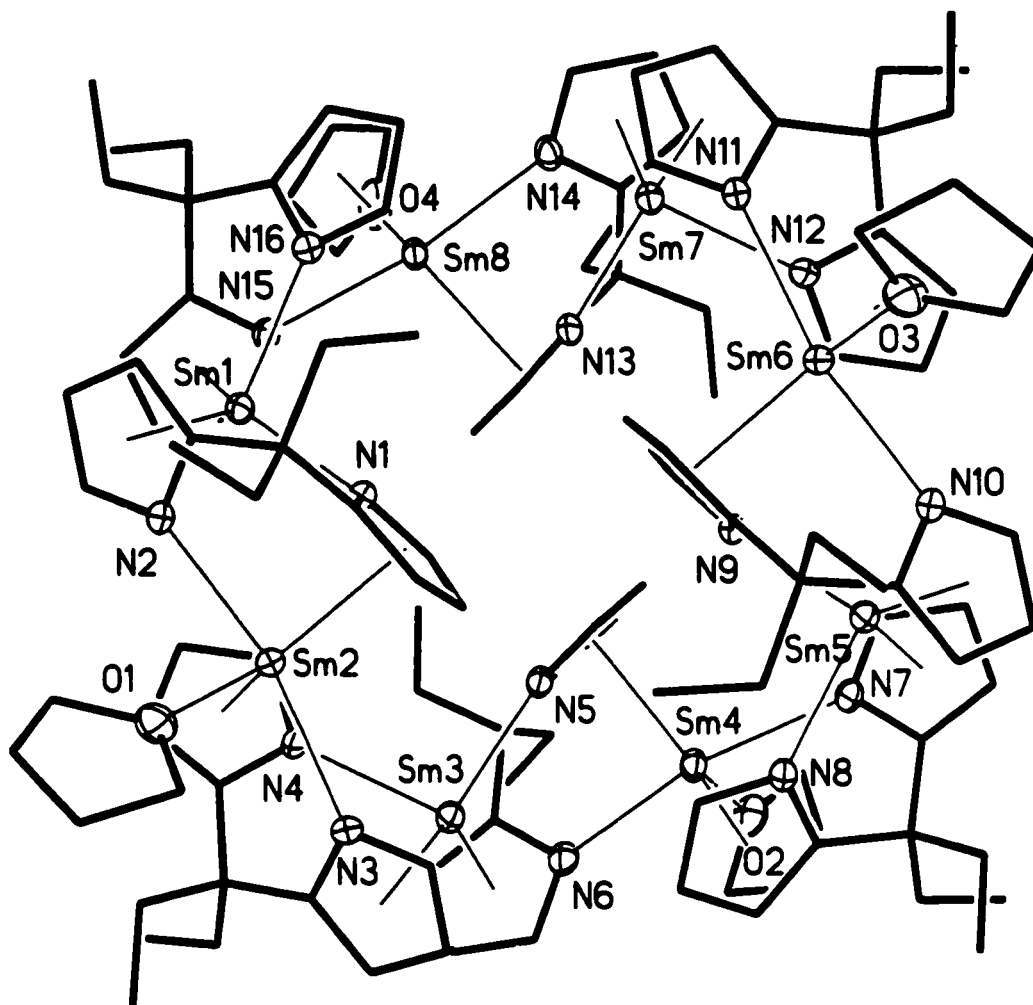


Figure 5.2: Thermal ellipsoid plot of $\{[1,1'\text{-diethyl}(\alpha\text{-C}_4\text{H}_3\text{N})_2]\text{Sm}\}_8(\text{THF})_4$ (**5.2**).

Thermal ellipsoids are drawn at the 30% probability level. All carbon atoms were resolved anisotropically but are not shown as ellipsoids.

Selected Bond Distances (Å) and Angles (deg): Sm(1)-N(1)=2.617(10), Sm(1)-N(2)_{centroid}=2.582(10), Sm(1)-N(16)=2.600(11), Sm(2)-N(2)=2.625(10), Sm(2)-N(3)=2.644(10), Sm(2)-O(1)=2.599(10), N(1)-Sm(1)-N(16) = 99.1(3), N(2)-Sm(2)-O(1) = 77.3(3), N(2)-Sm(2)-N(3) = 162.7(3), N(3)-Sm(2)-O(1) = 85.4(3), N(2)-Sm(2)-N(4)_{centroid} = 101.8(3), N(2)-Sm(2)-N(1)_{centroid} = 85.1(3),

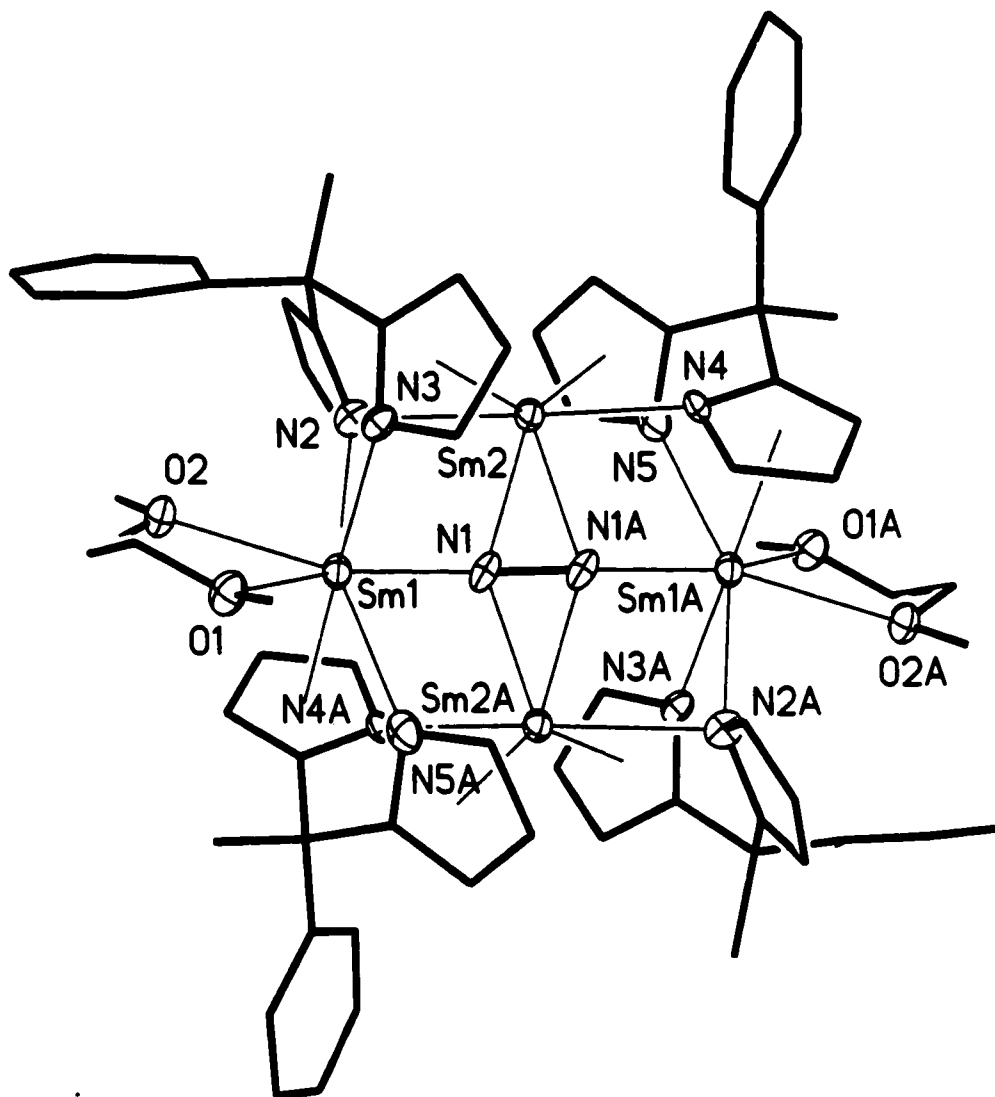


Figure 5.3: Thermal ellipsoid plot of $[\{[(C_6H_5)(CH_3)C(\alpha-C_4H_3N)_2]Sm\}_4(DME)_2](\mu-N_2)]$

(5.3). Thermal ellipsoids are drawn at the 30% probability level. All carbon atoms were resolved anisotropically but are not shown as ellipsoids.

Selected Bond Distances (Å) and Angles (deg): N(1)-N(1A)=1.42(2), Sm(1)-N(1)=2.149(11), Sm(2)-N(1)=2.316(13), Sm(2)-N(1A)=2.316(13), Sm(1)-O(1)=2.588(10), Sm(1)-O(2)=2.629(10), Sm(1)-N(2)=2.585(12), Sm(2)-N(2)=2.828(12), Sm(1)-N(3)=2.586(12), Sm(1)-N(5A)=2.817(14), Sm(1)-N(1)-N(1A) = 167.0(13), N(2)-Sm(1)-N(3) = 66.3(4), N(1)-Sm(1)-N(3) = 80.8(4)

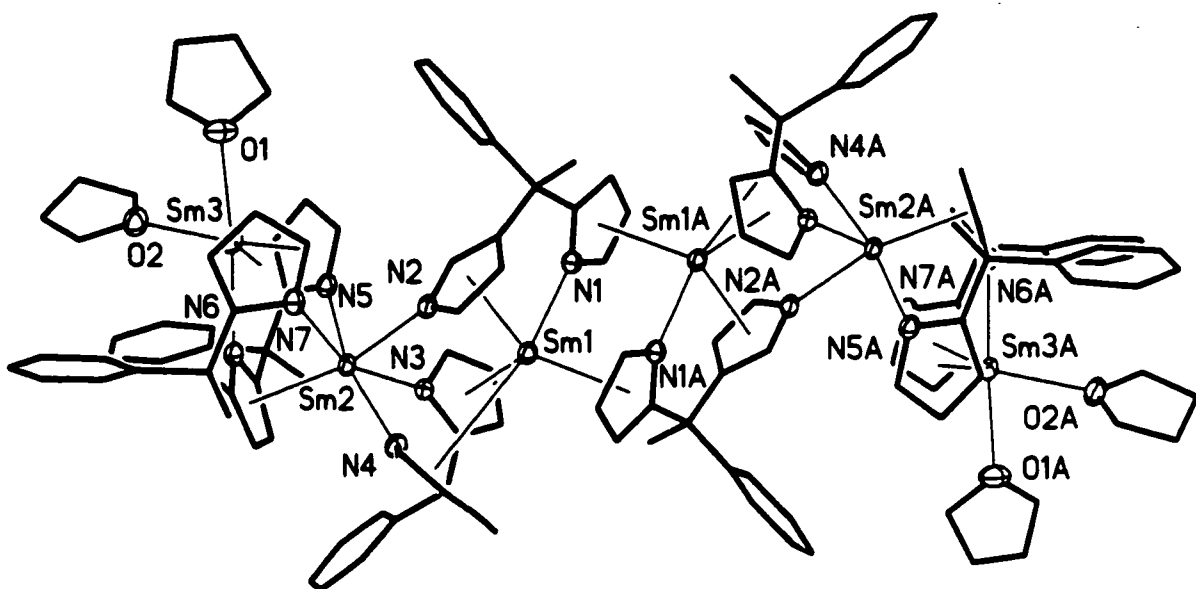


Figure 5.4: Thermal ellipsoid plot of $\{[(C_6H_5)(CH_3)C(\alpha-C_4H_3N)_2] [(C_6H_5)(CH_3)C(\alpha-C_4H_3N)(\beta-C_4H_3N)] [((C_6H_5)(CH_3)C)_2(\alpha-C_4H_3N)_2(\alpha,\alpha-C_4H_2N)] Sm_3\} THF_2$ (5.4).

Thermal ellipsoids are drawn at the 30% probability level. All carbon atoms were resolved anisotropically but are not shown as ellipsoids.

Selected Bond Distances (Å) and Angles (deg): Sm(1)-N(1)=2.583(6), Sm(1)-N(2)_{centroid}=2.670(6), Sm(1A)-N(1)_{centroid}=4.042(6), Sm(1)-N(3)_{centroid}=2.708(6), Sm(2)-N(2)=2.771(6), Sm(2)-N(3)=2.481(6), Sm(2)-N(4)=2.392(6), Sm(2)-N(5)=2.544(6), Sm(2)-N(7)=2.495(6), Sm(3)-N(6)=2.602(6), Sm(3)-N(5)_{centroid}=2.581(6), Sm(3)-O(1)=2.575(6), Sm(3)-O(2)=2.574(6), N(2)-Sm(2)-N(4)= 84.1(2), N(2)-Sm(2)-N(7)= 78.6(19), N(3)-Sm(2)-N(7)=155.2(2), N(3)-Sm(2)-N(4)= 74.4(2), N(4)-Sm(2)-N(5)=159.5(2), O(1)-Sm(3)-O(2)= 77.3(2), N(6)-Sm(3)-O(2)= 77.36(2),

V.6 Conclusion

Two new dinitrogen complexes from the reactions of divalent samarium and dipyrrolides were synthesised, as was the divalent precursor to one of them from the reaction carried out under an argon atmosphere. A serendipitous result from the reaction of non-analytically pure methylphenyl-methyldipyrrole and $[\text{Sm}\{\text{N}(\text{SiMe}_3)_2\}_2(\text{THF})_2]$ gave the first example of a samarium-tripyrane complex, giving insight in the bonding mode of such novel compounds.

References

- 1 Bochkarev, M.N., Fedushkin, I.L., Fagin, A.A., Petrovskaya, T.V., Ziller, J.W., Broomhall-Dillard, R.N.R., *Angew. Chem. Int. Ed. Engl.* **1997**, 36, No. 1/2
- 2 Bochkarev, M.N., Fagin, A.A, *Chem. Eur. J.*, **1999**, 5, no.10
- 3 a) Girard, P., Namy, J. L. Kagan, H.B., *J. Am. Chem. Soc.* **1980**, 102, 2693; W. J. b)Evans, I. Bloom, W. E. Hunter, and J. L. Atwood, *J. Am. Chem. Soc.* **1983**, 105, 140;
c)W. J. Evans, S. C. Engerer, P. A. Piliero, A. L. Wayda, *J. Chem. Soc. Chem. Commun.* **1979**, 1007;
d)W. J. Evans, S. C. Engerer, P. A. Piliero, A. L. Wayda, *Fundamentals of Homogeneous Catalysis*, Tsutsui, M. Ed., Plenum Press, New York, **1979**, 3;
e)W. J. Evans, M. A. Ansari, J. W. Ziller, S. I. Khan, *Organometallics*, **1995**, 14, 3;
f)W. J. Evans, T. A. Ulibarri, J. W. Ziller, *J. Am. Chem. Soc.* **1990**, 112, 219;
g)W. J. Evans, L. A. Hughes, T. P. Hanusa, *J. Am. Chem. Soc.* **1984**, 106, 4270;
h)W. J. Evans, L. A. Hughes, T. P. Hanusa, *Organometallics*. **1986**, 5, 1285;
i)W. J. Evans, D. K. Drummond, S. G. Bott, J. L. Atwood, *Organometallics*. **1986**, 5, 2389;
j)W. J. Evans, R. A. Keyer, H. Zhang, J. L. Atwood, *J. Chem. Soc., Chem. Commun.* **1987**, 837;
k)W. J. Evans, D. K. Drummond, J. W. Grate, H. Zhang, J. L. Atwood, *J. Am. Chem. Soc.* **1987**, 109, 3928;
l)W. J. Evans, D. K. Drummond, *J. Am. Chem. Soc.* **1989**, 111, 3329;

- m) W. J. Evans, R. A. Keyer, G. W. Rabe, D. K. Drummond, J. W. Ziller, *Organometallics*, **1993**, *12*, 4664;
- n) W. J. Evans, J. W. Grate, R. J. Doedens, *J. Am. Chem. Soc.* **1985**, *107*, 1671;
- o) W. J. Evans, T. A. Ulibarri, *J. Am. Chem. Soc.* **1987**, *109*, 4292;
- p) W. J. Evans, J. W. Grate, L. A. Hughes, H. Zhang, J. L. Atwood, *J. Am. Chem. Soc.* **1985**, *107*, 3728;
- q) W. J. Evans, D. K. Drummond, *J. Am. Chem. Soc.* **1988**, *110*, 2772;
- r) W. J. Evans, D. K. Drummond, *Organometallics*, **1988**, *7*, 797;
- s) W. J. Evans, D. K. Drummond, L. R. Chamberlain, R. J. Doedens, S. G. Bott, H. Zhang, J. L. Atwood, *J. Am. Chem. Soc.* **1988**, *110*, 4983;
- t) W. J. Evans, D. K. Drummond, *J. Am. Chem. Soc.* **1986**, *108*, 7440;
- u) W. J. Evans, T. A. Ulibarri, J. W. Ziller, *J. Am. Chem. Soc.* **1990**, *112*, 2314;
- v) X. Zhang, G. R. Loppnow, R. McDonald, J. Takats, *J. Am. Chem. Soc.* **1995**, *117*, 7828;
- w) G. Desurmont, Y. Li, H. Yasuda, T. Maruo, N. Kanehisa, Y. Kai *Organometallics* **2000**, *19*, 1811.
- 4 Z. Pikramenou, *Coord. Chem. Rev.* **1990**, *172*, 99
- 5 Evans, W.J., Ulibarri, T.A., Ziller, J.M., *J. Sm. Chem. Soc.*, **1988**, *110*, 6877
- 6 J. Jubb, S. Gambarotta, *J. Am. Chem. Soc.* **1994**, *117*, 4477
- 7 a) Dube, T, Gambarotta, S., Yap, G.P.A., *Angew. Chem. Int. Ed.*, **1999**, *38*, 1432-1435;
- b) Guan, J., Dube, T., Gamabarotta, S., Yap, G.P.A., *Organometallics*, **2000**, *19*, 4820-4827;

- c) Dube, T., Ganesan, M., Conoci, S., Gambarotta, S., Yap, G.P.A.,
Organometallics, **2000**, 19, 3716-3721;
- 8 Ganesan, M., Gambarotta, S., Yap G.P.A., *Angew. Chem. Int. Ed.*, **2001**, 40, 766-
769
- 9 R. J. Errington, *Advanced practical inorganic and metalorganic chemistry*,
Blackie Academic & Professional, **1997**
- 10 Evans, W.J., Drummond, D.K., Zhang, H., Atwood, J.L., *Inorg. Chem.*, **1988**,
27,575
- 11 Dube, T., Conoci, S., Gambarotta, S., Yap, G.P.A., *Organometallics*, **2000**, 19,
1182-1185;

The reaction of $\text{YbI}_2(\text{THF})_2$ with diphenylmethyldipyrrolide yielded an octameric divalent Yb macrocycle as a major product, but two additional compounds were also obtained from the same reaction. An increase in the reaction time permitted the crystallization of both minor components, which were discovered to be a tetrameric cyclic Yb(II)-oxo complex and a monomeric Yb(III) complex. The presence of these side products leads to believe that octameric structure plays an important role in the stabilization of the Yb centers, since the same intermediate which is the building block of the octamer may also undergo different reaction leading to THF deoxygenation and disproportionation pathways. The major octameric compound was analogous to the Sm(II) dipyrrolide octameric clusters obtained under an argon atmosphere, which are thought to represent the intermediate species in the formation of dinitrogen complexes. Finally, the large octameric structure may be deformed by hosting small units, a characteristic that might find uses in host/guest transformations.

The reactions of $\text{SmI}_2(\text{THF})_2$ and $\text{YbI}_2(\text{THF})_2$ with the alkali salts of 2,5-dimethylpyrrole, or the reduction of the correspondent trivalent species with the appropriate alkali metals, led to the formation of divalent mono- and polynuclear complexes. This mono-pyrrolide ligand seems to be less activating than previous tetra- and dipyrrolides, suppressing the reactivity of low-valent samarium towards solvent and dinitrogen molecules. This lower activity might be linked to the retention of many alkali cation atoms, which seems more substantial than in dipyrrolide chemistry. Multiple complexes were obtained, which permitted the comparison and analysis of different system variables. First of all, there were substantial differences between the samarium and ytterbium complexes, which might indicate that ligand-metal interactions are highly

influenced by the size of the metal atom in the case of mono-pyrroles. Using different starting materials of the same metal (i.e. SmI_2 instead of SmCl_3) gave very similar structures, which suggests that the nature of the halide does not greatly influence the structure. Further analysis of the complexes obtained brought forth the observation that the bonding mode adopted by the ligand and the lanthanide metal is greatly dependent on the nature of the alkali cation present in the structure.

The reaction of $[\text{Sm}\{\text{N}(\text{SiMe}_3)_2\}_2(\text{THF})_2]$ with highly delocalized pyrrole supporting schiff base ligands yielded three distinct complexes, two of which had samarium atoms that had been oxidized to the trivalent state. The first of these complexes was formed by the dimerization of two ligands through the formation of a C-C bond. This carbon-carbon bond was brought about by the formation of stabilized radical species when the divalent samarium was bound by the ligand. These transient complexes combine through radical-radical coupling to form the bonding between ligands yielding two $\text{Sm}(\text{III})$ atoms. The oxidation pathway for the second compound is still unclear, but ionic complex obtain was clearly made up of $\text{Sm}(\text{III})$ atoms. The third complex was also formed by the dimerization of two species, but the units are linked through π interactions and there was no evidence of a radical process. X-ray characterization of this last complex clearly indicated the presence of divalent samarium centers. The analysis of this compound gave rise to novel observations for $\text{Sm}(\text{II})$ complexes. While typical divalent samarium complexes are dark in colour and they display high magnetic moment susceptibilities, our compound was light in colour and it had characteristics usually attributed to trivalent samarium containing complexes.

The reaction of $[\text{Sm}\{\text{N}(\text{SiMe}_3)_2\}_2(\text{THF})_2]$ with two dipyrrolide ligands, diethyldipyrromethane and methylphenyldipyrromethane, gave rise to two new dinitrogen complexes where the dinitrogen molecule was reduced by an electron from four different samarium centers. The precursor for the first dinitrogen complex was also obtained by carrying out the reaction under an argon atmosphere. The precursor is as expected an octameric macrocyclic structure which has previously been reported for analogous dipyrrolide ligands. The same treatment under argon with the methylphenyldipyrromethane did not lead to any tractable crystalline materials, possibly due to its asymmetric nature. Finally, a serendipitous result from the reaction of divalent samarium and methylphenyldipyrromethane gave the first example of a lanthanide complexed by a tripyrrane ligand.

Future work on the treatment of low-valent lanthanides with pyrrolide ligands can take quite a few possible pathways, but the previous investigations offer up a few promising avenues of research:

- i) Since tetra- and mono-pyrroles are apt to retain alkali metals in their structures and that these affect the structures, reactions with alkali free $[\text{Sm}\{\text{N}(\text{SiMe}_3)_2\}_2(\text{THF})_2]$ might yield novel compounds, possibly activating dinitrogen.
- ii) If chiral schiff bases that support two pyrrole moieties can be synthesized, especially ones resistant to ligand dimerization, low-valent lanthanide complexes

of these ligands might prove very interesting as stoichiometric chiral reductants in organic chemistry.

- iii) The use of divalent Yb (chapter 2) and Sm (chapter 5) octameric species with free interstitial spaces might complement each other in the study of their ability to host small molecules. The characterization of the subsequent transformations caused by the highly reactive samarium centers would profit from the analysis of the less reactive ytterbium complexes, which could possibly give some information on the transitional species.
- iv) Further study of tripyrrolide ligands could yield a new trianionic chiral ligand system that might lead to the development of a new chemistry. The resemblance of these ligands to the previously studied systems bodes well for their reactivity while their ability to support chiral centers increases their value in stoichiometric or catalytic systems.

Appendix

Table 1: Crystal Data and Structure Analysis Results for Complexes 2.1, 2.2, 2.3, 2.4 and 2.5

	2.1	2.2	2.3	2.4	2.5
Formula	C ₁₆₆ H ₁₂₈ N ₁₆ Yb ₈	C ₁₆ H ₁₂₈ K ₃ N ₆ O ₉ Yb ₆	C ₇₅ H ₇₂ K ₃ N ₆ O ₃ Yb	C ₆₆ H ₆₀ N ₆ O ₃ Yb ₆	C ₂₆₀ H ₂₇₂ Li ₂ Li ₂ N ₁₆ O ₁₉ Yb ₈
Formula weight	3755.18	2548.62	1395.73	1701.52	5137.84
Space group	Tetragonal, P4/n	Monoclinic, C2/c	Monoclinic P2(1)n	Monoclinic, P2(1)	Triclinic, P-1
A (Å)	26.859 (3)	26.131 (7)	13.934 (2)	14.183 (1)	17.254(4)
B (Å)	26.859 (3)	17.197 (5)	24.974 (3)	14.065 (1)	19.145(4)
C (Å)	24.152 (3)	25.325 (7)	19.565 (2)	14.911 (1)	19.659(4)
β(deg)	90	109.186 (5)	107.783 (2)	103.209 (1)	84.757(4)
Volume (Å ³)	17423 (3)	10748 (5)	6483 (1)	2895.6 (4)	5465(2)
Z'	4	4	4	2	1
T(°K)	236(2)	203 (2)	236(2)	236(2)	233
D _{calcd} (g cm ⁻³)	1.432	1.575	1.430	1.952	1.561
μ _{calcd} (cm ⁻¹)	4.296	3.586	1.689	6.454	3.476
F ₀₀₀	72.32	5080	2860	1648	2568
R, R _w ² , ^a GoF	0.0483,0.1475,1.029	0.0324,0.0485,1.019	0.0393,0.0661,1.015	0.0319,0.0558,1.010	0.0581,0.1213,1.043

$$^a R = \sum_o - F_c / \sum F_o R_w = [(\sum (F_o - F_c)^2 / \sum_w F_o^2)]^{1/2} .$$

Table 2. Crystal Data and Structure Analysis Results for Complexes 3.1, 3.2 and 3.3

	3.1	3.2	3.3
Formula	$C_{34}H_{56}ClLi_2N_3O_4Sm$	$C_{30}H_{55}ILi_2N_5O_{1.5}Sm$	$C_{60}H_{96}N_6Na_2O_6Sm_2$
fw	770.50	800.92	1344.11
Space group	Triclinic, P-1	Monoclinic, P2(1)/C	Triclinic, P-1
a (Å)	11.307(4)	21.147(1)	11.564(2)
b (Å)	13.137(5)	10.1298(5)	16.366(3)
c (Å)	17.091(6)	19.766(1)	19.305(4)
α (deg)	89.778(4)	90	64.990(3)
β (deg)	81.829(4)	117.247(1)	80.609(3)
γ (deg)	66.946(4)	90	78.348(3)
V (Å ³)	2308(1)	3764.4(3)	3230(1)
Z'	2	4	2
Radiation (K α Å)	0.71073	0.71073	0.71073
F(000)	796	1384	1612
T (K)	173(2)	203(2)	203(2)
D _{calcd} (Mg m ⁻³)	1.108	1.382	1.413
μ _{calcd} (mm ⁻¹)	1.360	1.863	2.408
R, wR _{2a}	0.0824, 0.2028	0.0488, 0.1083	0.0422, 0.1022
GoF	1.013	1.052	1.030

$$a R = \Sigma o - Fc / \Sigma F_o R_w = [(\Sigma (F_o - F_c)^2 / \Sigma w F_o^2)]^{1/2} .$$

Table 3: Crystal Data and Structure Analysis Results for Complexes 3.4, 3.5, 3.6 and 3.7

	3.4	3.5	3.6	3.7
Formula	$C_{32}H_{52}Cl_2Li_2N_4O_2Yb_2$	$C_{48}H_{86.36}Cl_4Li_4N_4O_6Yb_2$	$C_{47}H_{72}Li_4N_4O_4Yb$	$C_{32}H_{48}K_2N_4O_2Yb$
Fw	955.64	1331.22	819.26	771.98
Space group	Monoclinic, P2(1)/c	Monoclinic, P2(1)/C	Triclinic, P-1	Orthorhombic, P2(1)2(1)2
a (Å)	11.475(2)	11.972(2)	9.0560(9)	11.244(2)
b (Å)	11.541(2)	11.064(2)	11.162(1)	15.124(2)
c (Å)	15.711(3)	23.357(3)	15.354(2)	10.302(2)
α (deg)	90	90	77.044(2)	90
β (deg)	109.508(3)	99.980(3)	86.608(2)	90
γ (deg)	90	90	76.605(2)	90
V (Å ³)	1961.3(6)	3047.1(8)	1471.4(3)	1752.0(4)
Z	2	2	2	2
Radiation (K α Å)	0.71073	0.71073	0.71073	0.71073
F(000)	936	1341	778	784
T (K)	203(2)	203(2)	203(2)	203(2)
Dcalcd (Mg m ⁻³)	1.618	1.451	1.849	1.463
μ calcd (mm ⁻¹)	4.905	3.269	5.296	2.938
R, wR2a	0.0536, 0.1214	0.0402, 0.0722	0.0424, 0.0990	0.0343, 0.0510
GoF	1.022	1.056	1.007	1.020

$$a R = \frac{\sum o - F_c}{\sum F_o R_w} = \left[\frac{\sum (F_o - F_c)^2}{\sum w F_o^2} \right]^{1/2} .$$

Table 4: Crystal Data and Structure Analysis Results for Complexes 4.1, 4.2, 4.3, and 4.4

	1	2	3	4
Formula	$C_{68}H_{96}N_{10}O_4Sm_4$	$C_{136}H_{192}N_{16}O_8Sm_8$	$C_{72}H_{76}N_{10}O_4Sm_4$	$C_{74}H_{80}N_7O_{3.5}Sm_3$
fw (g/mol)	1718.95	3381.86	1746.83	1574.50
space group	Triclinic	Orthorombic	Monoclinic	Monoclinic
a(Å)	11.1020(10)	32.986(2)	9.0634(11)	12.6987(10)
b(Å)	12.4004(11)	28.819(2)	13.5294(17)	31.230(2)
c(Å)	13.5795(12)	33.030(2)	26.030(3)	18.8470(15)
α (deg)	101.4330(10)	90	90	90
β (deg)	91.272(2)	90	99.334(2)	90.700(2)
γ (deg)	113.313(2)	90	90	90
V(Å ³)	1672.2(3)	31400(4)	3149.6(7)	7327.1(10)
Z'	1	8	2	4
radiation (Mo K α)	0.71073	0.71073	0.71073	0.71073
T(K)	203(2)	203(2)	203(2)	203(2)
Dcalcd (g cm ⁻³)	1.707	1.431	1.842	1.427
μ calcd (mm ⁻¹)	3.514	2.993	3.734	2.421
F000	854	13440	1716	3148
R, Rw 2 ,a GoF	0.0340,0.0571, 1.038	0.0598,0.1602, 1.056	0.0589,0.1273, 1.033	0.0563,0.1375, 1.018

$$a R = \Sigma o - Fc / \Sigma FoRw = [(\Sigma (Fo - Fc)^2 / \Sigma wFo^2)]^{1/2} .$$

Table 5. Crystal Data and Structure Analysis Results for Complexes 5.1, 5.2 and 5.3

	5.1	5.2	5.3
formula	$C_{52}H_{64}N_8O_5Sm_2$	$C_{80}H_{100}N_{12}O_{6.5}Sm_2$	$C_{52}H_{80}N_8O_6Sm_2$
fw (g/mol)	1191.94	1634.42	1213.94
space group	Monoclinic	Triclinic	Orthorombic
a(Å)	17.9715(16)	12.7933(9)	11.1931(10)
b(Å)	116.2171(14)	16.9239(12)	17.9546(17)
c(Å)	18.1897(16)	18.9680(14)	26.580(2)
α (deg)	90	80.7450(10)	90
β (deg)	110.655(2)	72.2360(10)	90
γ (deg)	90	88.9190(10)	90
V(Å ³)	4932.9(8)	3858.1(5)	5341.6(8)
Z'	4	2	4
radiation (Mo K α)	0.71073	0.71073	0.71073
T(K)	203(2)	203(2)	203(2)
Dcalcd (g cm ⁻³)	1.591	1.407	1.510
μ calcd (mm ⁻¹)	2.413	1.567	2.232
F000	2384	1680	2480
R, R _w ² , χ^2 , a GoF	0.0506, 0.0951, 1.002	0.0839, 0.2280, 1.056	0.0431, 0.1373, 1.010

$$a R = \Sigma o - Fc / \Sigma F_o R_w = [(\Sigma (F_o - F_c)^2 / \Sigma w F_o^2)]^{1/2} .$$